PROBING LOCALIZED STATES DISTRIBUTIONS IN SEMICONDUCTORS BY LAPLACE TRANSFORM TRANSIENT PHOTOCURRENT SPECTROSCOPY

MARIANA JEKOVA GUEORGUIEVA

A thesis submitted in partial fulfilment of the
requirements of the University of Abertay Dundee
for the degree of Doctor of Philosophy

June 2005

I certify that this thesis is the true and accurate version of the thesis approved by the examiners.

Signed [redacted].....

Date ..3rd October 2005.....

(Director of Studies)

Contents

Abstract

The structure of the thesis is as follows:

Chapter I addresses the question of how the disorder of non-crystalline semiconductors influences their electronic properties. The concept of the mobility edge and mobility gap is introduced and a definition of the density of electronic states (DOS) is given. The DOS will be referred to frequently in this work. Also charge transport and photoconductivity in amorphous semiconductors are briefly described.

In chapter I the Multiple Trapping model (MT), widely used to describe charge transport in amorphous semiconductors, is formulated in the context of the transient photoconductivity (TPC) experiment. A brief review of the existing mathematically approximate methods (Naito H. *et al*, 1996; Nagase T. *et al*, 1999; Ogawa N. *et al*, 2000) based on the *Laplace* transformation for solving the MT system of equations is given. One of the main objectives of this work was to develop an exact procedure for solving the *Fredholm* integral equation of the 1st kind arising from the MT system of equations in the context of TPC experiment. The newly developed method is termed *Exact Laplace Transform (ELT)* method. The method could formally be divided in two parts. The first part is concerned with finding an exact solution of the *Fredholm* integral equation of the 1st kind. The second part of the method is a semi-analytic procedure based on a polynomial approach for simulation of *I-t* data from a model DOS distribution. The method has been thoroughly studied by application to computer simulated *I-t* data. The *ELT* method is found to have the finest resolution of $\sim kT/6$ (when applied to simulated *I-t* data) which is clearly an improvement over the approximate methods which have resolution of $\sim$ 2-3 kT. Furthermore, it has been shown that the polynomial approach could be used to obtain information on the free carrier recombination lifetime, τ_f and the procedure has been discussed.

The *Tikhonov* regularization method (Tikhonov A. N., 1963; Weese J., FTIKREG program, 1992), regarded as one of the most reliable methods for extracting information from noisy experimental data, has been applied to computer simulated data. It has been shown that the newly developed exact method and the *Tikhonov* regularization method perform equally well in terms of accuracy and resolution when applied to computer simulated, noise free *I-t* transients.

In the same chapter the approximate and exact methods have been applied to simulated *I-t* data with and with no noise introduced. The reliability of all methods has been discussed.

At the end, the approximate and exact methods have been used to extract information on DOS in light-soaked plasma enhanced chemical vapour deposition (PECVD) $a-Si:H$, and on

discrete levels in single crystal *Tin*-doped $CdTe$. The results have been compared with other publications.

In chapter II the time-of-flight (TOF) experiment and the mathematics describing it are briefly reviewed. The *ELT* and the *Tikhonov* regularization methods have been adapted for the case of the *post-transit* TOF experiment and applied to computer simulated TOF *I-t* data. The performance of the exact methods and the widely used approximate $txI(t)$ approach (Seynhaeve *et al*, 1989) has been studied. In order to simulate post-transit *I-t* data the polynomial approach has been used with model DOS distributions and under the assumption of near equivalence of *post-transit* régime in TOF experiment and *post-recombination* conditions in the context of the TPC experiment. The *ELT* and the *Tikhonov* regularization proved superior to the existing $txI(t)$ approach (Seynhaeve *et al*, 1989). All three methods (the *ELT*, the *Tikhonov* and the $txI(t)$ method) have been applied to experimentally obtained TOF data on $a-Si:H$ and the results have been discussed.

A summary of the principle results from this work is given in the final chapter (Conclusions).

Objectives

1. To provide an exact semi-analytic solution of the *Fredholm* integral of the 1st kind arising from the multiple trapping (MT) model, widely used to describe charge transport in amorphous semiconductors.

2. To illustrate the characteristics of the exact solution via numerical simulations, and comparison with existing mathematically approximate methods, and the *Tikhonov* regularization method.

3. To apply the exact methods to experimental transient photoconductivity (TPC) data, obtained on amorphous hydrogenated silicon (*a-Si:H*), and single crystals.

4. To analyse critically the available methods (based on *Laplace* transformation) to extract information about Density of States (DOS) distributions from transient photoconductivity data.

Introduction

The periodicity of the atomic structure is central to the theory of crystalline semiconductors. A crystalline structure is ordered in the sense that knowledge of the unit cell of the lattice allows the prediction of the positions of all atoms in the material over many bond lengths. Thus the environment in which the electrons move in a crystalline material is known ***a-priori***. A consequence of the order is the existence of bands - in a particular sample of a solid there are some ranges of total electron energy where electrons can be found (allowed bands), and other ranges where there are no electrons (forbidden bands). Bands are described by energy-momentum dispersion relations, which in turn, determine the effective mass, electronic excitations etc.

In contrast, amorphous semiconductors are '*disordered*', and this is the main feature which distinguishes them from crystalline materials. The lack of long range order introduces a range of localized states at the extremities of the valence and conduction bands of an amorphous semiconductor. These localized states are also a characteristic feature of disordered solids and have a determining influence on electron transport and related properties. It is their presence which leads to new forms and mechanisms of transport not generally found in the crystalline case. Research over the last 30 years shows that despite the apparent disorder, the band structure remains a valid concept for the *a-periodic* state too, though the bands are no longer described in terms of the energy-momentum (the $E_n(\mathbf{k})$ functions in the reciprocal lattice space are no longer periodic), but in terms of the density of states (DOS - the number of states per unit energy range per unit volume). DOS will be referred to very often in this work.

Anderson's work of 1958, 'The absence of diffusion in certain random lattices', has had a profound effect on the understanding of the behaviour of electrons in non-crystalline media (Mott N. F., 1987). The concept of 'localisation' has been introduced, and a transition in the nature of electronic states between delocalized and localized has been considered as an order parameter is varied (Mott N. F. and Davis E. A., 1979). Now it is generally accepted that valence and conduction bands and a band gap exist. Figure 1 (a) is a schematic representation of the density of states distribution near a band edge of an amorphous semiconductor. In the valence and conduction bands the disorder (different bond lengths and bond angles) produces 'tails' of (localized) states, and somewhere within this tail there is a mobility edge (Mott N. F., 1966), a critical energy separating localized from extended states.

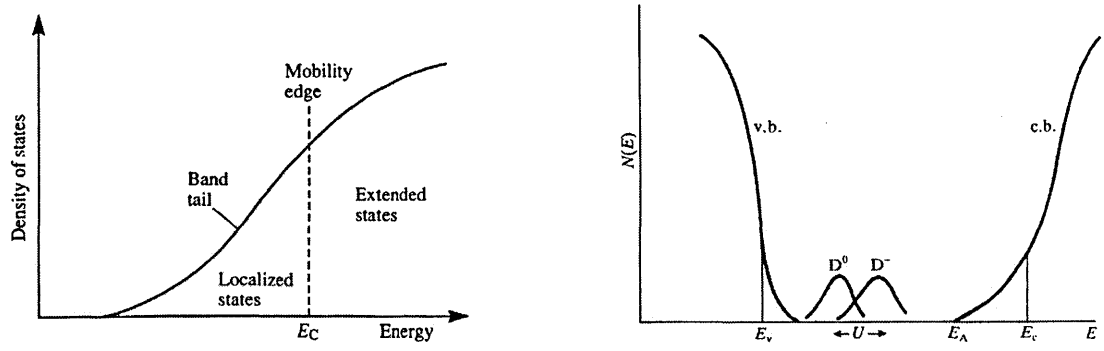

(a) **(b)**

Figure 1

(a) *The density of states distribution near the band edge of an amorphous semiconductor, showing the localized and extended states separated by the mobility edge (Street R. A., 1991).*

(b) *Schematic DOS distribution in amorphous silicon or germanium showing the bands, the band tails, and the defect states in the band gap (Mott N. F., Conduction in non-crystalline materials, 1987).*

A further contribution to the density of states in mid-gap comes from the co-ordination defects such as dangling bonds. The current model for amorphous silicon and germanium, figure 1 (b), is that most of the deep states are caused by dangling bonds. A dangling bond occurs when a silicon atom is so placed that it can form only three bonds with neighbours. Dangling bond can be positive (D^+), neutral (D^0) or negative (D^-) depending on the number of electrons at a given state. These defects are known as *amphoteric* defects, as they can act as donors, and also as acceptors. For amorphous silicon it is expected that the energy of the D^- state is further from the valence band edge than D^0 and D^+, i.e. that the energy required to remove an electron from a D^- state is smaller, because of the electrostatic repulsion between the two electrons on the site. The difference of the D^0 state and the D^- state is called a *correlation* (or Hubbard) energy, U. The correlation energy in the case of amorphous silicon is positive. In $a-As_2Se_3$ and other chalcogenide glasses it is suggested that U is negative, i.e. D^- is closer to the valence band edge because of fast local changes in the lattice configuration when D^- is created (Mott N. F. and E., A. Davis, 1979).

The density of dangling bond states depends on the conditions under which the material has been fabricated and they play an important role in amorphous semiconductors as they mediate the recombination processes. Shockley – Read statistics (Shockley W. and Read W.T, 1952)

take into account all possible transitions between the bands and defect states in amorphous semiconductors.

A distinction should be made between the deep states, mediating recombination, and states close to the band edges which act as temporary traps of charge. Carriers captured by these states are more likely to be thermally re-emitted than to capture a free carrier of the opposite sign. The presence of traps affects time resolved conductivity measurements, e.g. transient photoconductivity measurement which is described in chapter I.

The probability of thermal re-emission of a trapped carrier can be obtained by consideration of the *detailed balance*, the principle that in thermodynamic equilibrium the forward and reverse rates of all processes are equal. Thus taking into account that in thermodynamic equilibrium the rate of capture is equal to the rate of re-emission, and using the *Fermi* occupation function, gives the emission probability for electrons $e_n = \nu \exp(-(E_c - E)/kT)$ in s^{-1}. A similar expression holds for the hole emission probability e_p. This expression along with the capture probability defined by capture coefficient and the density of states are used in the analysis of the photoconductivity in chapter I.

Deep defects determine the electrical and optical properties of amorphous semiconductors by controlling trapping and recombination processes. It is generally accepted that at intermediate and high temperature (i.e. above 150 K for electrons in $a-Si:H$), the excess carriers interact with the localized tail states by a continuous process of trapping and thermal release. In this multiple trapping (MT) mode the observed transport takes place in the *extended* states, but the carriers–tail states interactions critically determine the propagation of the carriers and the drift mobilities (cases (i) and (ii) below). Below about 80 K there occurs a fundamental change in the predominant transport path and mechanism. In this low-temperature regime excess carriers now move through the localized tail states by phonon assisted hopping (case (iii)). (Mott N. F. and Davis E. A., 1979)

i. Thermal release to E_C.

The probability per second, P_r, which is equal to the inverse of the release time, τ_r, is approximately given by:

$$P_r = \frac{1}{\tau_r} \approx 10^{13} \exp\left(-\frac{E_C - E}{kT}\right)$$

ii. Further thermalization (downward hopping)

This is dependent on the electron wavefunction overlap of neighbouring sites in the tail states. The probability, P_{th}, is proportional to $\exp(-2\alpha R)$, where α^{-1} is the extension of the carrier wavefunction and R is the average distance between sites below energy

E. R is determined by the density of states distribution, $g(E)$, in the tail states. Near the bottom of the tail states the decreasing $g(E)$ increases the distance R and thus would be expected to lead to an appreciable slowing down in the rate of thermalization.

iii. **Phonon assisted hopping around energy E_F.**

$$P_h \propto \exp(-2\alpha R) \times \exp(-W / kT)$$

in addition to the wavefunction overlap, the hopping transport depends also on the hopping activation energy, W. This is the dominant transport mechanism at low temperatures, where probabilities for thermal release to the conduction band, and further downward thermalization are negligible. As the temperature is lowered the number and energy of phonons available for absorption decrease so that the tunnelling is restricted to seek centres which are not nearest neighbours but which instead lie energetically closer and within the range kT (so called Variable Range Hopping, VRH).

In this work a multiple trapping conduction mechanism has been assumed.

Illuminating a semiconductor with a constant intensity of light of an appropriate wavelength changes the conductivity by altering the carrier densities. This simple fact is used in photoconductivity experiments to study defect distributions in disordered semiconductors. Photoconductivity (Mott N. F. and Davis E. A., 1979) is a complex process of generation, transport and recombination of excess (above the thermal equilibrium) photogenerated carriers. In a semiconductor, generation of carriers is connected to the optical absorption coefficient and the quantum efficiency of generation of free electron and/or holes. Transport is characterised by the free carrier mobility μ_0 and the free carrier lifetime τ_f.

The conductivity σ of a sample may be defined as the current that flows across unit cube when the voltage between opposite faces is unity. Thus for a semiconductor where both holes and electrons are present the conductivity is given by $\sigma = ne\mu_e + pe\mu_h$, where $e = 1.6 \times 10^{-19} C$, and μ is the mobility. A very useful first approximation is to say that μ is a constant for a given carrier and material. In general μ depends on the temperature, and on the doping density when this is high, because of the effect on the collision time. It is assumed for a particular set of experimental conditions that conduction is dominated by a particular conduction path for which the mobility-charge density product is greatest. At high temperatures the dominant path is at the mobility edge, and is moving into localized states at lower temperatures. The transport analysis used in this work assumes unipolar conduction (the carriers are electrons) through extended states only.

The main objective of this work has been to develop an exact method for extracting information on the density of states distribution from photoconductivity data.

In this work it has been assumed that the photocurrent (defined as the excess current per unit volume produced by the radiation) is mainly carried by electrons. The photocurrent for a field F is given by $I = eF\mu_D G\tau = eF\mu_D \Delta n$, where μ_D is the drift mobility for electrons, τ is the lifetime, Δn is the excess density of the carriers due to the radiation, and G is the number of carrier pairs generated per unit time and per unit volume. After the radiation is cut off, Δn decays and from the transient photoconductivity measurements detailed information on the nature and energy distribution of localized states within the material under examination can be obtained. Such trapping centres critically determine the quality and commercial usefulness of disordered thin films.

Transient and modulated photocurrent measurements, TPC and MPC (Brüggemann *et al*, 1990; Main C. *et al*, 1992; Reynolds S. *et al*, 2000), have been used for many years to obtain transport information from disordered thin-film semiconductors. One of the main objectives of such analysis is spectroscopic – to determine the energy distribution of various species of gap states which influence carrier mobilities and lifetimes. The major problem with spectroscopic interpretation of the time-domain photoresponse $I(t)$ following a short laser pulse is that the instantaneous response is a result of simultaneous interaction of free photocarriers with the *whole* ensemble of gap states via multi-trapping process. Early analytical methods involved mathematical/physical approximations and even assumptions on the form on the density of states. The *Fourier* and *Laplace* (Naito H. *et al*, 1995; Main C., 1997; Nagase T. *et al*, 1999) methods avoid many of the pitfalls incurred by earlier transient analyses. Both methods use information from the *whole* transient response (rather than instantaneous values) in computing the density of each selected section of the gap state distribution, but still mathematical approximations have been used in the analysis.

The motivation for this work was the need for a reliable and exact method of computation of the density of states of amorphous semiconductors, which would represent a valuable diagnostic tool for material quality.

I. Transient Photoconductivity (TPC) Experiment

The idea behind the TPC experiment is schematically represented in figure 1.1. In the TPC experiment coplanar electrodes are deposited on the top surface of the sample and the photocurrent response *I-t* of the semiconductor as a function of time is measured following a short pulse of light. Under certain conditions (Ohmic contacts) the transient photodecay reflects solely the equilibration process of the excess carrier density mediated by the localized states. The photocurrent varies over many orders of time and magnitude and contains information on the localized states densities and the associated trapping and recombination parameters. The TPC experiment therefore could be used to probe the DOS distribution in amorphous semiconductors if a suitable mathematical analysis could be devised.
The TPC system used in our laboratories is described in detail elsewhere (Reynolds S. *et al*, 2000).

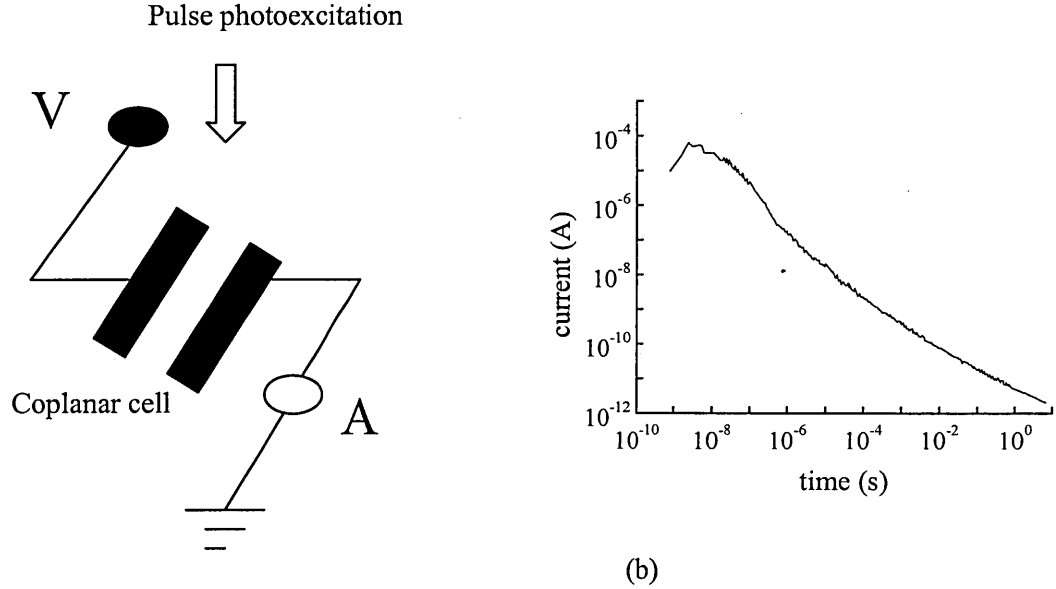

Figure 1.1 *The idea behind the TPC experiment (a), and the measured photocurrent as a function of time (b).*

1.1 Multiple Trapping (MT) model – formulation of the problem

The MT model is frequently used for the description of phenomena near and above room temperature. The model assumes, that carriers are trapped in localized states where they are immobile until thermally re-emitted to extended states (Schmidlin F. W., 1977)). The model is relatively simple, and it can be used to analyze photocurrent transient data in terms of a small number of transport parameters, and to obtain significant trends in these parameters with

temperature, electric field, and sample properties. Figure 1.2 is an illustration of the MT model. The progress of a typical carrier (an electron) in extended states (conduction band) is frequently interrupted by capture and release events from a set of states in the gap.

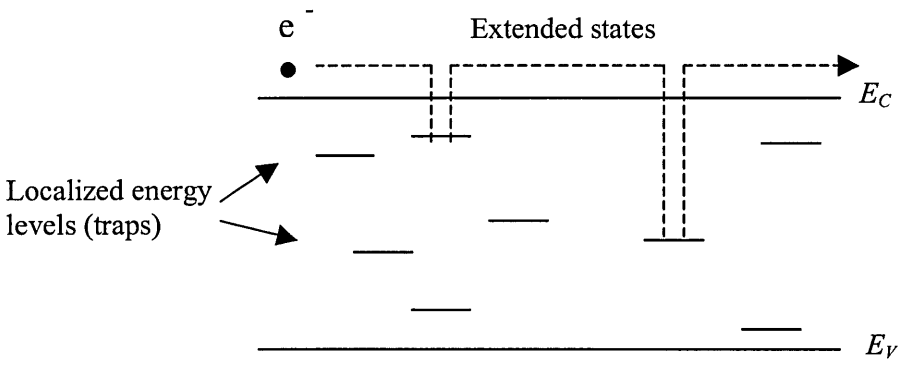

Figure 1.2 *Multiple trapping conduction mechanism*

Following Schmidlin the term 'trap' is used for any localized state which basically immobilizes a carrier for an observable length of time. In contrast with this, the term 'transport state' is used for any state which determines the microscopic mobility (μ) of a charge carrier. In other words traps are states which are sufficiently isolated from each other spatially so that direct transitions between them are negligible. Transport states, on the other hand, are sufficiently interconnected spatially to sustain what appears to be a continuous drift speed (μE, where E is the local electric field). Thus the microscopic mobility is entirely determined by transitions between transport states alone, whereas capture and release rates are determined by transitions between transport states and traps. (A given release rate, γ_i however, can be produced by different combinations of attempt-to-escape frequency, ν_i, and activation energies E_i.)

The MT model assumes that the excess carriers are residing initially in extended states. Subsequently, they become trapped in localized states at various depths. The time before re-emission varies with trap depth, with the shallower states releasing trapped carriers first. Further trapping and release occur, and the energy distribution of excess carriers evolves towards greater depths with time. This process is known as *thermalization.* Direct transitions between traps are neglected. The main problem which makes the extraction of information about DOS complicated is the fact that a continuous distribution of localized states in the material's gap results in *simultaneous* interactions of excess free carriers with a range of localized states, with rather complicated trapping/recombination dynamics. Consequently, the observed features in a transient decay are related to *both* the capture and release times from traps but they do not coincide with either the capture or release times.

To describe the TPC experiment in terms of the MT model the following assumptions are made:

i. The current is carried solely by carriers in free states which interact through trapping and release with a trap distribution,

ii. The photoconduction is unipolar, meaning that the mobile carriers are either holes or electrons,

iii. The capture cross section of all states are equal,

iv. The localized states are not saturated. This is achieved if the photocurrent is measured under small-signal condition. In this case the recombination kinetics of photocarriers is expected to be *monomolecular*[1].

The transient photoconductivity experiment is described with a set of coupled first order differential rate equations (1.1) and (1.2) with initial conditions (1.3), in which each type of trap is simply characterized by a capture probability ω_i and a release probability γ_i (Schmidlin F. W. (1977), Lakin W. D. *et al* (1977), Noolandi J.(1977)).

$$\frac{dn(t)}{dt} = -\sum_i \frac{dn_i(t)}{dt} - \frac{n(t)}{\tau_f} + n_0\delta(t) \tag{1.1}$$

$$\frac{dn_i(t)}{dt} = \omega_i n(t) - \gamma_i n_i(t) \tag{1.2}$$

Initial conditions:

$$n(t=0) = n_0,\ n_i(t=0) = 0 \tag{1.3}$$

$n(t)$ is the free carrier density at time t, $n_i(t)$ is the trapped carrier density at the i^{th} localized state at time t, n_0 is the injected free carrier density, τ_f is the free carrier recombination lifetime, $g(E_i)$ is the density of states at the the i^{th} localized level below the mobility edge, $\omega_i = \sigma \upsilon g(E_i)$ is the capture rate constant and $\gamma_i = \nu \exp(-E_i / kT)$ is the release rate

[1] The condition, in which the recombination rate depends on the excess density of only one of the recombining species is called *monomolecular* recombination. The condition, in which the recombination rate depends on the densities of the both recombining species is called *bimolecular* recombination.
In the case of *monomolecular* recombination the excess electron density is proportional to the excess generation. In the case of *bimolecular* recombination the excess electron density varies as the square root of the excess generation.

constant at the i^{th} localized level, σ is the capture cross section, υ is the thermal velocity, ν is an attempt-to-escape frequency, k is the *Boltzmann* constant and T is the absolute temperature.
The *delta*-function defines the initial condition for the transient photocurrent experiment. It should be noted that in general both the pre-factor ν and the activation energy E_i may vary and contribute to a distribution of release rates.

1.2 Early work on TPC analysis, thermalization energy concept

Historically, the first precise and analytic solution of the multiple trapping equations, in the context of the time-of-flight experiment, is due to Schmidlin F. W. (1977) and Noolandi J. (1977). A mathematical analysis of considerable complexity leads to a solution in the form of convolution of modified *Bessel* functions of first order and must, in general, be evaluated numerically. Although Schmidlin's result is analytic it is difficult to interpret. To overcome this difficulty, during the past 20 years, a variety of approximate techniques assuming a MT mechanism of charge transport, and based on *Fourier* (Main *et al*, 1992; Main C., 1997) and *Laplace* transformations (Naito H. *et al*, 1994; Ogawa N. *et al*, 2000) have been developed. The fact that they are mathematically simple and straightforward makes them attractive, but unfortunately, they have inferior resolution in comparison with the existing exact methods (cf. Exact methods of solving the *Fredholm* integral equation of the 1st kind).

The early approximate methods made use of the *thermalization energy*[2] concept, introduced by Arkhipov and Rudenko (1978), and independently Tiedje and Rose (1980), Orenstein and Kastner (1981) (the so-called TROK model), and Orenstein J. *et al* (1982). The *post*-transit analysis of the time-of-flight experiment still uses this approach (TOF experiment; Seynhaeve's PhD thesis, 1989; Seynhaeve *et al.* (1989)) and yields the DOS proportional to $t \times I(t)$. Seynhaeve G., *et al* (1985) have shown that that there are important limitations to the range of validity of the *thermalization energy* analysis. It has been shown that the *thermalization approximation* does not work for structured distributions of localized tail states and for exponential tails whose width is smaller than kT, where kT is the thermal energy (Marshall J. M. and Main C., (1983)), but the thermalization energy model is useful historically for the insight it gives.

---

[2] The *thermalization energy* concept is based on the following consideration. If E is the depth of an electron trap below the conduction band mobility edge then the immobilization time of a trapped electron is equal to the thermal release time t, which is defined by $t = \nu^{-1} \exp(E/kT)$, where ν is the attempt-to-escape frequency which is of order $10^{12}\ s^{-1}$. Then the energy $E_{th} = kT \ln \nu t$ separates those states above $E_{th}(t)$ for which the most probable number of release events in the time t is greater than unity, from the deeper states where an electron is unlikely to be thermally released in the time t.

The physical approximation used is that above the $E_{th}(t)$ electrons are thermalised and have a *Boltzmann* distribution. This assumption is increasingly valid as one departs from $E_{th}(t)$ since the electrons in the shallower states have had ample opportunity to 'thermalise' as a result of many thermal excitations. Below $E_{th}(t)$, by definition, the electron distribution remains 'frozen' into the initial form that parallels the density of traps. As the time progresses the thermalization energy moves further into the gap, releasing charge which is subsequently re-trapped into the deep traps thus increasing their occupation.

A review of the methods which make use of the thermalization energy concept is out of the scope of this work. Only one of them, the *post-transit* TOF experiment, is briefly discussed. In the post – transit TOF experiment the current is due solely to the *emission* of carriers from localized states, *i.e.* where no re-trapping occurs. It is shown that this case could be easily treated with the existing exact methods and an exact solution could be obtained (cf. chapter II). In Chapter II a comparison is made between Seynhaeve's *post-transit* approach and the exact methods developed as a part of this project. Other methods known as 'multi-point' methods, which make use of current-time data over a range of times (e.g. *Voltera* integral equation (Michiel H., J. *et al* (1983), and methods based on the *Fourier* transformation of the photocurrent data (Main C. *et al*, 1992; Main C., 1997; Webb D.P., PhD thesis (1994)) are out of the scope of this work.

The following section is a summary of the work of the Osaka group (Naito H. *et al*, 1996, Nagase T. and H. Naito, 1998), which was used as a starting point for the development of the Exact *Laplace* transform (*ELT*) method. The MT equations are solved using the *Laplace* transform, which is a widely used method of solving systems of differential equations. It is assumed that the *Laplace* transform $\mathcal{L}\{n(t)\} = \hat{n}(s)$ and $\mathcal{L}\{n_i(t)\} = \hat{n}_i(s)$, denoted by ($\hat{}$) over the corresponding variable, exists and is defined, in the cases of free and trapped carriers respectively, by:

$$\hat{n}(s) = \int_0^\infty n(t)\exp(-st)dt\,, \qquad \hat{n}_i(s) = \int_0^\infty n_i(t)\exp(-st)dt$$

The application of the theorem for *Laplace* transform of derivatives $\mathcal{L}f'(t) = s\hat{f}(s) - f(0)$ leads to a linear system of algebraic equations (LAE).

$$s\hat{n}(s) - n(0) = -s\sum_{i=1}^{n}\hat{n}_i(s) - \frac{\hat{n}(s)}{\tau_f} + n_0 \tag{1.4}$$

$$s\hat{n}_i(s) = \omega_i\hat{n}(s) - \gamma_i\hat{n}_i(s) \tag{1.5}$$

$$\hat{n}_i(s) = \frac{\omega_i}{s+\gamma_i}\hat{n}(s), \qquad \hat{n}(s) = \frac{n_0 + n(t=0)}{\frac{1}{\tau_f} + s + \sum_{i=1}^{n} \frac{s\omega_i}{s+\gamma_i}}$$

After replacing the summation by integration the last line reads:

$$\hat{n}(s) = \frac{2n_0}{\hat{a}(s)} = \frac{2n_0}{\frac{1}{\tau_f} + s + s\int_0^{E_F} \frac{\sigma v g(E)}{s + \nu \exp(-E/kT)} dE}, \qquad \frac{2n_0}{\hat{n}(s)} = \hat{a}(s) \tag{1.6}$$

The free carrier density $n(t)$ and the photocurrent $I(t)$ are related by $I(t) = q\mu_0 Fn(t)$, where q is the electronic charge, μ_0 is the microscopic mobility and F is the applied electric field. Then the last expression can be written in terms of the initial value of the photocurrent $I(0)$ and the *Laplace* transform of it $\hat{I}(s)$. After differentiating with respect to the *Laplace* variable s, an integral equation for the density of states, termed a *Fredholm integral equation of the 1st kind*, is obtained (Naito H. *et al*, 1996; Nagase T. *et al*, 1998, 1999).

$$\frac{d}{ds}\left(\frac{2I(0)}{\hat{I}(s)}\right) - 1 = \int_0^{E_F} \sigma v g(E) \frac{\nu \exp(-E/kT)}{[s + \nu \exp(-E/kT)]^2} dE \tag{1.7}$$

It relates the *Laplace* transformation of (noisy) transient photoconductivity data with the density of localized states. The numerical inversion to obtain the function of interest, $g(E)$, is known as an '*ill-posed*' problem (cf. General definition of ill-posed problems).

It has been assumed that this *Fredholm* integral equation cannot be solved for the DOS using methods from linear algebra, the reason being its ill-posed nature. In this work it will be shown that despite its ill-posed nature, it is possible to obtain an exact solution for the DOS without using any mathematical/physical approximations. In order to be able to make a comparison and to analyse the results, a brief review of the approximate methods for solving the *Fredholm* integral equation of the first kind will be given.

1.3 Approximate Laplace transform methods of solving the Fredholm Integral Equation of the 1st kind

The approximate methods developed by the Osaka group (Naito H. *et al*, 1996, Ogawa N. *et al*, 2000), *Laplace Transform* (*LT*) and *High Resolution Laplace Transform* (*HLT*), are based on a simple mathematical approximation, namely the kernel of the integral in the *Fredholm* integral equation of the 1st kind (or a variant of it) is replaced by a suitably weighted *delta* function peaked at energy E_0 to yield $g(E_0)$. The approximate methods based on *Laplace* (alternatively on *Fourier*) transformations are straightforward but unfortunately they do not have a good resolution. Discrete levels (and features in the DOS) are returned 'broadened' by several kT and in the case of a steep exponential tail the recovered slope is wrong.

1.3.1 *Laplace* transformation (*LT*) method

In the *LT* method, developed by Naito *et al* (1996), the problematic part of the *Fredholm* integral equation of the 1st kind, namely the kernel function, is replaced by a *delta* function positioned at a given energy, $E_0 = kT\ln(\frac{\nu}{s})$, where the kernel has a maximum

$$h(s,E) = \frac{\nu \exp(-E/kT)}{[s+\nu\exp(-E/kT)]^2} \approx \frac{kT}{s}\delta(E-E_0)$$

This mathematical simplification leads to a simple expression relating the localized states distribution with the *Laplace* transformation of the photocurrent transients

$$g(E_0) = \frac{1}{\sigma\upsilon kT}\left\{\frac{d}{d\ln(s)}\left[\frac{I(0)}{\hat{I}(s)} - s\right]\right\} \qquad (1.8)$$

Another more precise but still approximate method developed later by the Osaka group is termed High Resolution *Laplace* Transform (*HLT*) method (Ogawa N. *et al*, 2000).

1.3.2 High resolution *Laplace* transformation (*HLT*) method

In the *HLT* method the approach is similar. After taking a derivative with respect to the *Laplace* variable s on the *Fredholm* integral equation of the 1st kind, the following equation relating the DOS and the *Laplace* transform of the measured photocurrent is obtained:

$$\frac{d^2}{ds^2}\left(\frac{I(0)}{\hat{I}(s)}\right) = -\int_0^{E_F} \sigma \upsilon g(E) h'(s,E) dE, \qquad h'(s,E) = \frac{2\nu \exp(-E/kT)}{[s+\nu \exp(-E/kT)]^3}$$

The *sharper* kernel function $h'(s,E)$ is replaced again by a *delta* function with appropriate weighting coefficient $\frac{kT}{s^2}\delta(E-E_0')$, and positioned at another energy $E_0' = kT\ln(\frac{2\nu}{s})$. A more precise but still approximate expression for the DOS is obtained:

$$g(E_0') = \frac{I(0)}{\sigma \upsilon kT} \frac{\hat{I}(s)\hat{I}''(s) - 2[\hat{I}'(s)]^2}{[\hat{I}(s)]^3} s^2 \tag{1.9}$$

In the calculation proposed by the Osaka group the integration, in order to find the *Laplace* transform of the photocurrent data, and differentiation have been done by simple numerical procedure over n sampling points.

In our computation procedure the *Laplace* transformation of the photocurrent data *I-t* has been calculated *semi analytically* by a simple procedure of connecting neighbouring *I-t* points by exponents and representing the integration over the accessible time domain as a summation of integrals between the neighbouring points (Appendix A2). The first and second derivatives of $\hat{I}(s)$ have been found using the theorem for multiplication by t^n (Spiegel M.R, 1965): $\hat{f}^{(n)}(s) = (-1)^n \int_0^{\infty} t^n f(t) e^{-st} dt$. This approach leads to a negligible round-off error.

It is obvious that the *HLT* method has a better resolution in comparison with the simpler *LT* method due to the sharper kernel function.

1.3.3 Energy resolution of the approximate methods

The well-known effect of broadening caused by the *delta*-function approximation can easily be estimated (figure 1.3) by applying both approximate methods to computer-generated *I-t* data from one discrete level. The Full Width of the Half Maximum (FWHM) is 93 *meV* (3.5 *kT*) for the *LT*, and 78 *meV* (3 *kT*) for *HLT* method respectively.

The mathematical approximation of replacing the problematic part of the *Fredholm* integral equation (the kernel function) with a *delta*-function leads to diminished resolution of the approximate methods.

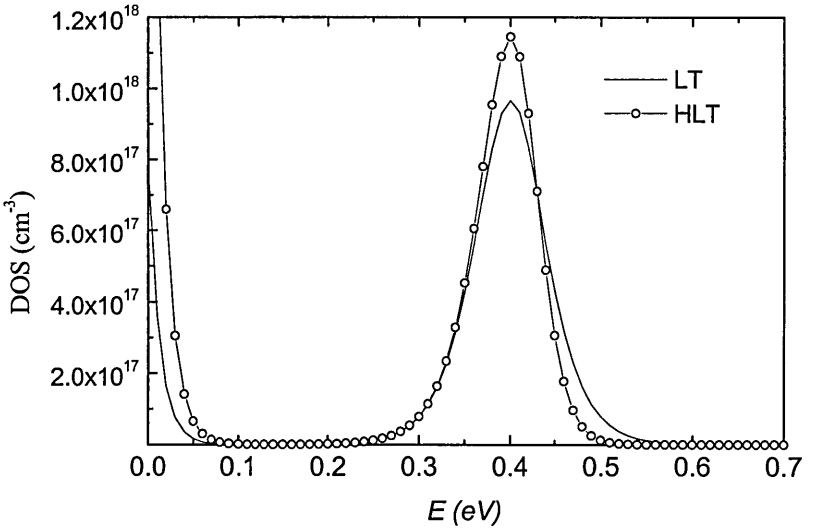

Figure 1.3 *Recovery of one discrete level of density 10^{17} cm^{-3} positioned at 0.4 eV using the LT and HLT methods.*

The example in figure 1.4 is self-explanatory. Our simulations showed that the approximate methods are incapable of reproducing the DOS in a case, for example, of two discrete levels positioned less than 80 *meV* apart (as it should be if a method has FWHM 93 *meV*).

In the case of two discrete levels positioned at around 70 *meV* the *LT* method resolves only one broad level with a maximum around the middle of the distance between the actual positions of the original two levels.

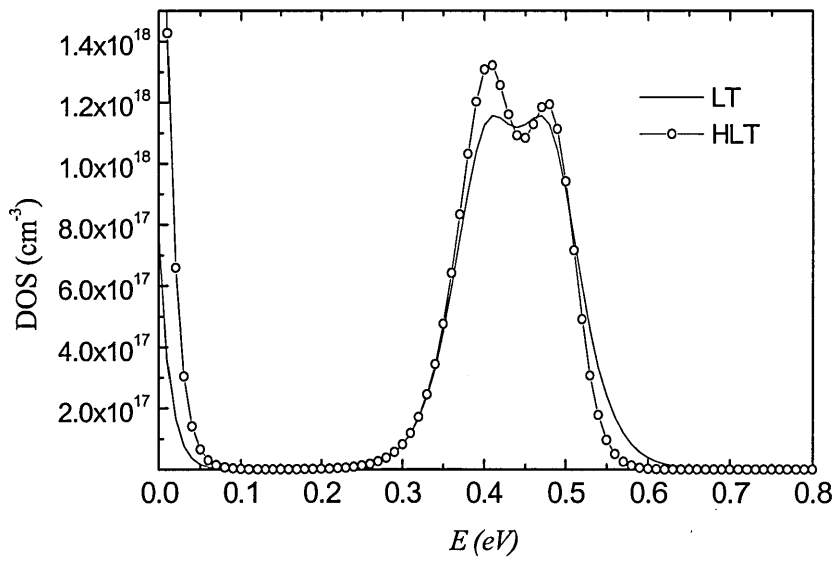

Figure 1.4 *Recovery of two discrete levels of equal density 10^{17} cm^{-3} placed at 0.4 and 0.48 eV using the LT and HLT methods.*

The *LT* and *HLT* methods have been applied to exponential and structured distributions. Figure 1.5 shows the TPC $I(t)$ computed for exponential localized states distributions with different values of the characteristic temperature, T_0. In the calculation an ambient temperature $T = 300K$ and free carrier recombination lifetime $\tau_f = 10^{-6}$ s have been assumed. The inflection points in the transients are due to the recombination of the photogenerated free carriers. The recombination lifetime determined from the graph is longer than τ_f. This is a result from frequent trapping and detrapping of free carriers into the exponential state distributions. The value of τ increases with T_0 because the trapping and detrapping of free carriers become much more frequent.

Figures 1.6 (a) and (b) show the exponential localized state distributions recovered from the TPC data in figure 1.5 which were obtained using the polynomial approach as described in 1.4.1.2. From figure 1.6 (a) it is seen that the *LT* method fails when steep distributions ($T_0 \leq T^{ambient}$) have to be recovered. The *HLT* method (figure 1.6 (b)) performs better but still the recovery of steep distributions is problematic (T_0=200K). This is in agreement with the results obtained from the Osaka group (Nagase T, *et al*, 1999).

The back-simulated TPC data using the *LT* DOS is wrong, as was expected, for steep distributions with $T_0 \leq T^{ambient}$ (200 K and even 300 K). This is clearly caused by the δ – function approximation.

In contrast, the *HLT* method, although approximate, reproduces quite well the starting distributions even when $T_0 \leq T^{ambient}$. The reason is that now the δ-function replaces a sharper Kernel function in comparison with the simple *LT* method. The back-simulated TPC data fit well the original $I(t)$ data (symbols in figure 1.5).

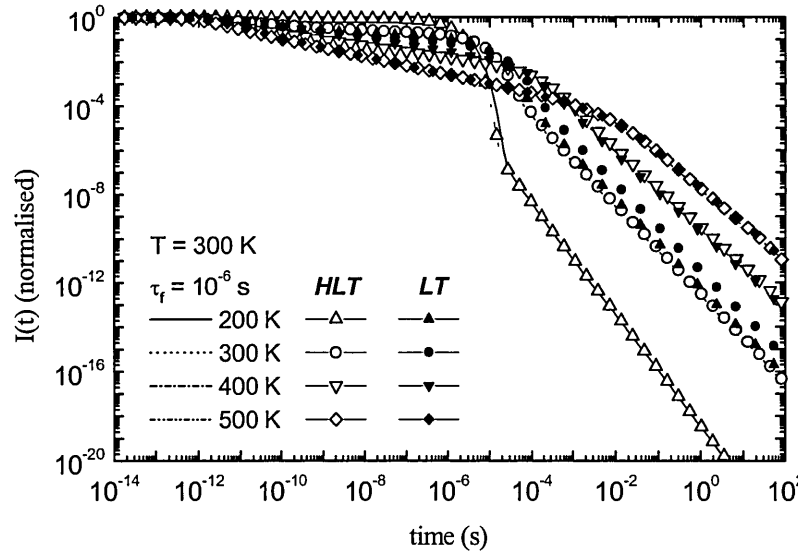

Figure 1.5 *TPC $I(t)$ transients computed for exponential localized state distributions with T_0=200 K, 300 K, 400 K, 500 K, and free carrier recombination lifetime $\tau_f = 10^{-6}$ s at T = 300 K. Symbols correspond to simulated I(t) using the recovered LT and HLT DOS.*

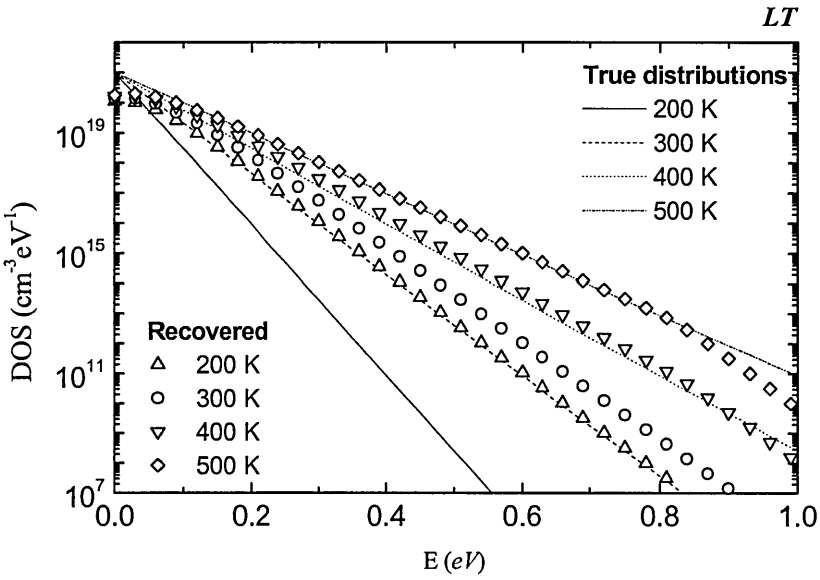

(a)

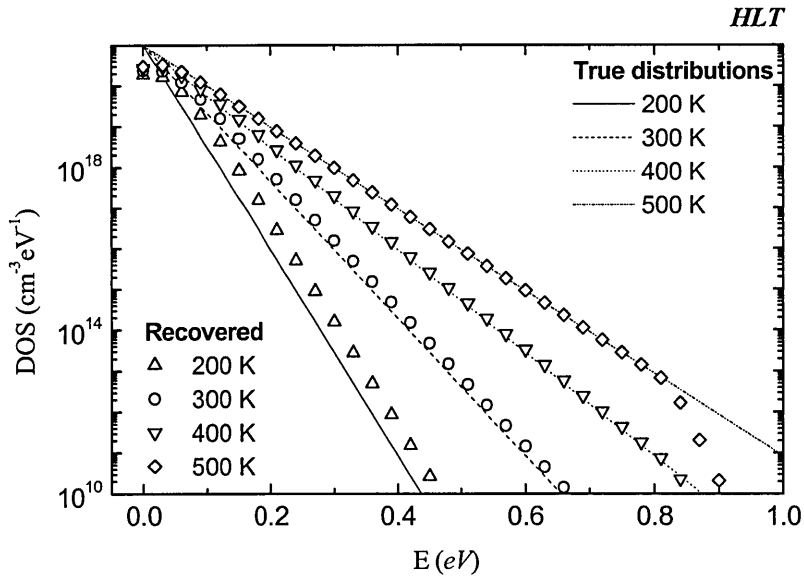

(b)

Figure 1.6 (a), (b). *Recovery of exponential distributions of states simulated with tail slope parameters T_0 = 200K, 300 K, 400 K, 500K from the current transients in figure 1.5. Lines indicate the model DOS distributions.*

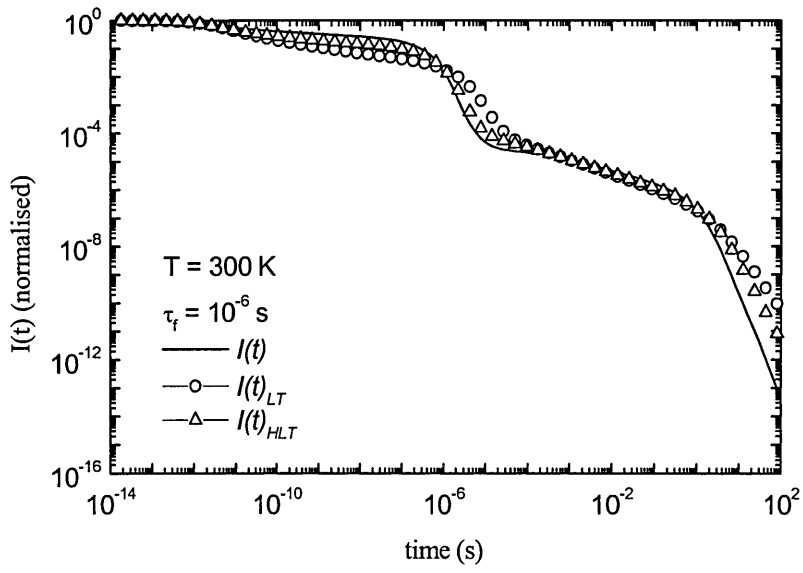

Figure 1.7 *TPC $I(t)$ computed for the structured distribution in figure 1.8. In the computation the free carrier recombination lifetime $\tau_f = 10^{-6}$ s at T = 300 K.*

Figure 1.7 shows the TPC $I(t)$ data computed for an exponential localized states distribution with T_o = *300 K* on which *Gaussian* distributions with different widths have been superimposed. The initial decay of the photocurrent transients, between 10^{-11} – 10^{-6} s is caused by trapping into the *Gaussian* distributed states.

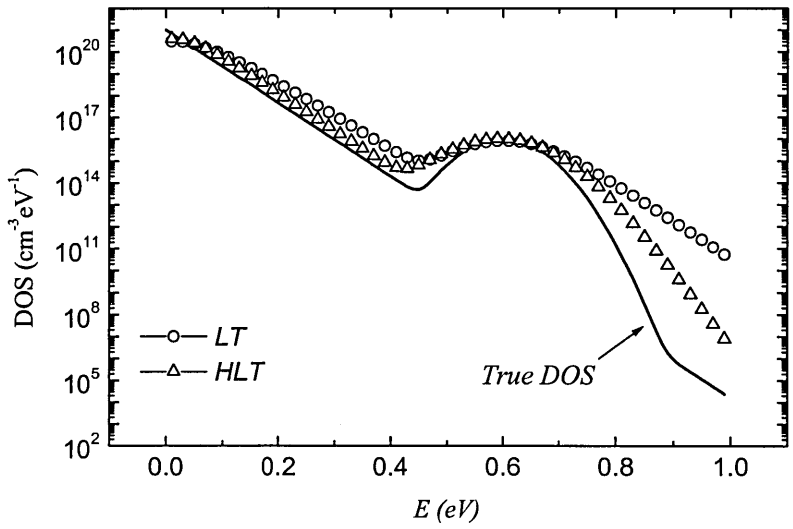

Figure 1.8 *Recovery of exponential plus Gaussian distributions:* T_o = *300 K,* g_{Go} = 10^{16} cm^{-3} eV^{-1}, E_0 = *0.6 eV* , E_W = *0.06 eV using LT and HLT methods.*

From figure 1.8 is seen that although the energy position and the density of the *Gaussian* distribution are well reconstructed by both methods, the calculated distribution significantly deviates from the original distribution especially in the deep energy region, and the deviations are bigger for the *LT* method. Even though the examined *Gaussian* distribution in figure 1.8 has a width E_W = 0.06 *eV* both methods still cannot reproduce it. The deviations from the true shape of the model distribution are clearly due to the δ - function approximation.

1.4 Exact methods of solving the Fredholm Integral Equation of the 1st kind

1.4.1 Exact Laplace Transform (*ELT*) method

1.4.1.1 Exact solution of the MT system of equations for the Density of States

One of the main objectives of this thesis was an exact solution involving no mathematical approximations of the *Fredholm* integral equation of the 1st kind arising from the MT system of equations to be found. The developed method is termed the *Exact Laplace Transformation* (*ELT*) method (Gueorguieva M. *et al*, 2000a) because it contains no mathematical or physical approximations (apart from the assumption that the transport is governed by the MT mechanism).

The starting point of the method is the *Fredholm* integral equation of the first kind (cf. MT – formulation of the problem):

$$\frac{d}{ds}\left(\frac{2I(0)}{\hat{I}(s)}\right)-1=\int_0^{E_F}\sigma\upsilon g(E)\frac{\nu\exp(-E/kT)}{[s+\nu\exp(-E/kT)]^2}dE \qquad (1.10)$$

Solving this integral equation for the function under the integral ($g(E)$) is known as an *ill-posed* problem, meaning that relatively small variations (errors) in the experimental data lead to relatively large changes in the solution, $g(E)$. The problem is ill-posed by its nature (described by the Kernel function) and so-called *regularization* methods are needed to obtain a reliable solution (cf. *Tikhonov regularization* method).

As it is described later in this work (the *Tikhonov regularization* method), a criterion of whether a problem is ill- or well- posed is the so-called *condition number*. In our calculation the product *Mathematica* has been used to calculate the singular values decomposition[3] of the matrix of the system corresponding to equation (1.10) and to obtain a value for the condition number. The calculated condition number is of order 10^{13} suggesting that the problem is extremely ill-conditioned.

It should be noted that the developed *ELT* method does not transform the ill-posed problem of solving the *Fredholm* integral equation of the 1st kind to a well-defined one. Starting from the *Fredholm* integral equation the method transforms it to a linear system of algebraic equations in

[3] Any matrix **m** can be written in the form $\mathbf{u}^T\mathbf{m}_D\mathbf{v}$, where $\mathbf{m}_D$ is a diagonal matrix with elements known as *singular values*, and **u** and **v** are row orthonormal matrices. The ratio of the largest singular value of a matrix to the smallest one gives the *condition number* of the matrix. A system is said to be *singular* if the condition number is infinite, and *ill-conditioned* if it is too large. Wolfram S, 1991.

the *Laplace* domain. Then, it obtains a unique solution of the system for a given set of experimental/ simulated *I-t* data. The key moment for obtaining a unique solution is to find a range for the *Laplace* variable s for which the matrix of the system of equations (1.4) & (1.5) becomes strictly diagonally dominant ensuring uniqueness of the obtained solution $g_i(E_i)$.

In our approach we begin by integrating a *discrete* form of the *Fredholm* integral equation with respect to the *Laplace* variable s to obtain an exact system of linear algebraic equations (LAEs) for n closely - spaced levels g_i:

$$\frac{2I(0)}{\hat{I}(s)} = \frac{1}{\tau_f} + s + \sigma\upsilon s\sum_{i=1}^{n}\frac{g_i}{s+\gamma_i}, \qquad \gamma_i = \nu\exp(-E_i/kT) \tag{1.11}$$

$$\left\|\sum_{j,i=1}^{n} a_{ij}(s_i)g_j = b_i(s_i),\ a_{ij}(s_i) = \frac{1}{s_i+\gamma_j},\ b_i(s_i) = \frac{1}{\sigma\upsilon}\left[\frac{1}{s_i}\left(\frac{2I(0)}{\hat{I}(s_i)} - \frac{1}{\tau_f}\right) - 1\right]\right. \tag{1.12}$$

It is known from linear algebra theory that the solution of these LAEs is unique provided the matrix of the system (1.12) is non-singular, i.e. the determinant is non-zero (Atkinson L.V. *et al*, 1989).

Our solution algorithm comprises two steps.

i An appropriate domain for the *Laplace* variable s is chosen which makes the system strictly diagonally dominant[4], i.e. $|a_{ii}| > \sum_{j=1, j\neq i}^{n}|a_{ij}|$. This is achieved by taking $s_i = -\gamma_i + \varepsilon_i$, where ε is a small quantity defined by $\varepsilon_i = \min_{\substack{j=1,n \\ j\neq i}}\frac{1}{n}(\gamma_i - \gamma_j)$.

ii Solving the system by the standard method of *Gaussian* elimination (Atkinson L.V. *et al*, 1989).

[4] **Theorem:** A strictly diagonally dominant matrix A is non-singular, i.e. the determinant of A is non-zero. Moreover, *Gaussian* elimination can be performed without row interchanges on $Ax = b$ to obtain unique solution and computation is stable with regards to growth of round-off errors. (Atkinson L.V *et al*, 1989)

In order to solve the system for DOS, *Laplace* transform of the TPC *I-t* data has to be done. An *analytic* procedure of calculating $\hat{I}(s)$ was developed. It comprises two steps:

i First, TPC current-time data are presented as a set of weighted exponents, $I(t) = \sum_i A_i \exp(\alpha_i t)$ (Appendix A1),

ii Second, the tabulated expression is used to calculate the *Laplace* transform of summation of exponents, $\hat{I}(s) = \sum_i \frac{A_i}{s - \alpha_i}$ (Appendix A2).

Two methods of fitting exponents to TPC *I-t* data were used and assessed:

The first method uses a proprietary subroutine (Garbow B. S. *et al* (1980)) employing the *Levenberg-Marquardt* algorithm, to calculate the weights of typically 100 exponential functions spaced at equal logarithmic intervals over the time range of interest.

The second method is based on *analytic* fitting of successive exponential functions to the residuals, which allows both weights and time-constants to be optimised (Appendix A1). It makes use of the *Least squares method* to find A_i and α_i for a minimum number of exponents which would fit the experimental current-time data. The requirement for a minimum number of exponents is consistent with the *principle of parsimony*, or *principle of simplicity*[5], which is widely used in regularization techniques. It is used as a further criterion to select one solution if many vectors (solutions) are compatible with the input data. A similar to the principle of parsimony approach has been adopted and rigorously proven from the physics point of view by Schmidlin (1977). He reached to the following conclusion: '*The experimental current transients can be extremely well approximated by very few traps having release times bracketing the experimental transit time.*' This confirms one of our results obtained when simulating current-time data using our polynomial approach. We found that essentially the same current-time data could be simulated from a range of different DOS profiles, although the solution for DOS is unique.

[5] Adoption of this principle, though seemingly obvious, leads to problems about the role of simplicity in physics, especially when we are choosing between hypotheses that are not (or are not known to be) equivalent. Probably, there are different criteria for what is the simplest hypothesis, and it is not clear whether a simpler hypothesis is more likely to be true or not (Kirsch A.).

Having found the *Laplace* transformation of the TPC *I-t* data for the required s domain defined by $s_i = -\gamma_i + \varepsilon_i$, the problem is to determine a vector with components $\{g_i(E_i); \quad i = 1,...,n\}$ from the transformed experimental data, $\{b_i(s_i); \quad i = 1,....,n\}$. The solution algorithm, as described above, allows determination of both g_i and E_i vectors simultaneously, and is truly 'spectroscopic' meaning that no assumptions as to the form of the DOS have to be made. In addition, the solution is unique i.e. there is only one vector $\{g_i(E_i); \quad i = 1,...,n\}$ compatible with given experimental data $\{b_i(s_i); \quad i = 1,....,n\}$.

The accuracy and resolution of the *ELT* method were tested and compared with the existing and recently developed approximate and exact methods, employing *Laplace* transformation of TPC data for determination of the density of electronic states in disordered semiconductors. Details are presented in the rest of the section and in the following publications: Gueorguieva M. J. *et al*, 2001; 2000a. The method was applied to study light-soaked materials (Gueorguieva *et al*, 2001) and crystalline semiconductors (Gueorguieva M. J. *et al*, 2002). The results are presented in sections Light-induced meta-stable states in PECVD $a-Si:H$, and 'Discrete' levels in single crystal *Tin*-doped $CdTe$.

1.4.1.2 Exact semi-analytic simulation of the current transients based on a polynomial approach

To investigate the potential accuracy and resolution of a DOS extraction procedure, it is necessary to simulate accurately the transient photocurrent response from a prescribed DOS distribution. A possible approach is to solve numerically the initial system of MT equations, using given (already calculated) discrete values $g(E_i)$, for $n_i(t)$ and $n(t)$ (Main C. *et al* 1992, Main C., 1997). The latter is proportional to the photocurrent transient.

In our approach the *Heaviside's* expansion theorem (Spiegel M.R., 1965) is used to analytically perform Inverse *Laplace* transformation in order to find current data in the time domain.

The *Laplace* transform of the TPC $I(t)$ data could be written as:

$$\hat{I}(s)=\frac{2I(0)}{\frac{1}{\tau_f}+s+\sigma\upsilon s\left(\frac{g_1}{s+\gamma_1}+\frac{g_2}{s+\gamma_2}+\ldots+\frac{g_n}{s+\gamma_n}\right)}=\frac{2I(0)\prod}{\prod\left(\frac{1}{\tau_f}+s\right)+\sigma\upsilon s\sum_{i=1}^{n}g_i\prod_i}=\frac{P(s)}{Q(s)}$$

$$\prod=\prod_{i=1}^{n}(s+\gamma_i),\qquad \prod_i=\prod_{\substack{j=1\\ j\neq i}}^{n}(s+\gamma_j),\qquad \gamma_i=\nu\exp(-E_i/kT).$$

In the above expression *P(s)* and *Q(s)* are polynomials, with the degree of $P(s)$ less than that of *Q(s)*. According to the *Heaviside's* expansion theorem the Inverse *Laplace* transform $\mathcal{L}^{-1}\left\{\hat{I}(s)\right\}$ exists:

$$I(t)=\mathcal{L}^{-1}\left\{\hat{I}(s)\right\}=\sum_{i=1}^{n+1}\frac{P(\alpha_i)}{Q'(\alpha_i)}e^{\alpha_i t}=\sum_{i=1}^{n+1}A_i e^{\alpha_i t}$$

The alphas, α_i, are the *n + 1* zeros of the denominator $Q(s)$, and $Q'(\alpha_i)$ is the first derivative of *Q(s)* calculated at the zeros α_i.

The fact that the denominator $Q(s)$ has exactly *n + 1* zeros is easily seen if we order the emission rates, γ_i, so that $\gamma_1 > \gamma_2 > \ldots > \gamma_n$ for energies $E_1 < E_2 < \ldots < E_n$. Then the equation

$$Q(s) = (\frac{1}{\tau_f} + s)(s+\gamma_1)(s+\gamma_2)...(s+\gamma_n) + \sigma\upsilon s(g_1\prod\nolimits_1 + g_2\prod\nolimits_2 + ... + g_n\prod\nolimits_n) = 0$$

is satisfied by a sequence of *negative* alphas, α_i, which fall between the successive *negatives* of the γ_i.

- Polynomial $Q(s)$ is always positive for positive *s*.
- Let us consider the sign of the denominator $Q(s)$ at points $s = 0, -\gamma_n, -\gamma_{n-1}, ..., -\gamma_1$ (negative *s*):

$$Q(s=0) = \frac{1}{\tau_f}\gamma_1\gamma_2...\gamma_n > 0$$

$$Q(s=-\gamma_n) = -\sigma\upsilon\gamma_n\prod\nolimits_n = -\sigma\upsilon\gamma_n g_n(\gamma_1-\gamma_n)(\gamma_2-\gamma_n)...(\gamma_{n-1}-\gamma_n) < 0$$

$$Q(s=-\gamma_{n-1}) = -\sigma\upsilon\gamma_{n-1}g_{n-1}\prod\nolimits_{n-1} = -\sigma\upsilon\gamma_{n-1}g_{n-1}(\gamma_1-\gamma_{n-1})(\gamma_2-\gamma_{n-1})...(\gamma_{n-2}-\gamma_{n-1})(\gamma_n-\gamma_{n-1}) > 0$$

.

.

.

$$Q(s=-\gamma_1) = -\sigma\upsilon\gamma_1 g_1\prod\nolimits_1 = -\sigma\upsilon\gamma_1 g_1(\gamma_2-\gamma_1)(\gamma_3-\gamma_1)...(\gamma_n-\gamma_1) \quad \begin{cases} > 0, & n = 2k \\ < 0, & n = 2k+1 \end{cases}$$

$$Q(s=-\infty) \quad \begin{cases} < 0, & n = 2k \\ > 0, & n = 2k+1 \end{cases}$$

The polynomial $Q(s)$ alternates its sign at the points $s = 0, -\gamma_n, -\gamma_{n-1}, ..., -\gamma_1$, and between γ_1 and infinity there is another root. As far as $Q(s)$ is of order *n+1* (for *n* discrete levels) and the above procedure finds *n+1* real and distinct roots, this ensures that between two successive points (γ_i, γ_{i-1}) there is only one zero. All roots α_i are negative. In the case with no recombination ($1/\tau_f = 0$) one of the roots is zero. Essentially the same result was also obtained by Schmidlin (1977) and Noolandi (1977) in the case of discrete distribution of traps. Another interesting fact in our computation, in Schmidlin's, and in Noolandi's work, is that all coefficients A_i are found to be positive, and $\sum_i A_i = 1$. Also, our results are consistent with Schmidlin's finding that the current transients in any real situation can be analysed in terms of relatively few discrete traps, meaning that only a few of given set of A_i and alphas, α_i, $i = 1,...,n+1$ contribute to the TPC I-t curve.

1.4.1.3 Energy resolution of the *ELT* method

In order to test the resolution of the *ELT* method first a hypothetical sample with two discrete levels placed only 4 meV apart (slightly less than $kT/6$ at 300 K) was considered. The photocurrent *I-t* data (solid line in fig. 1.10) were simulated using the polynomial approach, assuming an 'experimental' temperature $T = 300K$, free carrier recombination lifetime $\tau_f = 10^{-6}s$, attempt-to-escape frequency $\nu = 10^{12}s^{-1}$, and capture coefficient $\sigma\upsilon = 10^{-8}cm^{-3}s^{-1}$.

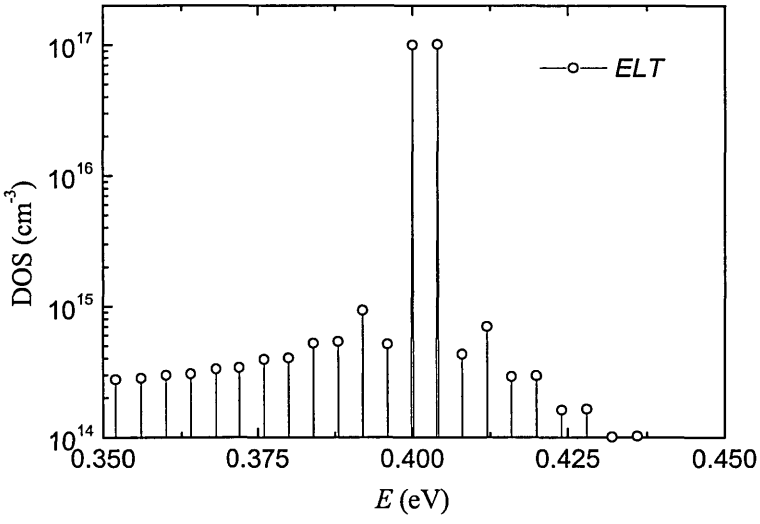

Figure 1.9 *Two discrete levels 4 meV apart. The DOS is recovered from the computer-generated $I(t)$ data (solid line) in figure 1.10.*

Figure 1.9 shows that in the ideal case of noise-free current-time data the *ELT* method can recover two discrete levels positioned less than $kT/6$ apart. The 'background noise', which is three or more orders of magnitude lower than the amplitudes of the discrete levels, is due to the computation (non zero solutions of the MT system of equations in the chosen energy interval). The resolution of *4 meV* is the finest resolution available. All other (known to us) methods would 'see' these two discrete levels as one level from which the dashed line in figure 1.10 is obtained.

Although not visible on this scale, the energy positions are recovered to an accuracy of typically $0.001\,eV$, and the broadening of typically 2-3 kT that accompanies the approximate methods (cf. Approximate methods, and Main C. *et al*, 1992; N. Ogawa *et al*, 2000) is absent.

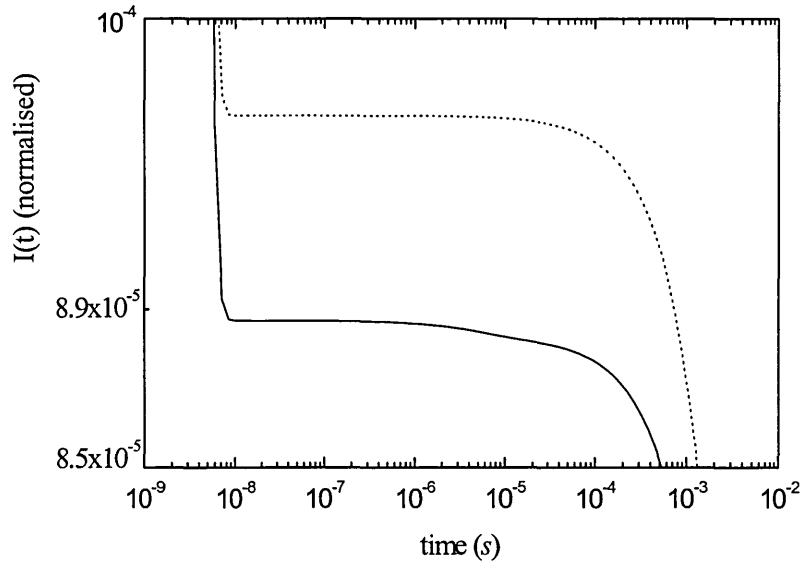

Figure 1.10 *$I(t)$ data simulated from two discrete levels of equal density ($1x10^{17}$ cm^{-3}), 4 meV apart (solid line), and $I(t)$ data simulated from one discrete level of double density ($2x10^{17}$ cm^{-3}) positioned at 0.4 eV below the band edge (dashed line). In the simulation T=300K and $\tau_f = 10^{-6}$ s were used.*

In figure 1.11 *I-t* data simulated from two discrete levels of equal density ($1x10^{17}$ cm^{-3}) positioned 10 *meV* apart (solid line) is shown. The method is capable of resolving both levels at their right positions and with right amplitudes. The sensitivity of the method is further demonstrated by simulation of two sets of *I-t* data from one level of double density placed at 0.4 and 0.41 *eV* respectively. The difference in the amplitudes of the two plateaus in *I-t* data is less that an order of magnitude but the method resolves the originating DOS (figures 1.12 a, 1.12 b and 1.12 c) accurately.

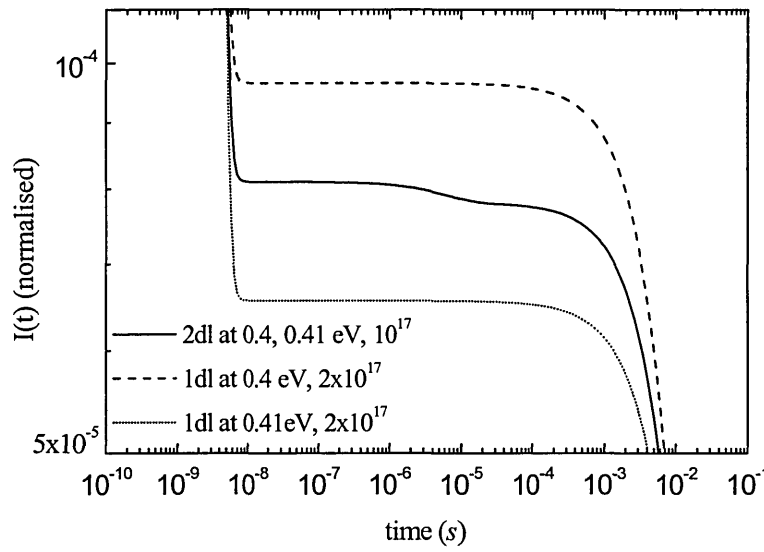

Figure 1.11 *$I(t)$ data simulated from <u>two</u> discrete levels of equal density ($1x10^{17}$ cm^{-3}) 10 meV apart (solid line). The dashed and dotted lines represent $I(t)$ data simulated from <u>one</u> discrete level of double density ($2x10^{17}$ cm^{-3}) positioned at 0.4 and 0.41 eV respectively. (In the simulation T=300K and $\tau_f = 10^{-6}$ s were used)*

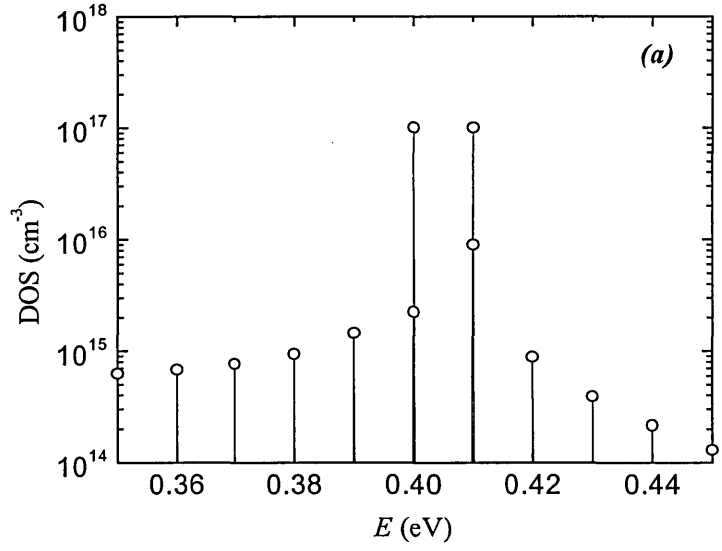

Figure 1.12 (a) *DOS recovered from the solid curve in figure 1.11. In the calculation T=300K and $\tau_f = 10^{-6}$ s were used.*

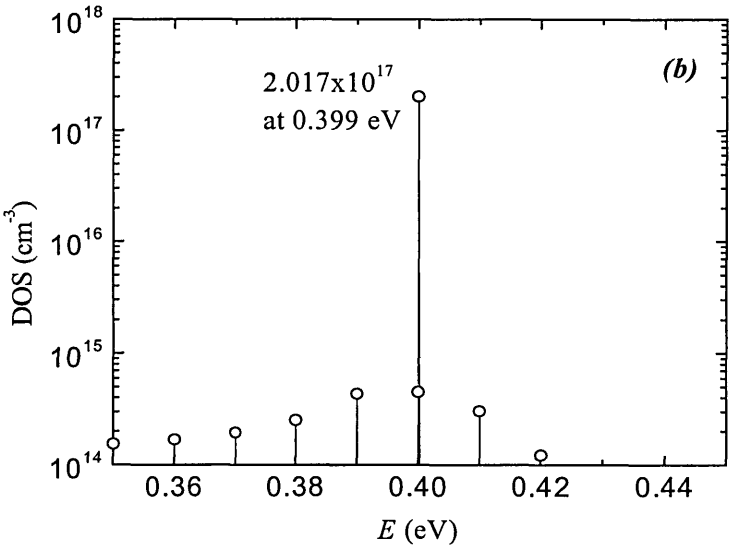

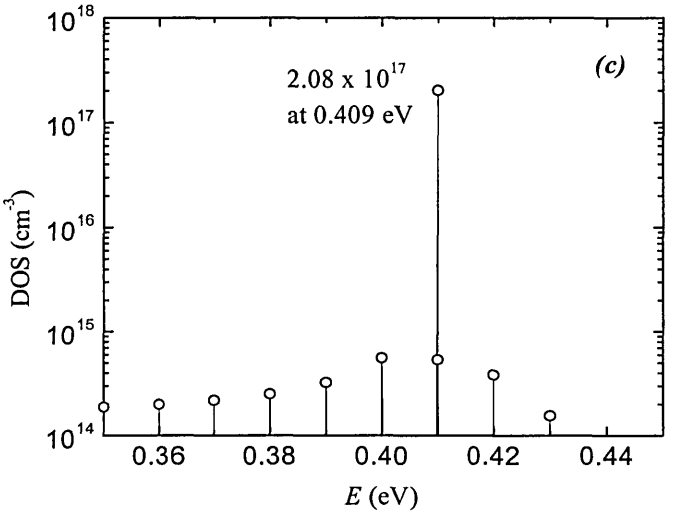

Figures 1.12 (b) and 1.12 (c). *DOS recovered from the dashed and dotted curves in figure 1.11. In the calculation T=300K and* $\tau_f = 10^{-6}$ *s were used.*

Second, the recovery of a range of exponential DOS distributions $g(E) = g_0 \exp(-E/kT_0)$, where E is the energy relative to the band edge and T_0 is the characteristic tail slope, from simulated $I(t)$ data is illustrated in figure 1.13 (Gueorguieva M. J. *et al*, 2000a). It can be seen that the recovered DOS (symbols) is an accurate representation of the original DOS for T_0 both above and below the 'experimental' temperature T. This represents a significant improvement in resolution over approximate LT methods which can introduce serious errors as T_0 approaches T, and offers a performance as good as that obtained using *Tikhonov* regularization (Nagase T., *et al* 1999), when operating on simulated data.

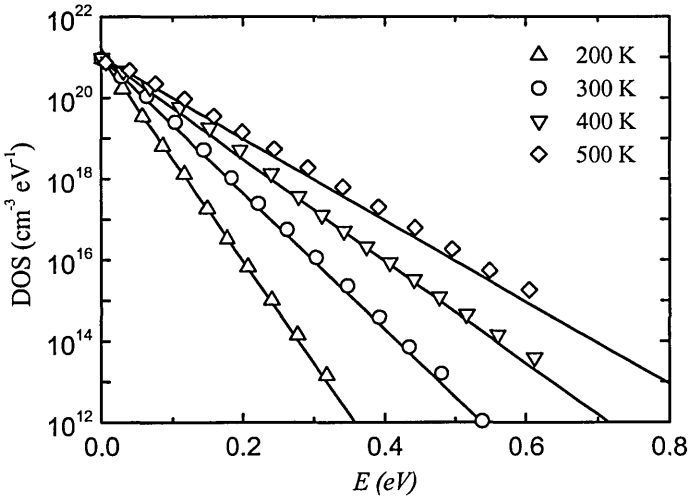

Figure 1.13 *Recovery of exponential distributions of states simulated with tail slope parameters T_0 = 200, 300, 400, 500 K. Solid lines indicate the model DOS distribution.*

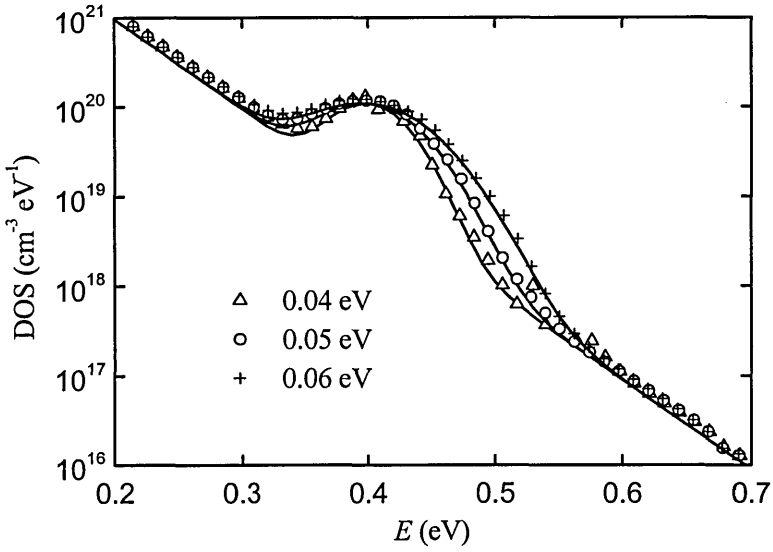

Figure 1.14 *Recovery of exponential plus Gaussian distributions using ELT method: T_0 = 500 K, $g_{G0} = 10^{21} cm^{-3} eV^{-1}$, $E_0 = 0.4eV$, E_W = 0.04, 0.05, 0.06 eV. Solid lines indicate model DOS distributions.*

In figure 1.14, a *Gaussian* distribution $g_G(E) = g_{G0} \exp\{-[(E - E_G)/E_W]^2\}$, where g_{G0}, E_G and E_W are the peak density, peak position relative to the mobility edge and width respectively, has been added to an exponential tail. The method is seen to recover the originating distributions accurately.

1.4.1.4 Determination of free carrier recombination lifetime in amorphous and crystalline materials assuming the MT mechanism as a physical model for transport

Since the determination of the free carrier recombination lifetime τ_f is of fundamental importance to the understanding of the nature of recombination centers in amorphous semiconductors, it is desirable to have a reliable way of estimating τ_f.

In the course of this work the *ELT* method along with the developed polynomial approach of simulation of current transients were used to obtain an estimate for the free carrier recombination lifetime in amorphous and crystalline materials. The approach is not new and in general is a fitting procedure. It has been used by the Osaka group (Nagase T., H. Naito, (1998)) to determine τ_f in arsenic triselenide ($a-As_2Se_3$). They make use of the approximate *LT* method to obtain density of localized states distribution from a given set of experimental photocurrent data. After that the obtained DOS is used to back-simulate $I(t)$ data solving the original system of MT equations with a chosen value for τ_f. The free carrier recombination lifetime is varied until a good fit is obtained.

In our approach:

i First, using the *ELT* method with a given current-time data set a unique solution for the localized state distribution is obtained.

ii Second, using the polynomial approach, computer-generated current-time transients related to the already found DOS are fitted to the experimentally obtained photocurrent traces. By varying τ_f the best fit is obtained, and the corresponding value for τ_f is considered to be the most plausible.

This procedure has been applied for investigation of the properties of crystalline materials (single crystal *Tin*-doped *CdTe*) (Gueorguieva M. J. *et al*, 2002), and also light-soaked PECVD amorphous hydrogenated silicon (Gueorguieva M. J. *et al*, 2001). The results from the light-soaked material are consistent with the understanding that the free carrier recombination lifetime is inversely proportional to the density of recombination centers.

Sensitivity of the Polynomial approach in determination of free carrier recombination lifetime.

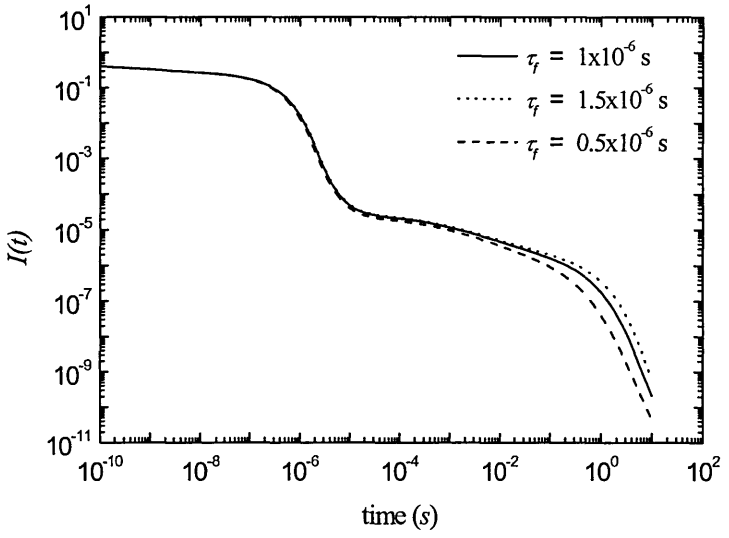

Figure 1.15 *Computer-generated* $I(t)$ *data produced with different values for the free carrier recombination lifetime* τ_f.

Figure 1.15 is an illustration of the fact that even a very small change in τ_f ($0.5\text{x}10^{-6}$) reflects in quite a big difference in the simulated current-time data. The values of τ_f in figure 1.15 have been chosen only for illustration and they are not the limit of the sensitivity of the polynomial approach.

1.4.2 Regularization methods

1.4.2.1 General definition of Direct and Inverse problems

Two problems are *inverse* to each other if the formulation of each of them requires full or partial knowledge of the other (Kirsch A.,1996). From this definition follows that it is quite arbitrary which of the two problems is called a direct and which is called an inverse problem. Often one of the problems has been studied earlier and, perhaps, in more detail. This one is usually called the *direct* problem, whereas the other is the *inverse* problem.

The solution of a *direct* problem involves finding effects based on a complete description of their causes. In contrast, finding a solution of an *inverse* problem entails determining unknown causes based on observation of their effects. In other words the *direct* problem can be formulated as the evaluation of an operator K acting on a known 'model' x in a model space X. The inverse problem then is the solution of the equation $K(x) = y$.

Direct problem: given x and K, evaluate $K(x)$.

Inverse problem: given y and K, solve for x.

In order to formulate an *inverse* problem, the definition of the operator K, including its domain and range, has to be given. *An Introduction to the Mathematical Theory of Inverse Problems* by Kirsch contains many references concerning the philosophy and the theory of ill-posed problems.

From the above general definition is obvious that there is a fundamental difference between a *direct* and an *inverse* problem. In most of the cases with practical importance the *inverse* problem *is* '*ill-pose*d' or *improperly posed* (in the sense of Hadamard) while the direct problem is '*well-posed*'.

1.4.2.2 General definition of ill-posed problem

Hadamard (Hadamard J., 1923; Kirsch A., 1996), introduced the concept of a *well-posed* problem, originating from the philosophy that any mathematical model of a physical problem has to have the following three properties:

1. There exists a solution of the problem (Existence).
2. There is at most one solution of the problem (Uniqueness).

3. The solution depends continuously[6] on the data (Stability).

If at least one of these three properties fails to hold the problem is called '*ill-posed*' in the sense of Hadamard. Conditions 1 and 2 are equivalent to saying that the operator K has a well-defined inverse K^{-1} and that the domain of K^{-1} is all of data space. In many cases the problem is not whether a solution exists, but that there is more than one solution. If there is more than one solution, then information about the problem described by a particular model is missing. In this case additional, in most cases *a priori*, information has to be introduced in the model. ("A lack of information cannot be remedied by any mathematical trickery", Kirsch A., 1996).

The requirement for stability is the most important one. If the solution of a problem does not depend continuously on the data, then in general the computed solution has nothing to do with the 'true' solution. The continuous dependence of the solution image on the data is a necessary but not sufficient condition for the stability of the solution. There are mainly two reasons. Firstly, in practice, only a finite number of data values can be measured, hence a continuum problem is always an idealization of an actual problem. Secondly, it is impossible to make 'exact' measurement and the data are always 'corrupted'. The difference between the 'ideal', error-free data and the measured data is called *noise*.

The stability with respect to perturbations in the right-hand side y of the solution x of the problem $K(x) = y$ can be quantified in terms of the *condition number*[7] of the model matrix K (Groetsch C. W., 1984; Öztürk F. and F. Akdeniz, 2000).

$$\|\Delta x\| . \|x\|^{-1} \leq cond(K) \|\Delta y\| . \|y\|^{-1}$$

Δy is a variation of y and Δx is the corresponding variation of x. The *condition number* $cond(K)$ for linear forward problem is defined as: $cond(K) = \|K\| . \|K^{-1}\|$, where $\| \ \|$ is the norm of a linear operator (or transformation). The *condition number* therefore gives an upper bound for the relative error in the solution caused by a given relative error in the right-hand side (Kirsch A., 1996). It gives an idea to what extent relatively small errors in y can lead to

---

[6] A function $f(z)$ is said to be *continuous* at z_0 if, given any $\varepsilon > 0$, there exists a $\delta > 0$ such that $|f(z) - f(z_0)| < \varepsilon$ whenever $|z - z_0| < \delta$. (Spiegel M. R., 1965)

[7] Any matrix $\mathbf{m}$ can be written in the form $\mathbf{u}^T \mathbf{m}_D \mathbf{v}$, where $\mathbf{m}_D$ is a diagonal matrix with elements known as *singular values*, and $\mathbf{u}$ and $\mathbf{v}$ are row orthonormal matrices. The ratio of the largest singular value of a matrix to the smallest one gives the *condition number* of the matrix. A system is said to be *singular* if the condition number is infinite, and *ill-conditioned* if it is too large. (Wolfram S., 1991)

relatively large changes in the solution $\underline{x}$. From the above relation is obvious that small values of $cond(K)$ are desirable. If $cond(K)$ is not too large, the problem is said to be *well-conditioned* and the solution is stable with respect to small variations of the data. Otherwise the problem is said to be *ill-conditioned.*

So-called *regularization techniques* are needed to obtain meaningful solution estimates for such *ill-posed* problems. Regularizing an inverse problem means restoring stability and constructing efficient numerical algorithms allowing a physically meaningful stable solution to be obtained.

The importance of solving inverse problems can be seen from the following incomplete list of applications: numerical differentiation of noisy data (perhaps the simplest known ill-posed problem), inverse *Laplace* transforms, image reconstruction, computer-based diagnostic imaging (e.g. computer assisted tomography (CAT)), indirect measurements and nondestructive testing, seismic analysis, calculation of relaxation spectra.

Regularization = Stabilization

In general, *regularization* or *stabilization* of solution to inverse problems involves a 'trade-off' between the 'size' of the regularized solution and the quality of the fit that it provides to a given data set. The 'size' of the regularized solution could be measured by the norm of the regularized solution, while the quality of the fit is measured by the norm of the residual vector (discrepancy term). What distinguishes the various regularization methods is how they measure these quantities, and how they decide on the optimal trade-off between the two quantities.
The regularization parameter α could be chosen using *a priori* or *a posteriori* (during the process of computing the regularized solution) information.

1.4.2.3 Tikhonov Regularization method

Many inverse problems can be formulated as operator equations of the form $Kf = g$, where f and g are functions and K is an integral operator.
Tikhonov (Tikhonov A. N., 1963) arrived to the following solution for the unknown function f, where λ is a regularization parameter and $R(f)$ is a particular functional[8]:

$$f_\lambda = \min\left\{\|Kf - g\|_2 + \lambda^2 \|R(f)\|_2\right\} \tag{1.13}$$

[8] **Theorem**: Let $K: X \to Y$ be a linear and bounded operator and $\alpha > 0$. Then the *Tikhonov functional*: $J_\alpha(x) := \|Kx - y\|_2 + \alpha\|x\|_2$ has a unique minimum $x^\alpha \in X$. (Kirsch A., 1996)

The sign $\|x\|_2$ stands for the *2*- norm[9] of a vector x.

Often the functional $R(f)$ is written as: $R(f) = \|\mathbf{L}f\|_2$ where L could be (i) an identity operator, (ii) first or (iii) second derivative of the regularized solution f. The first case, $\mathrm{L} = I$ (I - identity operator). The case, $\mathrm{L} = f'$ (first derivative of the regularized solution), corresponds to an imposed requirement for *maximum flatness* of the solution, and the third case, $\mathrm{L} = f''$ (second derivative of the regularized solution), means that a requirement for *minimum roughness* has been imposed.

i. The first term in the Tikhonov's original formulation is a 'discrepancy' term, the *2*-norm of the vector, which measures the agreement of a model to the data. Minimizing only this term is equivalent to the classical χ^2 problem. The agreement can be very good but the solution becomes unstable, widely oscillating, or in other ways unrealistic, reflecting the fact that the first term alone typically defines an ill-posed problem (Press W. H. *et al*, 1992).

ii. The second, regularization term measures the 'smoothness' of the desired solution. This term gives the 'size' of the regularized solution. Minimizing this term itself is supposed to give a solution that is 'smooth' or 'stable' or 'likely' but it has nothing at all to do with the measured data. The presence of this term could lead to a stable solution provided that the regularization parameter λ is properly chosen.

iii. The size of the regularization parameter λ is related to the degree of regularization imposed on the solution. A very small lambda ($\lambda \to 0$) would lead to the classical *least-squares* method. The fit will be good but the obtained solution will be dominated by contributions from the data errors, and consequently it will be highly unlikely that it will be close to the 'true' solution. On the other hand, too big value of the lambda would mean that too much regularization/stabilization has been imposed on the solution, and as a result it will not fit the given data properly leading to a too big discrepancy term. (Increasing λ makes the reconstruction smoother and the inversion more approximate.)

The regularization term has something to do with a priori expectation, or knowledge, of a solution, while the first (discrepancy) term has something to do with a posteriori knowledge. The regularization parameter λ gives the delicate compromise between the two.

---

[9] *Euclidean 2*-norm of a vector $x = (\xi_1,...,\xi_n)$ is defined as $\|x\|_n = \left(\sum_{i=1}^{n} \xi_i^2\right)^{1/2}$

In this work the proprietary subroutine FTIKREG (Weese J., 1992), based on the *Tikhonov* regularization method has been applied to computer-generated (with and without noise), and noisy experimental data in order to find the density of localized states distribution in amorphous and crystalline materials. The FTIKREG program and its non-linear version (NLREG, Weese J., 1993) as well as a user manual are available from the CPC Program Library, Queen's University of Belfast, N. Ireland.

The FTIKREG program

The following paragraph is a résumé of the FTIKREG user manual (Weese J. 1992, 1993) intending to give only an idea about problems to which the FTIKREG program could be applied, and about the way it has been used in this work.

First, the continuous problem (*Fredholm* integral equation of the first kind) is replaced by a linear algebra problem by discretization of the integral equation, this is known as *Discrete Tikhonov* regularization method. The FTIKREG program minimizes the following quantity:

$$V_\lambda(f) = \sum_{i=1}^{n} \frac{1}{\sigma_i^2} \left(g_i^\sigma - K(f)(t_i) + \sum_{j=1}^{m} a_j b_j(t_i) \right)^2 + \lambda R(f) \tag{1.14}$$

In the *Linear Tikhonov* method (FTIKREG program), $K(f)(t_i)$ is a *linear* integral operator of type:

$$K(f)(t) = \int_{s_{\min}}^{s_{\max}} K(t,s) f(s) ds \tag{1.15}$$

In the *non-linear* version of the method (NLREG program) (Weese J., 1993), the kernel function is a *non-linear* integral operator, two examples of which are:

$$K(f)(t) = \left(\int_{s_{\min}}^{s_{\max}} K(t,s) f(s) ds \right)^2 \tag{1.16}$$

$$K(f)(t) = \int_{s_{\min}}^{s_{\max}} K(t,s) e^{f(s)} ds \tag{1.17}$$

The kernel function $K(f)(t_i)$ depends on the experiment. The data g are usually taken at distinct values $t = t_i$, $i = 1,...,n$. This leads to a data set $\{g_i^\sigma;\ i = 1,...,n\}$ where the superscript

($^{\sigma}$) indicates that the data are affected by (relative/ absolute) errors of size σ_i. The problem of finding the function f is actually a problem of determining a vector $\vec{f}$ from the data $\{g_i^{\sigma};\ i=1,...,n\}$. In addition, provided that the functions $\{b_j(t_i);\ j=1,...,m\}$ are given, the programs give an estimate for the coefficients $\{a_i;\ i=1,...,m\}$. The regularization term $R(f)$ depends on the function f only, but not on the coefficients $\{a_i;\ i=1,...,m\}$.

According to the theory, the required 'unique' solution highly depends on the choice of the regularization parameter λ. This parameter has essentially the same meaning as the bandwidth of a filter for smoothing noisy data. If this parameter is too small, the result will show artefacts caused by the data errors. If this parameter is too large, the result will be over-smoothed. In order to obtain a reliable estimate for the regularization parameter λ, the FTIKREG and NLREG programs use a self-consistent method, developed by Honerkamp J., and J. Weese (1990), for calculation of the regularization parameter. This method, according to the authors, is a robust and reliable way of calculation of λ and accordingly, the regularization solutions do not (should not) differ too much with different sets of data when noise is present.

1.4.2.4 Tikhonov regularization in the context of TPC experiment

The starting point for the analysis of TPC current-time data by the *Tikhonov* regularization method is the *Fredholm* integral equation of the first kind arising from the MT system of differential equations (cf. MT model – formulation of the problem):

$$\frac{d}{ds}\left(\frac{2I(0)}{\hat{I}(s)}\right)-1=\int_0^{E_F}\sigma\upsilon g(E)\frac{\nu\exp(-E/kT)}{[s+\nu\exp(-E/kT)]^2}dE \tag{1.18}$$

The *Tikhonov* method minimizes the quantity:

$$V(\lambda)=\sum_{i=1}^{n}\frac{1}{\sigma_i^2}\left(c_i^{\sigma}-\int_0^{E_F}K(s,E)g(E)dE\right)^2+\lambda\|g(E)\|_2 \tag{1.19}$$

$c_i^{\sigma} = \frac{d}{ds}\left(\frac{2I(0)}{\hat{I}(s)}\right) - 1$ is found from the measured photocurrent, $K(s,E)$ is the kernel function in the *Fredholm* integral equation (1.18), $\|g(E)\|_2$ is the norm of the vector $\vec{g}$, and λ is the regularization parameter. The coefficients $\{a_i;\ i = 1,...,m\}$ have been set to be zeros.

According to the theory, with an appropriate value for the regularization parameter λ, the first (discrepancy) term on the right-hand side of (1.19) forces the result to be compatible with the experimental/simulated photocurrent data. The second (regularization) term imposes a requirement for smoothness on the obtained estimate for the vector $\vec{g}$. Furthermore, as far as the DOS distribution is known to be a positive quantity, a requirement for a positive regularized solution has been imposed.

Mathematically, the *TPC Tikhonov* method is clearly more complicated in comparison with the *post-transit* TOF *Tikhonov* case (cf. Chapter II).

i. The kernel function is more complicated, due to the more complicated physical model allowing trapping and release of carriers, while the post-transit case deals with extraction of trapped carriers only.
ii. The input data for the FTIKREG program are in the *Laplace* domain. This inevitably introduces an error caused by the finite set of data used in the *Laplace* transformation. This could give rise to correlated errors in the input data.

In the case of correlated errors in the 'final' (input) data c_i^{σ}, the equation (1.19) is not correct any more and a variant of it should be minimized by the *Tikhonov* method (T. Roths, private correspondence; Press W. H., *et al*, Numerical Recipes in FORTRAN, 1992), namely:

$$V(\lambda) = \sum_{i=1}^{n}\sum_{j=1}^{n}\left[c_i^{\sigma} - \int_0^{E_F} K(s_i,E)g(E)dE\right] C_{i,j}^{-1}\left[c_j^{\sigma} - \int_0^{E_F} K(s_j,E)g(E)dE\right] + \lambda\|g(E)\|_2 \quad (1.20)$$

$C_{i,j}^{-1}$ is the inverse of the covariance matrix $C_{i,j}$ given by:

$$C_{i,j} = \left\langle c_i^{\sigma} \cdot c_j^{\sigma} \right\rangle = \left\langle \left(\frac{d}{ds}\left(\frac{2I(0)}{\hat{I}(s_i)}\right) - 1\right) \cdot \left(\frac{d}{ds}\left(\frac{2I(0)}{\hat{I}(s_j)}\right) - 1\right) \right\rangle$$

The covariance matrix takes into account the correlations of the data errors. Only in case of not correlated errors the covariance matrix reduces to $C_{i,j} = \sigma_i^2 \delta_{i,j}$, with $\delta_{i,j}$ being the *Kronecker* delta which is 1 for $i = j$ and 0 for $i \neq j$ - accordingly $C_{i,j}^{-1}$ is σ_i^{-2} for $i = j$ and 0 for $i \neq j$. Hence, only then this equation reduces to equation (1.19).

A reliable computation in the case of correlated errors in the input data would require a change in the algorithm of the FTIKREG program. As far as this was physically impossible the following procedure for reconstructing 'ideal' from noisy photocurrent data has been adopted.

i. First, the *lmdif1* subroutine (Garbow B. S. *et al*, 1980) has been used to fit set of exponents $A_i \exp(\alpha_i t)$ to a given *I-t* data set.

ii. Second, the obtained coefficients (A_i, α_i), $i = 1,...,n$ have been used to reconstruct 'ideal' *I-t* data coinciding with the original photocurrent data, but with no noise included, and starting from times much shorter than the experimentally available (10^{-16} *s*).

iii. Third, *Laplace* transformation of these data is calculated according to the procedure explained in Appendix (A2).

In all our calculations an independent statistical errors model has been assumed.

1.4.2.5 Energy resolution of the *Tikhonov* method

As with the *ELT* method the *Tikhonov* regularization method is in theory capable of arbitrarily high resolution as no inherent mathematical approximations have been made. As a check on the operation of the *Tikhonov* method we have simulated the current decay, $I(t)$ in fig. 1.16, from two discrete levels (fig. 1.17) of equal density positioned at 0.60 and 0.61 eV. Then following appropriate *Laplace* transformation of the data the *Tikhonov* method was applied. The result from this calculation is shown in fig. 1.17. The *Tikhonov* method returns only two values that are significantly greater than zero, which correspond very closely in energy to the originating levels. Closer investigation reveals a small difference in energy, and a small inequality in the density, affecting the re-calculated TPC $I(t)_{Tikh}$ (symbols in figure 1.16).

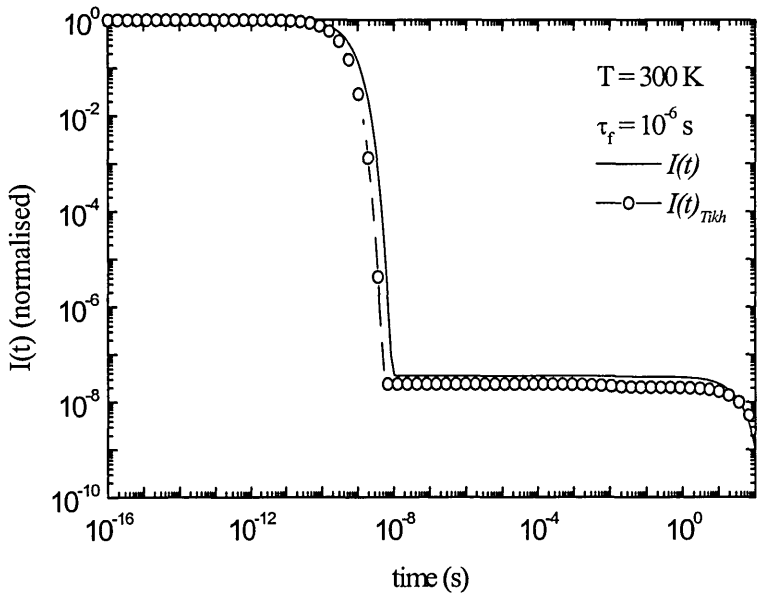

Figure 1.16 *TPC $I(t)$ corresponding to two discrete levels of density 10^{17} cm^{-3} positioned at 0.6 and 0.61 eV below the band edge. Symbols: re-simulated data from the recovered DOS in fig. 1.17.*

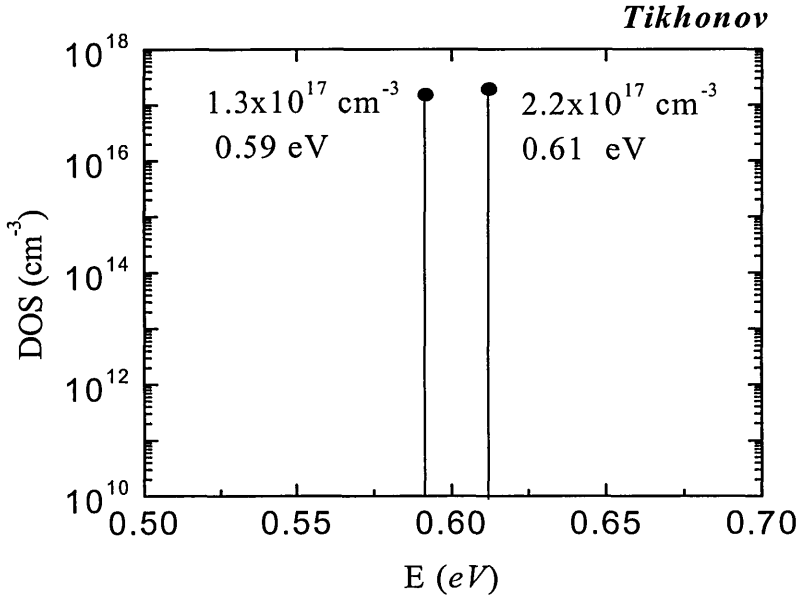

Figure 1.17 *Recovery of two discrete levels of density 10^{17} cm^{-3}, at 0.60 and 0.61 eV, using Tikhonov regularization method.*

The performance of the *Tikhonov* method has been further checked on a model DOS comprising an extensive exponential tail (fig. 1.18 and 1.19); and also an exponential tail plus *Gaussian* distributions with different widths (fig. 1.20 and fig. 1.21). The latter is a more realistic model for a disordered semiconductor.

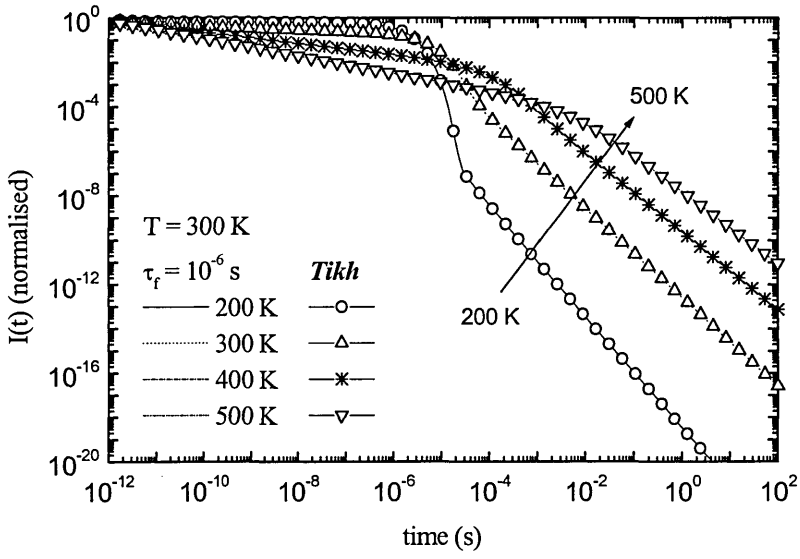

Figure 1.18 *TPC $I(t)$ transients computed for exponential localized state distributions with T_0=200 K, 300 K, 400 K, 500 K, and free carrier recombination lifetime $\tau_f = 10^{-6}$ s at T = 300 K. Symbols correspond to $I(t)$ simulated from the recovered DOS in figure 1.19.*

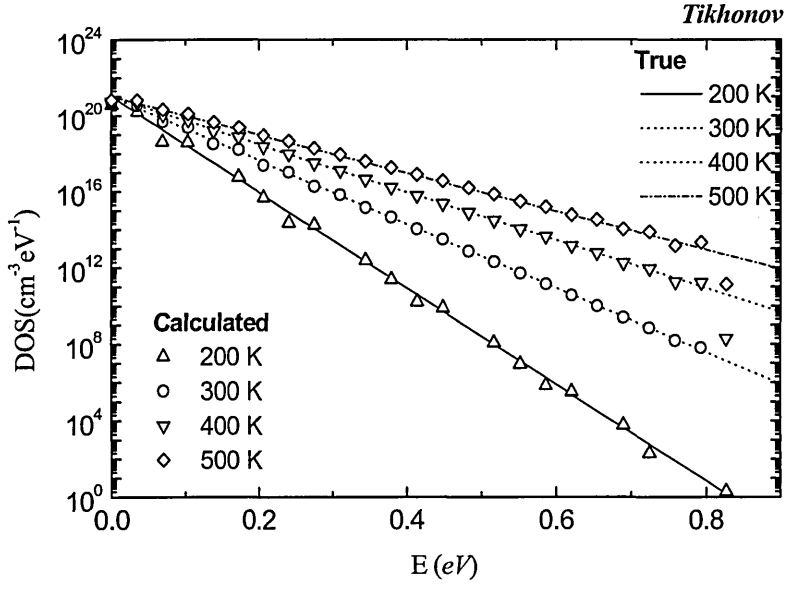

Figure 1.19 *Recovery of exponential distributions of states simulated with tail slope parameters T_0 = 200K, 300 K, 400 K, 500K from the current transients in figure 1.18. Lines indicate the model DOS distributions.*

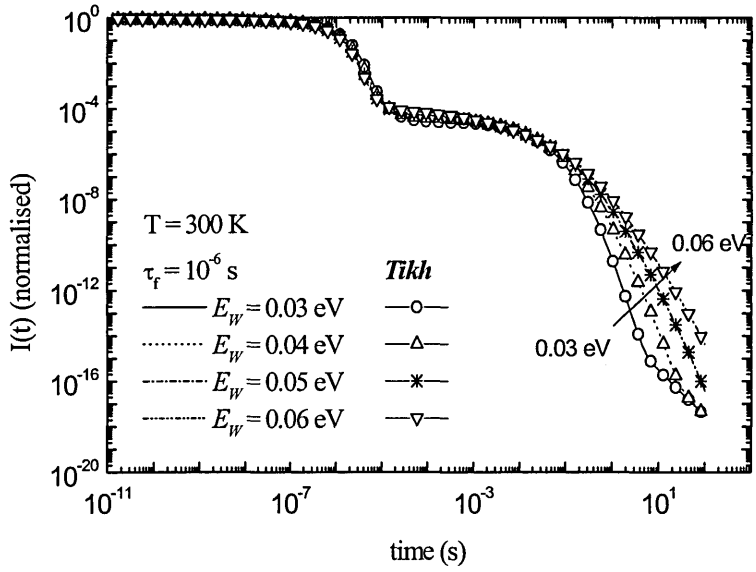

Figure 1.20 *TPC I(t) data simulated from exponential plus Gaussian distributions:* T_o = 300 K, $g_{Go} = 10^{16}$ cm^{-3} eV^{-1}, $E_0 = 0.6$ *eV*, E_W = 0.03, 0.04, 0.05 and 0.06 *eV*. *Symbols correspond to I(t) simulated from the recovered DOS in figure 1.21.*

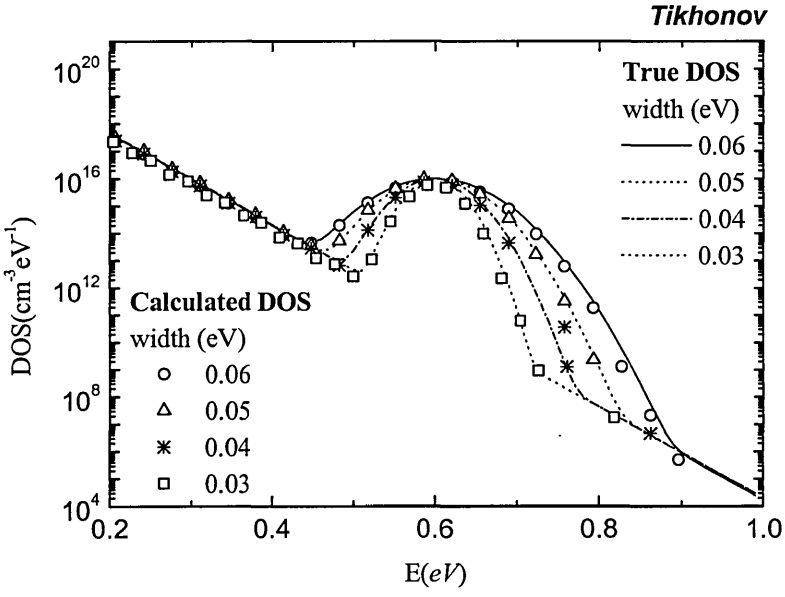

Figure 1.21 *Recovery of exponential plus Gaussian distributions from TPC data in figure 1.20 using the Tikhonov method.*

The above simulations show that the *Tikhonov* method is capable of resolving features in the DOS to an arbitrary narrow width, since no mathematical approximations are required. Simulation of the current-time curves from the recovered DOS yields excellent agreement in all considered cases with the originating (simulated) data.

1.4.3 Energy resolution of the approximate and exact methods - comparison

Amorphous semiconductors are expected to exhibit extensive, frequently exponential, DOS distributions (the 'band tails') associated with structural disorder, and broad local maxima associated with 'dangling bond' defects. Here, we have investigated the recovery of such features, and additionally discrete levels, by simulations of *I-t* data followed by use of all four methods, *LT*, *HLT*, *ELT* and *Tikhonov regularization* method.

Figure 1.22 illustrates the application of the above methods to recover the DOS from simulated *I-t* data for two closely spaced discrete levels, placed at 0.60 and 0.61 eV below the band edge. Although features as sharp as this are not anticipated to occur in disordered materials, the results show that the exact methods could be successfully applied to the study of crystalline semiconductors with specific defect levels (Gueorguieva M. J. *et al*, 2002).

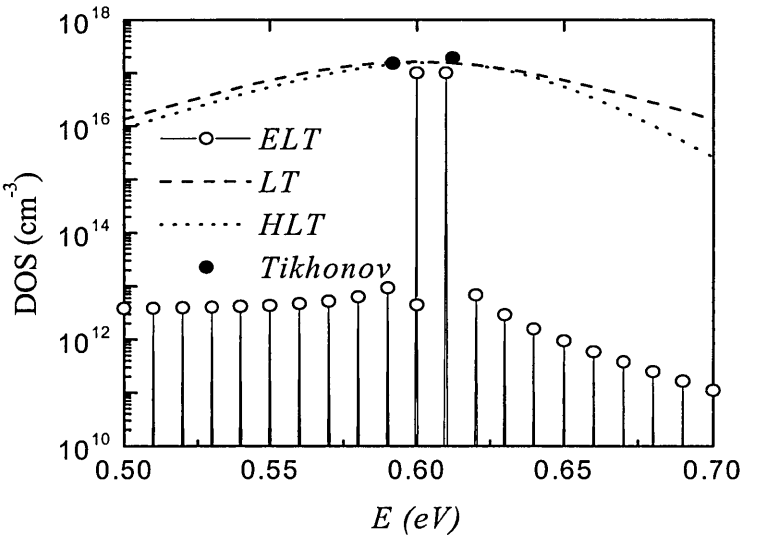

Figure 1.22 *Recovery of two discrete levels of density 10^{17} cm^{-3}, at 0.60 and 0.61 eV , using LT, HLT, ELT and Tikhonov methods.*

As it has already been shown (cf. *ELT* method) the *ELT* method has the finest known to us resolution of 4 meV. The *Tikhonov* method has a resolution approximately $kT/3 = 12\ meV$, and it recovers the two levels in Figure 1.22 but at slightly wrong positions (0.592 and 0.612 eV). The *LT* and *HLT* methods fail to recover two levels as has been expected, as they have resolution 93 meV (3.5 kT) and 78 meV (3 kT) respectively (cf. Approximate methods for solving the *Fredholm* integral equation of the 1st kind).

Figure 1.23 compares the methods in recovering the DOS from simulated *I-t* when the original distribution consists of an exponential band-tail, of characteristic energy 26 meV, and a *Gaussian* feature centered at 0.6 eV, with peak density $10^{16}\ cm^{-3}eV^{-1}$, and characteristic width 60 meV.

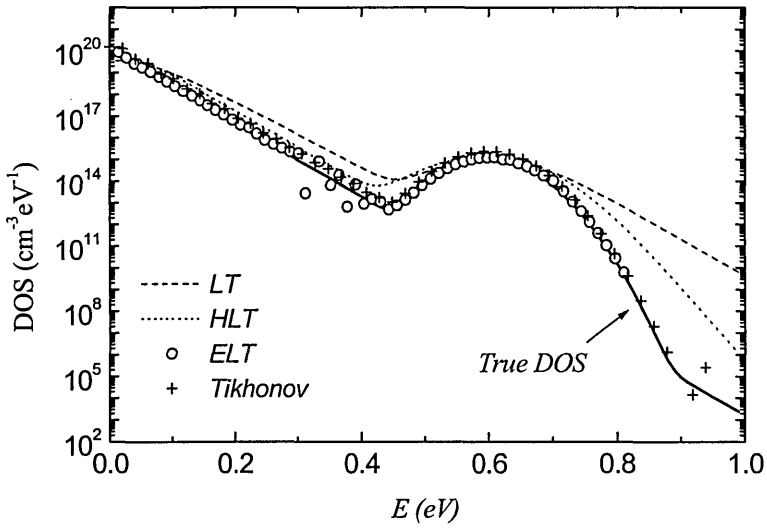

Figure 1.23 *Recovery of exponential plus Gaussian distributions:* $T_o = 300\ K$, $g_{Go} = 10^{16}\ cm^{-3}\ eV^{-1}$, $E_0 = 0.6\ eV$, $E_W = 0.06\ eV$ *using LT, HLT, ELT and Tikhonov methods.*

The approximate nature of the *LT* and *HLT* methods is the reason for the broadening effect observed in the recovered DOS profiles in figure 1.23. Although the position of the *Gaussian* feature is resolved properly by both approximate methods they fail to resolve the steeper parts correctly especially for energies deeper than 0.7 eV. In contrast, the *Tikhonov* and *ELT* methods provide excellent recovery, particularly in regions where the distribution is steep.

As a further check on the accuracy of the approximate and exact methods the current transients corresponding to the recovered DOS in fig. 1.23 are simulated and shown in figure 1.24. The result is a good illustration of the fact that the approximate methods (*LT* and *HLT*) are incapable

of recovering the 'true' DOS distribution even when applied to 'ideal' computer-generated data. On the other hand the *Tikhonov* and *ELT* methods, being exact, produce the closest fit to the original *I-t* data, suggesting that they could be used to obtain information on the recombination lifetime (cf. Determination of the free carrier recombination lifetime in amorphous and crystalline semiconductors).

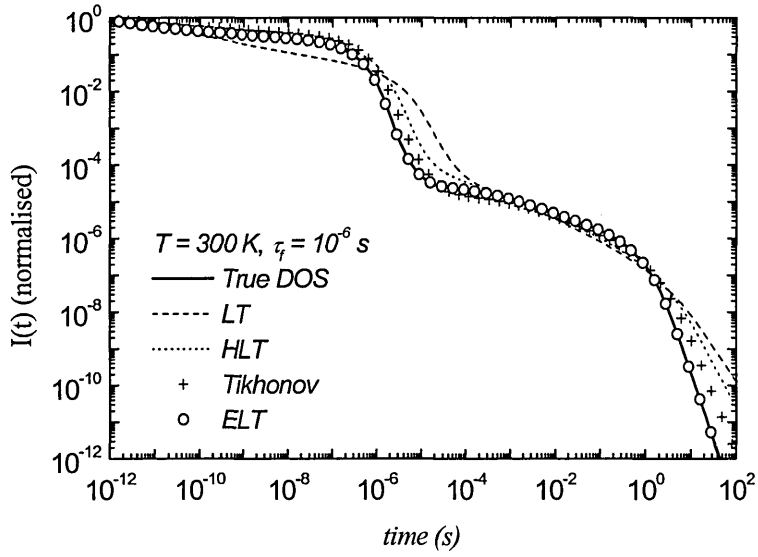

Figure 1.24 *$I(t)$ data simulated from the DOS in figure 1.23. In the simulation $T = 300K$ and $\tau_f = 10^{-6} s$ were used.*

While the recovered DOS (fig. 1.23) and the re-calculated current transients (fig. 1.24) are just what should be expected for the performance of the approximate and mathematically exact methods, a note should be made that a close fit to the original *I-t* data is a necessary but not sufficient requirement for uniqueness of the solution for DOS. Our calculations, Schmidlin's work (1977), and also Lakin *et al*, (1977) have shown that any real situation can be adequately analysed in terms of relatively few discrete traps characterized with their emission and capture properties. On the other hand, as we realise that we do not have any other objective way of determining the most plausible DOS rather than closeness of the original and the simulated *I-t* curve, the above criterion has been used throughout this work for choosing the most reliable solution for DOS.

1.4.4 Effect of experimental noise and missing short-time data on recovery of the electronic density of states from TPC data

Effect of experimental noise on the TPC DOS

The performance of all four methods in the presence of noise has been studied by application to a computer generated current transients. Typically 200 $I(t)$ points were generated, and noise was introduced by multiplying each point by a random number from a Gaussian distribution. The standard deviation was varied between 1% and 20 %, spanning the range of noise amplitudes commonly observed.

Figure 1.25 is an illustration of the 'noisy' current transients used in the calculation below.

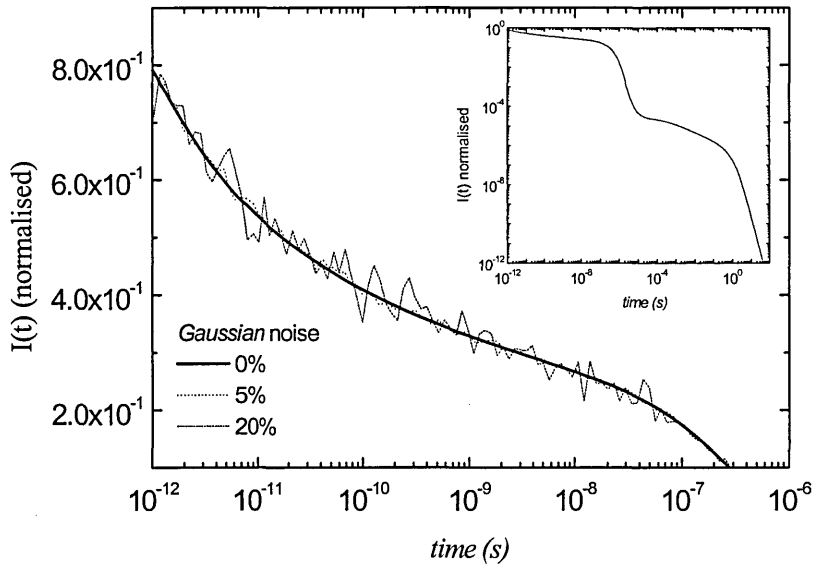

Figure 1.25 *TPC $I(t)$ computed for an exponential band tail and a Gaussian feature superimposed (parameters in the simulation: $T_0 = 300K$, $g_{Go} = 10^{16}\ cm^{-3}\ eV^{-1}$, $E_0 = 0.6\ eV$, $E_W = 0.06\ eV$). Gaussian noise up to 20 % has been introduced and its effect on the $I(t)$ data is shown in linear-log scale. The inset is a log-log graph of $I(t)$ over the whole time interval.*

Measurements on a range of disordered semiconductors indicate that noise (the random fluctuations, expressed as a fraction) in the experimental data is *Gaussian* with a standard

deviation of 5 %, across the entire time-span (Reynolds S. *et al*, 2001a). This confirms that practical DOS extraction methods are required to operate at noise levels of this order.

Exact methods

Tikhonov regularization method

As it has been already discussed, the *Tikhonov regularization* method is regarded as the best known to extract information from noisy experimental data. The method is well-suited to yielding an optimal DOS in the presence of noise as the solution obtained is a compromise between two important requirements; to match the 'true' and 'estimated' solutions and to achieve a smooth solution.

The effectiveness of the method is illustrated in figure 1.26. In the absence of noise, the recovered DOS corresponds very closely to the model DOS over the entire energy range. When Gaussian noise is introduced the features of the DOS remain, although artefacts appear as the solution is influenced somewhat by fluctuations in the data. This method gives a satisfactory reconstruction of the DOS at noise level even 20 %.

In all simulations in this section an exponential tail of 25 meV with a *Gaussian* feature ($E_G = 0.6\ eV$; $E_w = 0.06\ eV$; $g_G = 10^{16}\ cm^{-3}eV^{-1}$) superimposed has been used. All curves are offset for clarity.

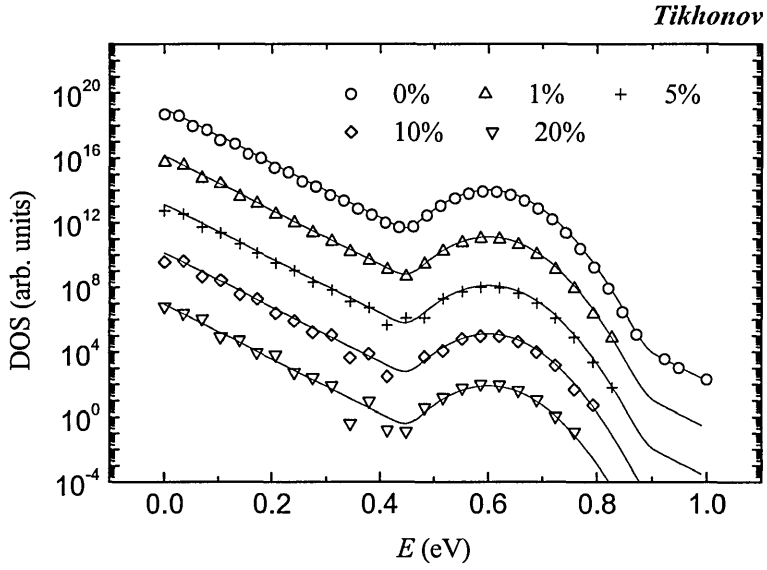

Figure 1.26 *Tikhonov regularization method used to recover DOS from simulated noisy data. Solid lines indicate the model DOS. The curves are offset for clarity.*

***Exact Laplace Transform (ELT)* method**

Since no mathematical approximations are employed, the *ELT* method is capable of extremely high theoretical resolution ($\sim kT/6$). As shown in figure 1.27, with zero noise the model DOS used here is accurately reproduced as far as 0.8 eV and the method functions reasonably well with 5 % noise added. However, the *ELT* method, as a mathematically exact procedure of obtaining an unique solution, is not as tolerant as the *Tikhonov* method to the presence of noise in the experimental data. The method gives no useful output at noise levels greater than 5 % unless the data are smoothed beforehand. We believe the smoothing procedure does not lead to loss of any physical information. In the calculation shown in figure 1.27, the *lmdif1* (Garbov B. S, 1980) subroutine was used to fit set of exponents to simulated noisy current-time data. Although the recovered DOS gets 'noisy' when increasing the random noise in the current-time data the tail and the *Gaussian* feature are recovered correctly.

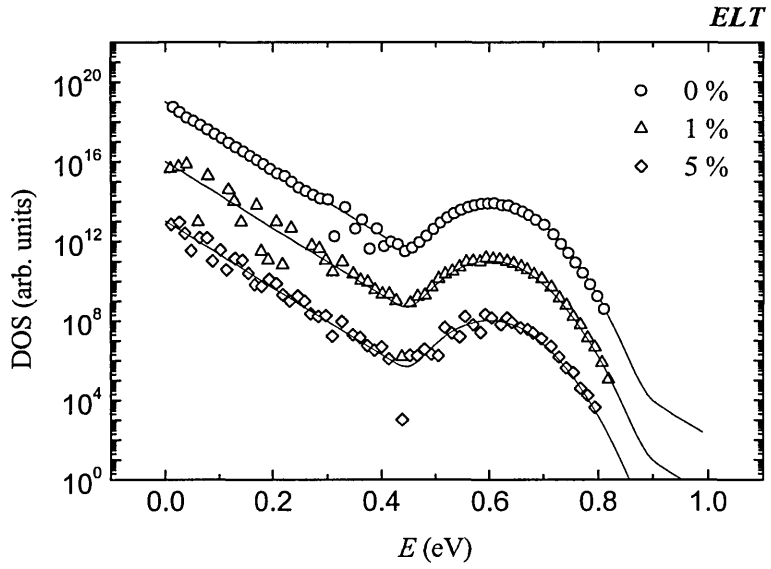

Figure 1.27 *ELT method used to recover DOS from simulated noisy data. Solid lines indicate the model DOS.*

Approximate methods

High resolution Laplace Transform (HLT) method

It is apparent from figures 1.28 and 1.29 that both approximate methods (*HLT* and *LT*) return DOS profiles that are relatively unaffected by a noise level of even 20 %.

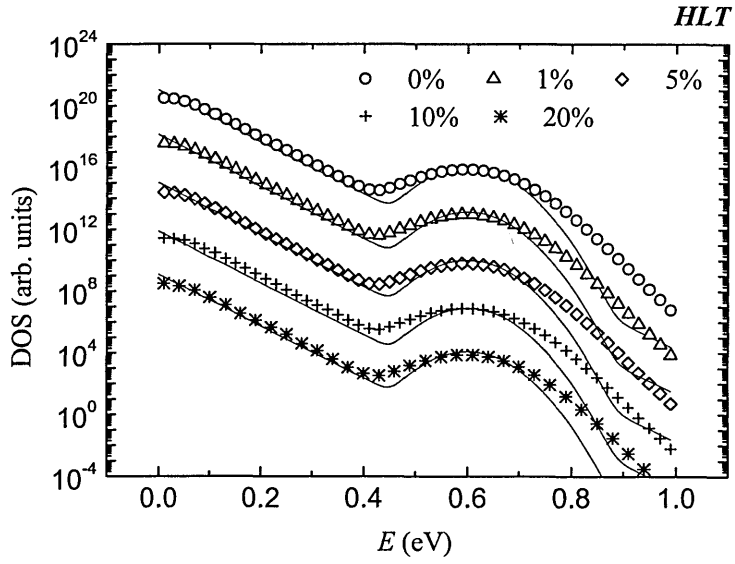

Figure 1.28 *HLT method used to recover DOS from simulated noisy data. Solid lines indicate the model DOS.*

Laplace transform (LT) method

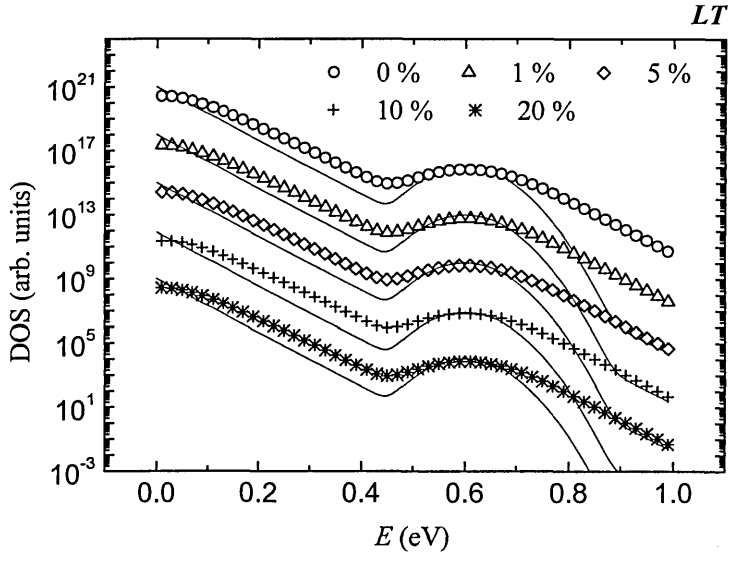

Figure 1.29 *LT method used to recover DOS from simulated noisy data. Solid lines indicate the model DOS.*

The finer resolution of the *HLT* method (in comparison with the *LT*) and the fact that the resolved DOS is virtually unaffected by the presence of noise in the experimental data makes it attractive when studying amorphous materials known to exhibit very broad and featureless distributions of states.

As was already mentioned, it is known and widely accepted that the random noise amplitude on a recorded photocurrent transient is typically 5% of the mean current at a given instant, and is approximately constant over the entire experimental time range. From the above calculations it is seen that this level of noise has a relatively small effect on the effectiveness of approximate DOS spectroscopies based on *Laplace* transform method, which can operate satisfactory with 20% noise. Mathematically the exact *ELT* method is more strongly affected by noise, and because of this the apparent benefits in resolution may not be achievable in practice. Solution techniques as *Tikhonov* regularization offer optimal resolution in a given noise context, and can recover a DOS with good resolution from a 20% noise background.

Effect of missing short-time data on recovery of the electronic density of states from TPC data

In figure 1.30 the simulated TPC $I(t)$ data from an exponential tail of $T_0 = 300K$ plus a *Gaussian* distribution with $g_{Go} = 10^{16}\ cm^{-3}\ eV^{-1}, E_0 = 0.6\ eV$, $E_W = 0.06\ eV$ is shown.

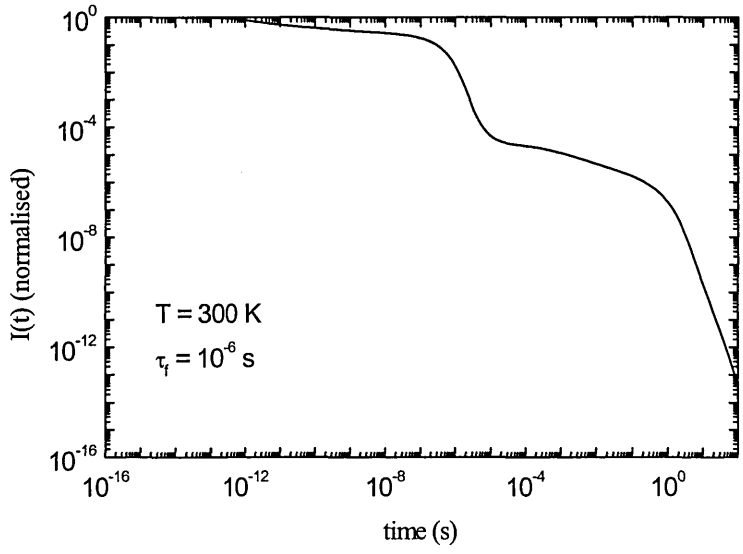

Figure 1.30 *TPC $I(t)$ computed for an exponential band tail and Gaussian feature superimposed. In the simulation $T_0 = 300K$, $g_{Go} = 10^{16}\ cm^{-3}\ eV^{-1}, E_0 = 0.6\ eV$, $E_W = 0.06\ eV$.*

The TPC data were analysed after successive removal of data points corresponding to short times (from 10^{-16} to 10^{-8} s). As far as our procedure of calculating the DOS from $I(t)$ involves *Laplace* transformation of the data, it is expected that the missing short-time data would result in considerable distortions in the recovered DOS. The reason being that the *Laplace* transformation has to be inferred from the whole time series of *I-t*. In figure 1.30 the effect of missing short-time data on $\hat{I}(s)$ is shown. It is obvious that any truncation of the transient *I-t* data gives rise to systematic errors of the calculated *Laplace* transform $\hat{I}(s)$ (figure 1.31) and accordingly, to *systematic errors* in the final (the transformed input data for FTIKREG program) data $c_i^{\sigma} = \frac{d}{ds}\left(\frac{2I(0)}{\hat{I}(s_i)}\right) - 1$.

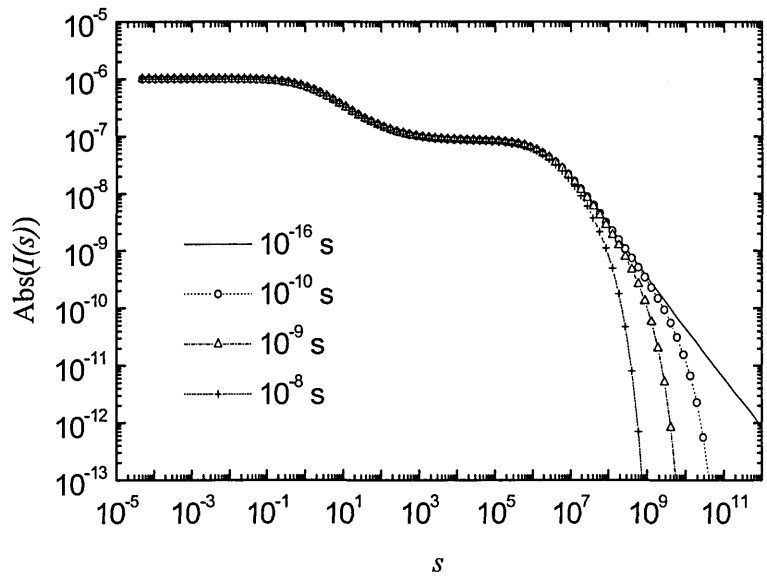

Figure 1.31 *Effect of missing short-time I-t data on the Laplace transformation* $\hat{I}(s)$.

This systematic error increases with increasing the argument s_i ($s_i \sim 1/t_i$). Furthermore, these systematic errors in the *Laplace* transform may give rise to correlations in the data after performing the numerical derivative, i.e. to correlations in $c_i^{\sigma} = \frac{d}{ds}\left(\frac{2I(0)}{\hat{I}(s_i)}\right) - 1$. If this occurs, the consequences will be artificial oscillations of the calculated DOS distribution (Roths T.,

private correspondence). This could be a possible explanation of the slightly 'noisy' DOS in figure 1.32.

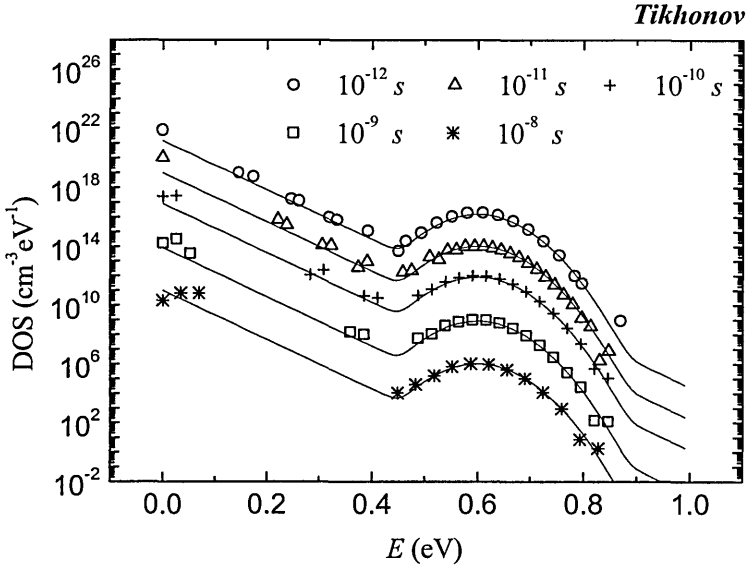

Figure 1.32 *Tikhonov regularization method used to recover DOS from truncated at different times I-t data. Solid lines indicate the model DOS.*

Another expected consequence of the truncation of the *I-t* data is the reduction of the accessible energy range, according to the relation $E = kT\ln(\nu t)$, as seen in figures 1.32, 1.33 and 1.34.

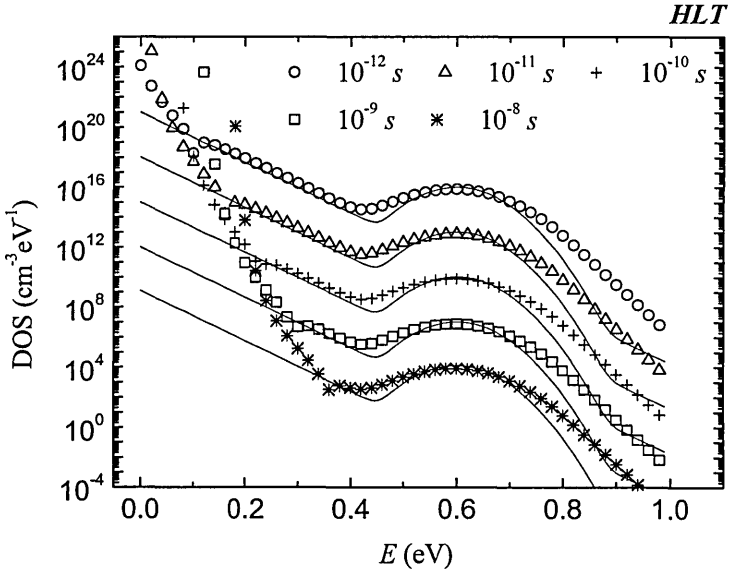

Figure 1.33 *HLT method used to recover DOS from truncated at different times I-t data. Solid lines indicate the model DOS.*

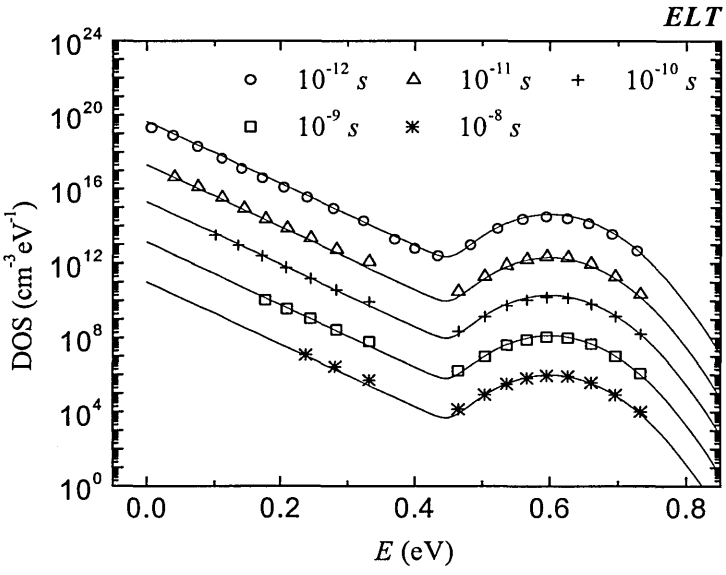

Figure 1.34 *ELT method used to recover DOS from truncated at different times I-t data. Solid lines indicate the model DOS. Curves are offset for clarity.*

Our simulations (fig. 1.32 – 1.34) show that the model DOS is recovered intact from the simulated data truncated up to 10^{-8} s. In the extreme case of truncation at 10^{-8} s the exponential tail, although consisting of only three points, is recovered with the right slope and the *Gaussian* feature is fully resolved. The missing points around 0.4 eV, in the *ELT* calculation, are due to a deficiency in our procedure of fitting exponents to *I-t* data, and are not a consequence of the truncation. If (for this particular model DOS) the *I-t* data up to 10^{-7} s are removed, the recovered DOS is a featureless exponent ('*' in figure 1.35).

Another effect of the truncation of the *I-t* data is the slight change in the amplitudes and positions of the recovered discrete values for DOS (figure 1.36) simply due to a 'wrong' *Laplace* transformation of the *I-t* data. The difference in the amplitudes for data truncated at 10^{-12} s and 10^{-8} s is less that one order of magnitude.

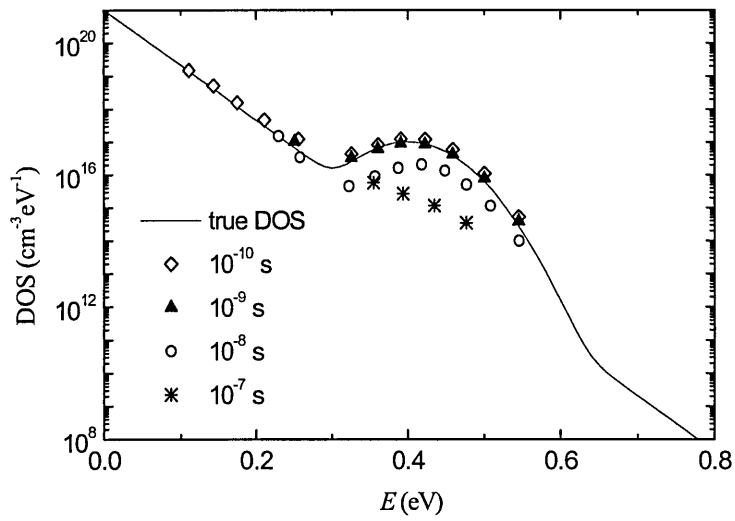

Figure 1.35 *DOS distributions recovered by ELT method from the TPC data in figure 1.30 after successive truncations of the short-time data. Curves are not offset. The inaccuracy in the recovered amplitudes is due to a 'wrong' Laplace transformation (figure 1.36).*

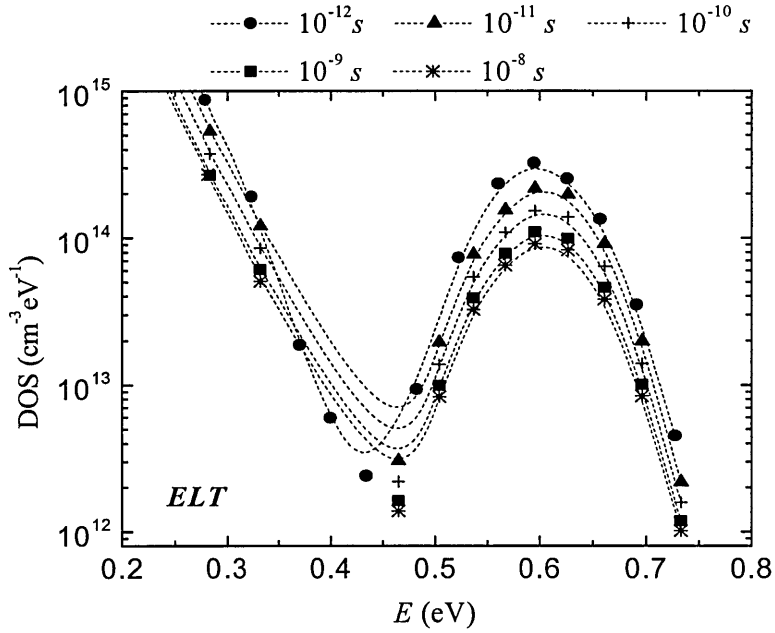

Figure 1.36 *The effect of truncation of the I-t data on the amplitudes and positions of the recovered discrete values for the DOS obtained using the ELT method. The curves are not offset. The slight difference in the overall shape is due to a 'wrong' Laplace transformation caused by missing short-time data.*

In general it could be concluded that missing short-time data would lead at least to 'truncation' and/or fluctuations in the recovered DOS. If in the TPC *I-t* data simulated from an exponential plus *Gaussian* distribution there is a steep descending section, then the recovered DOS profiles could be reduced to featureless exponential distributions, if the data from before the fall are removed, as figure 1.35 shows.

1.5 Application of the approximate and exact methods to experimental data obtained on amorphous and crystalline materials.

In this chapter we further assess the prospects for practical application of the existing approximate and exact methods for calculation of density of electronic states by analysing photocurrent transients obtained from a PECVD-prepared hydrogenated amorphous silicon film (Gueorguieva M. J. *et al*, 2001a) and from a single crystal tin-doped *CdTe* sample (Gueorguieva M. J. *et al*, 2002). As an amorphous material the $a-Si:H$ sample contains a broad distribution of tail and defect states, whereas the $CdTe:Sn$ sample would be expected to display sharper features associated with discrete defect levels. The choice of these two contrasting systems therefore allows a rigorous experimental comparison of these methods to be made.

1.5.1Exact methods - *ELT* and *Tikhonov regularization* methods

Light-induced meta-stable states in PECVD $a-Si:H$

PECVD $a-Si:H$ films typically 0.7 μm thick were prepared in a commercial reactor, and equipped with coplanar Al contacts to form a gap cell 5 mm in length with a separation of 0.4 mm. Light soaking was carried out by exposure to a simulated AM1 source.

The set of current-time decays obtained following progressive light soaking of $a-Si:H$ thin films is presented in figure 1.37, and the corresponding DOS distributions calculated using *ELT* and *Tikhonov* regularization methods are shown in figure 1.38. The DOS scaling is arbitrary, because parameters such as pre-trapping current, attempt-to-escape frequency and free carrier mobility are not known explicitly. Here, we have collectively scaled the family of plots to agree broadly with literature values for defect density of order 10^{16} cm^{-3} in annealed PECVD $a-Si:H$ (Carlson D. E., 1998). However, the scaling of the plots relative to one another is correct if it is assumed that the DOS alone is modified by light soaking.

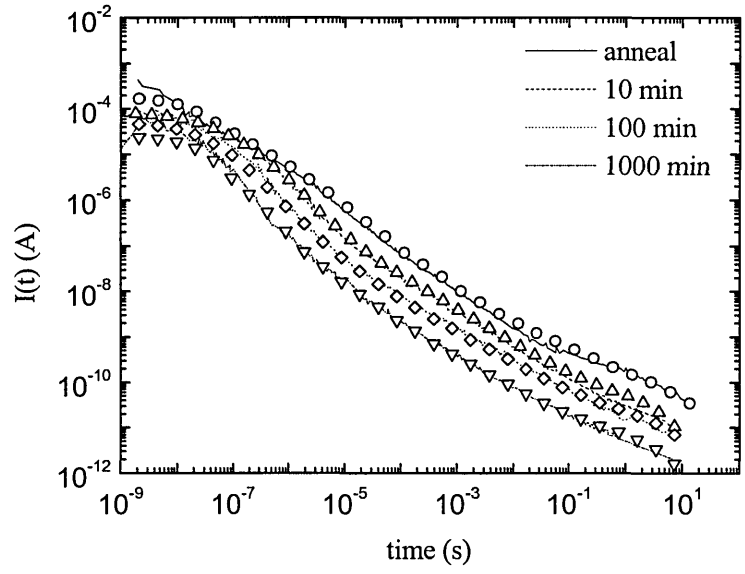

Figure 1.37 *Current-time decays at 300 K in PECVD $a-Si:H$ following progressive light-soaking (lines), and simulated TPC I(t) data using DOS obtained with ELT method (open symbols). Best fits to the experimental decays were obtained using τ_f = (10, 4, 3.5, 1.8) x 10^{-6} s for the annealed and progressively light soaked samples, respectively.*

In order to obtain a reasonably smooth DOS using the *ELT* method, the current decays required pre-filtering to reduce the effect of random noise (The *I-t* data were reconstructed using a set of exponents. The new *I-t* curve is noise free.). We believe this procedure does not significantly affect the physically important features of the decay, which in the case of $a-Si:H$ vary quite gradually with time.

As a check on the operation of the methods, we have simulated the current decay, using the polynomial approach, from each obtained DOS. The results are plotted in figure 1.37 using open symbols, alongside the experimental data. The free carrier recombination lifetime τ_f was varied to achieve an optimal fit to each current-time decay. This process thus yields additional information and, as expected, the values are found to decrease with increasing light soaking (Nagase T., 1998).

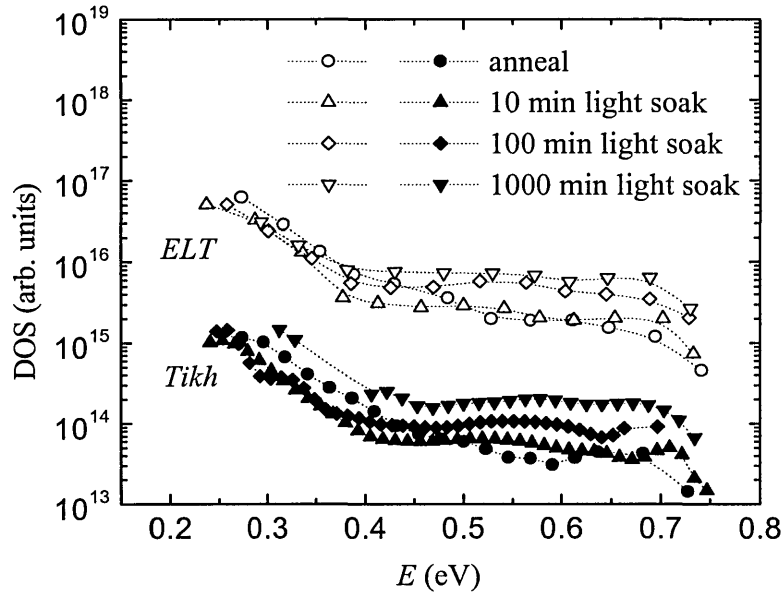

Figure 1.38 *DOS plots obtained using ELT and Tikhonov regularization methods for* $a-Si:H$. *Dashed lines are smooth curves illustrating the trend of the points. The ELT and Tikhonov DOS are offset for clarity.*

It is clear from figure 1.37 that a change in the shape of the current decay accompanies light soaking. Most prominent is the progressively more pronounced fall in current, commencing at times of the order of 10^{-7} s, due to electron trapping into metastable defects. The effect on the DOS revealed in figure 1.38 is an increase in the defect 'plateau' density by a factor of 5-10, with no clear systematic change in the distribution of shallower (tail) states. We do not detect an increase in a specific defect band with either method. However, since the decays simulated from the DOS curves are a good fit to the experimental data we would argue this interpretation is self-consistent.

Figure 1.38 also demonstrates that the *ELT* and *Tikhonov* regularization methods give essentially equivalent performance when applied to TPC data obtained from $a-Si:H$. This may be anticipated since we expect a fairly broad and extensive distribution of states in amorphous materials, and thus the potential benefits of the methods, particularly the resolution of sharp features of which such methods are capable, are not being exploited.

The *Tikhonov* method occasionally returns a rather sparse DOS. For example in the plot obtained following 1000 min light-soaking the DOS is essentially zero between 0.32 and 0.40 eV. However, a simulation based on this DOS is found to give as good a fit to the experimental current decay as the other (less sparse) data sets. Thus the dashed line connecting the points is added simply to indicate the assumed DOS profile based on physical plausibility rather than on mathematical accuracy. When applying the *Tikhonov* method it was not found necessary to

smooth the current-time data beforehand. This might prove advantageous in cases where signal to noise ratio is poorer, *e.g.* where low optical excitation is necessary to avoid saturation of the low density of deep states in high quality $a-Si:H$ (Reynolds S., *et al*, 2000).

'Discrete' levels in single crystal *Tin*-doped *CdTe*.

The $CdTe:Sn$ single crystal of [100] orientation was grown by the Bridgman method. A sample of size of 1 cm x 1 cm x 1.55 mm thickness was used for electrical measurements. Conductive paint contacts were applied to produce a gap cell approximately 5 mm in length with a 1 mm gap.

TPC decays obtained for the tin-doped *CdTe* sample at three different temperatures are shown in figure 1.39, and the corresponding DOS versus energy plots are given in figures 1.40 and 1.41. The simulated current decays are shown as open symbols on figure 1.39. Temperature dependencies of capture properties and carrier mobility have not been taken into account.

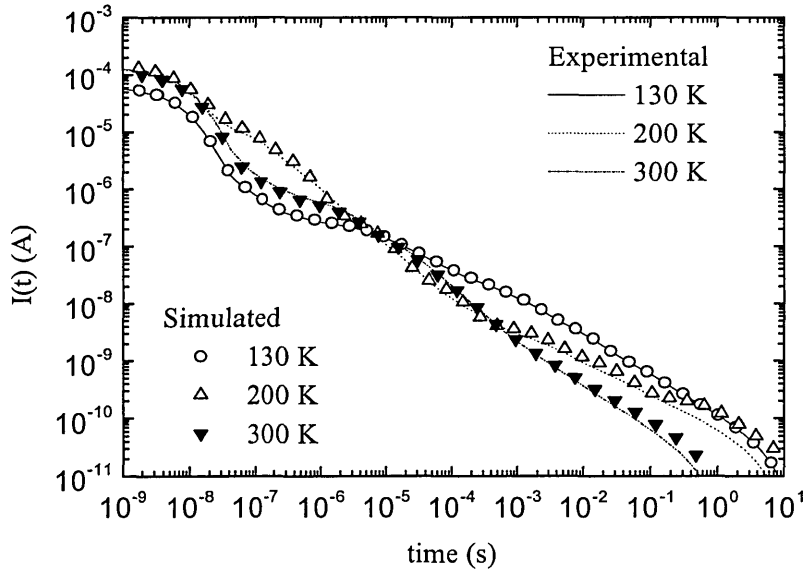

Figure 1.39 *Current-time decays in $CdTe:Sn$ for 130 K, 200 K and 300 K (lines), and simulated TPC I(t) data using DOS obtained with ELT method (symbols). (In the simulation: 130 K $\tau_f = 10^{-5}$ s; 200 K and 300 K $\tau_f = 4x10^{-7}$ s.)*

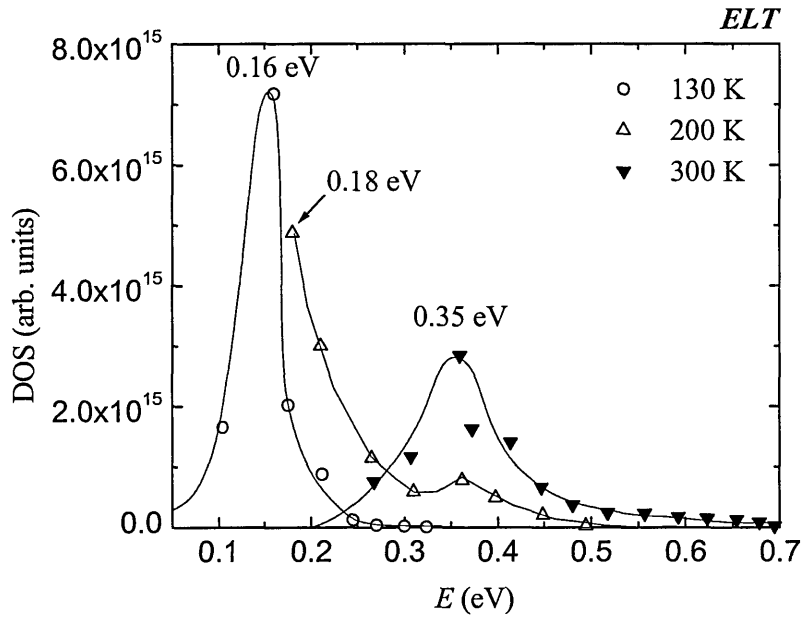

Figure 1.40 *DOS plots obtained using ELT method for CdTe : Sn . The lines are smooth curves illustrating the trend of the points.*

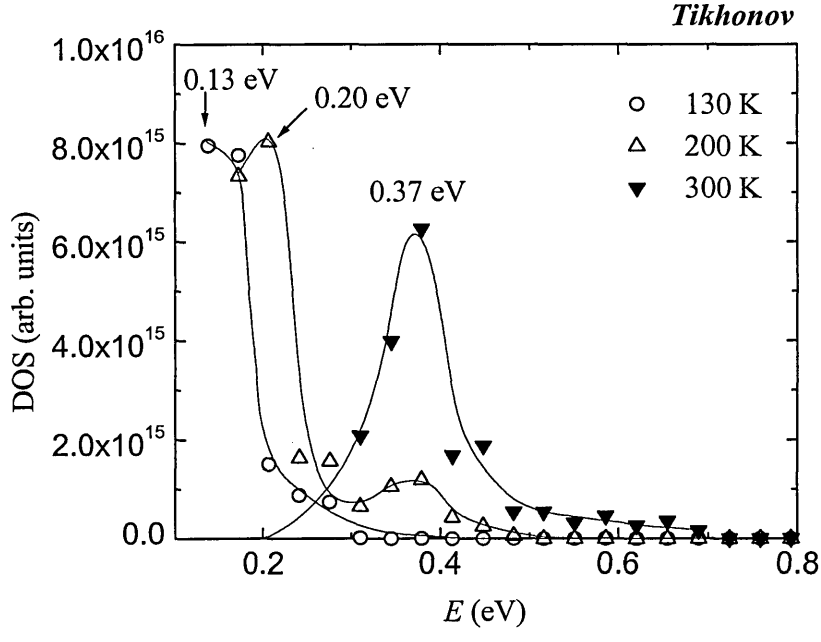

Figure 1.41 *DOS plots obtained using the Tikhonov regularization method for CdTe : Sn . The lines are smooth curves illustrating the trend of the points.*

Previous studies (Panchuk O. *et al*, 1999; Mathew X. 2003) have reported a wide range of localized discrete levels in the energy gap of *CdTe : Sn* . The TPC DOS plots obtained from the

$CdTe:Sn$ sample as shown in Figs. 1.40 and 1.41 indicate the presence of three main features, at approximately 0.15 eV, 0.19 eV and 0.36 eV below the conduction band edge with an estimated error of ±0.03. The temperature-independence of the energetic position of these features suggests the assumed attempt-to-escape frequency of $10^{12}\ s^{-1}$ is appropriate in all three cases. However, the *amplitude* of the 0.36 eV peak appears to be strongly temperature-dependent. The reason for this is presently unclear.

Both *ELT* and *Tikhonov* methods are capable in principle of resolving features in the DOS to an arbitrary narrow width, since no mathematical approximations are required. Therefore, it is possible in principle that each of the data points shown in figs. 1.40 and 1.41 corresponds to a distinct discrete level rather than deriving from an 'envelope' of three physically broadened levels. However, because of the dependence on both amplitude and energy position on temperature via the multiple-trapping kinetics, it is unlikely that a collection of distinct discrete levels would behave in the 'connected' way we observe. As shown in Fig. 1.39 the simulated TPC decays agree well with the experimental data, provided the free carrier lifetime is used as a fitting parameter, indicating the self-consistency of the analysis, although the variation in τ_f with temperature does not follow any obvious physical relationship.

1.5.2 Approximate methods (*LT* and *HLT* methods)

Light-induced meta-stable states in PECVD $a-Si:H$

We applied both approximate methods (*LT* and *HLT*) to the two sets of *I-t* data which have been studied by the exact methods. The results are shown in figure 1.42.

A comparison between Fig. 1.38 and Fig. 1.42 shows that the approximate *LT* and *HLT* methods, as it was expected, are good enough to study broad and featureless distributions of states as the existing in amorphous materials. As the exact methods, both approximate methods detect increase by approximately factor of 10 in the DOS distributions due to prolonged light soaking. Provided that the distribution is broad and featureless, the back-simulated *I-t* data will coincide very well with the original photocurrent data (symbols in figure1.43). In figure 1.43 the simulated *I-t* data using the worst performing, the approximate *LT* method, are shown.

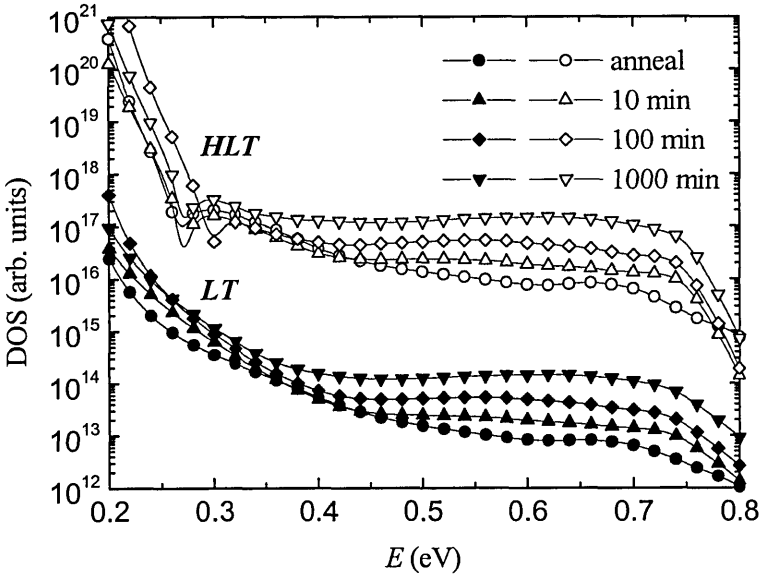

Figure 1.42 *DOS plots obtained using LT and HLT methods for* $a-Si:H$ *. Lines are smooth curves illustrating the trend of the points. The LT and HLT plots are offset for clarity.*

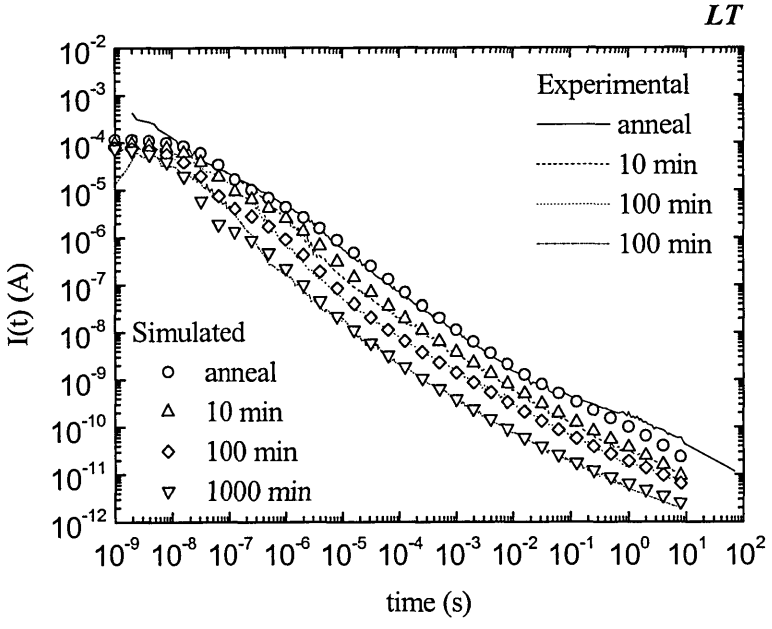

Figure 1.43 *Current-time decays at 300 K in PECVD* $a-Si:H$ *following progressive light-soaking (lines), and simulated TPC I(t) data using DOS obtained with LT method (open symbols). Best fits to the experimental decays were obtained using* τ_f *= (10, 4, 3.5, 1.8) x* 10^{-6} *s for the annealed and progressively light soaked samples, respectively.*

The simulated *I-t* data coincide very well with the original data. The fitting procedure in order to obtain information on the free carrier recombination lifetime, τ_f, gives the same values as those obtained with the exact methods (with a small difference for the annealed sample). Although it is not shown in the graph, essentially the same result is obtained using the *HLT* method. This supports the view that the approximate methods are good enough when applied to materials known to exhibit very broad and featureless distributions of states, as the $a-Si:H$.

Discrete levels in single crystal *Tin*-doped *CdTe*.

Applied to the *Tin*-doped *CdTe* the worst performing *LT* method resolves two features at around 0.16 *eV* and 0.37 *eV*.

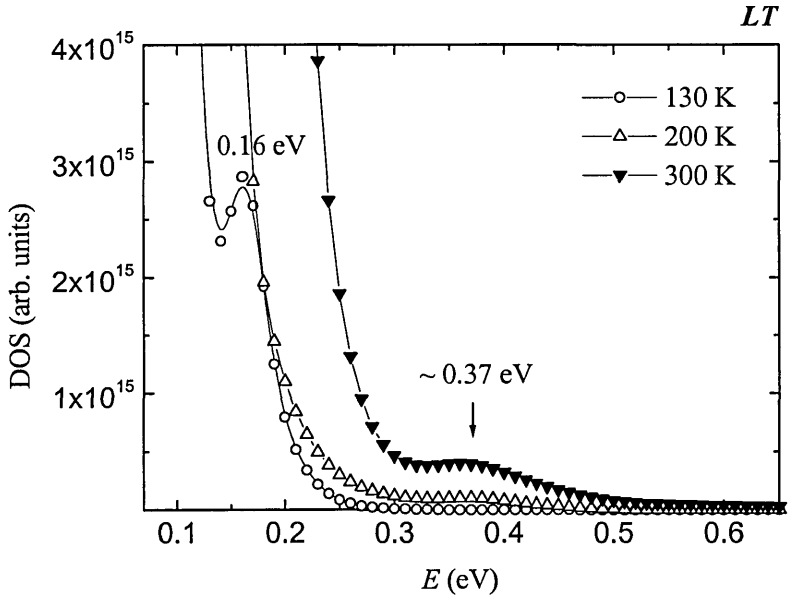

Figure 1.44 *DOS plots obtained using the LT method for* $CdTe:Sn$.

Although the positions of the recovered two peaks coincide very well with those obtained with the exact methods, both peaks are broadened (*e. g.* at 300 *K*, $\mathrm{FWHM}_{LT} \sim 0.16\ eV$ while $\mathrm{FWHM}_{Tikh} = 0.09\ eV$). The overall 'wrong' shape of the DOS (broadened features and high DOS at shallow energies) drastically affects the simulated *I-t* data up to times $10^{-5}\ s$. For times longer than $10^{-5}\ s$ the simulated *I-t* traces coincide with the originating data. The reason is that at long times the current is dominated by release from the deep state (at $\sim 0.37\ eV$), which although broadened, is recovered by the method. The simulation in fig. 1.45 was done with the same values for τ_f which have been obtained by a fitting procedure using the exact and the *HLT* methods. The lack of agreement between experimental and simulated *I-t* data shows that

the approximate *LT* method does not function correctly, and its application to systems known to contain sharp features is not appropriate. This view is supported as well by the fact that the re-calculated *I-t* traces do not fit the originating data for the same values of τ_f with which all other methods reproduce correctly the experimental data, hence the method should not be used to obtain information on τ_f.

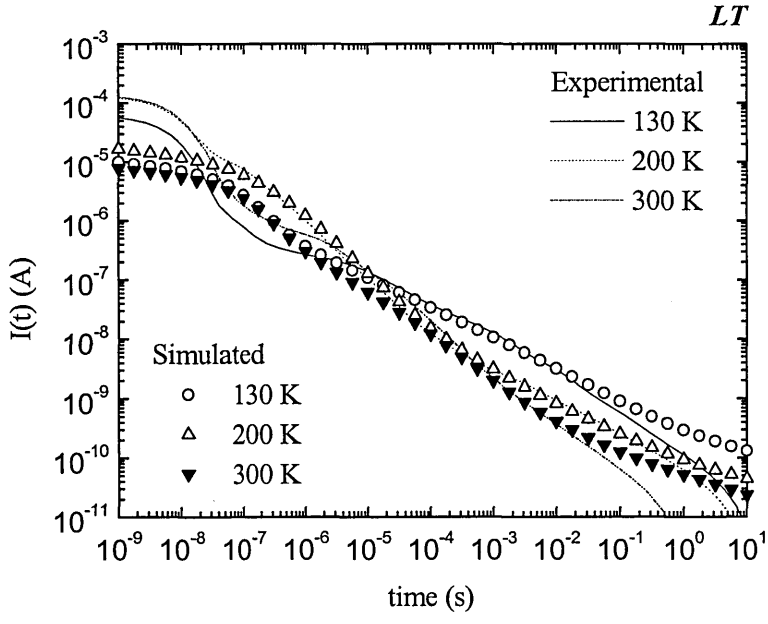

Figure 1.45 *Current-time decays in CdTe : Sn for 130 K, 200 K and 300 K (lines), and simulated TPC I-t data using DOS obtained with LT method (symbols). (In the simulation: 130 K,* $\tau_f = 10^{-5}$ *s; 200 K and 300 K* $\tau_f = 5x10^{-7}$ *s.)*

Due to its better resolution, the *HLT* method (fig. 1.46) recovers all three levels which have been detected with the exact methods. The *I-t* data simulated using the *HLT* DOS profiles are shown in figure 1.47.

Although the DOS distributions obtained with the *HLT* method are slightly broader in comparison with the distributions recovered with the exact methods (at 300 K, $FWHM_{HLT}$ = 0.13 *eV* and $FWHM_{Tikh}$ = 0.09 *eV*, $FWHM_{ELT}$ = 0.10 *eV*) the simulated *I-t* curves coincide very well with the originating *I-t* data for all three temperatures. This fact could be explained by the already mentioned result of our simulations and Schmidlin's work (1977) that any real situation could be adequately analysed in terms of relatively few discrete traps. Only a few points in the DOS profile (the main features of the DOS distribution) affect the shape of the simulated *I-t* curve. A plausible explanation could be the fact that *I-t* data are simulated as a

summation of exponents with coefficients A_i and α_i, ($I = \sum_i A_i \exp(\alpha_i t)$) and the *alphas* are proportional to the amplitudes of the recovered DOS (cf. *ELT* method).

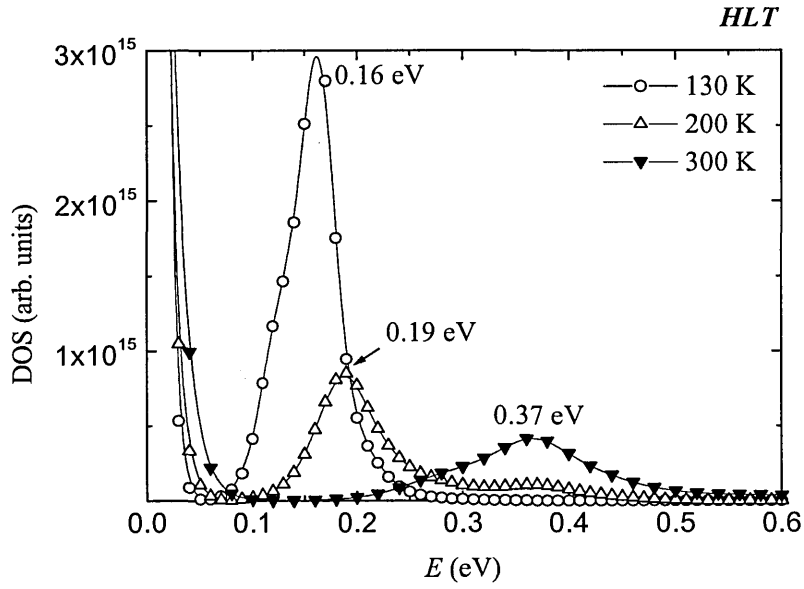

Figure 1.46 *DOS plots obtained using the HLT method for* $CdTe:Sn$.

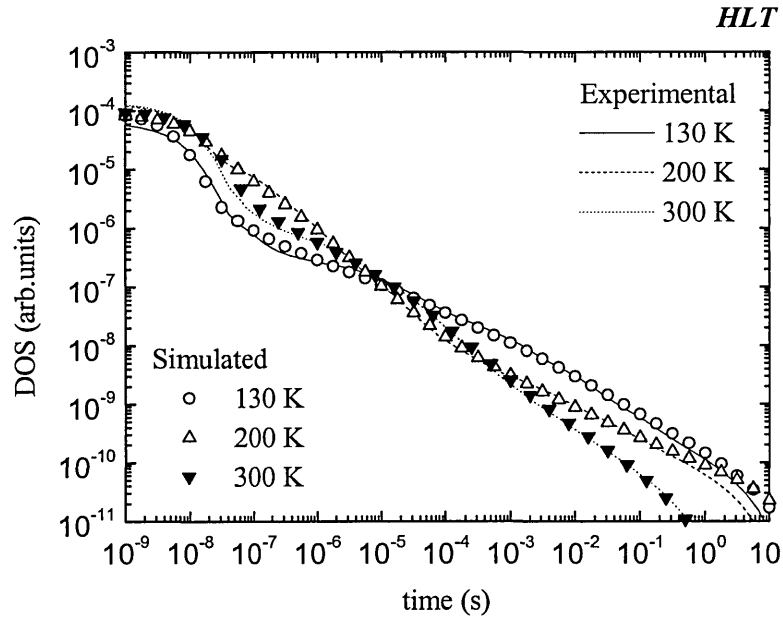

Figure 1.47 *Current-time decays in* $CdTe:Sn$ *for 130 K, 200 K and 300 K (lines), and simulated TPC I(t) data using DOS obtained with HLT method (symbols). (In the simulation: 130 K,* $\tau_f = 10^{-5}$ *s; 200 K and 300 K* $\tau_f = 5x10^{-7}$ *s.)*

TPC DOS analysed by a mathematically exact method (*ELT*) and a method based on the *Tikhonov* regularization are found to perform equally well when applied to data obtained from amorphous and crystalline semiconductors. Simulation of the current-time curves from the recovered DOS yields very good agreement in all cases with the originating experimental data over the range 10 ns – 1 s. All methods reveal a featureless increase by a factor of 5-10 in the deep defect density on light soaking of PECVD $a-Si:H$. It appears that although the exact methods do function correctly in the study of amorphous semiconductor systems, the capability to resolve discrete levels will seldom be required, and mathematically approximate methods (Naito H. *at al*, 1996; Nagase T. and H. Naito, 1998; Ogava N. *et al*, 2000; Main C. *et al*, 1992; Main C. 1997) will suffice in most cases.

In contrast, using the approximate *HLT* method and the exact techniques, three gap states, at 0.15 eV, 0.19 eV and 0.36 eV have been identified in $CdTe:Sn$, suggesting that TPC experiments combined with these methods of analysis may provide useful supplementary information to the more common defect spectroscopies used on crystalline materials such as thermostimulated current (TSC), deep level transient spectroscopy (DLTS) and photo induced current transient spectroscopy (PICTS). Further work to assess the prospects for such applications is in progress.

The approximate *LT* method has been found inappropriate to apply in the case of crystalline material because of its poor resolution.

II. Time of Flight Experiment

The time-of-flight (TOF) experiment has been used for quite a long time to investigate localized states distribution in amorphous materials. A comprehensive review of the experiment and its application could be found in Seynhaeve G., PhD thesis, 1989; and Marshal J.M., 1983. In the TOF experiment the sample is deposited in a sandwich structure consisting of a bottom electrode, a thin film of the material under study and a semitransparent top electrode. The electrodes must be 'blocking' to the injection of the charge type under study, so that ideally, no other excess charge is introduced. A sheet of charge (excess electrons and holes) is created close to the top contact by a short pulse of a strongly absorbed light. Then, the electrons or holes can be caused to drift across the sample by applying a field of the appropriate polarity. The movement of the charge is observed by monitoring the induced current.

For the TOF experiment some prerequisites have to be met (Seynhaeve, PhD thesis).

i. First, the field $F(x)$ should be uniform to ensure a constant drift velocity, $\upsilon_d = \mu_d F(x)$, through the sample. In a semiconductor, free charge carriers in thermal equilibrium are always present. When a voltage is applied these carriers will screen the field, resulting in a non-uniform internal field of which the shape is not readily known. The time constant of the relaxation, known as the dielectric relaxation time is equal to the product of the resistivity ρ and the permittivity ε of the material. So, when the excess carriers can complete a transit between the moment at which the voltage is switched on and the dielectric relaxation time, the field in which they drift will be uniform.

ii. Second, a strongly absorbed light should be used to ensure generating carriers in very thin layer close to the top electrode. Deeply penetrating light creates electrons and holes in much broader layer resulting in a different shape of the pre-transit current. Also the duration of the lightflash must be much smaller that the transit time.

iii. Third, the *deep-trapping* time must be larger than the free carrier *transit* time. The *Deep-trapping* time is defined as the average time it takes for an electron to get trapped in a deeper state. There it can either recombine with a hole or escape to the conduction band. If it escapes it should happen after a time larger than the macroscopic transit time because otherwise the electron can still contribute to the *pre-transit* current. So, whether trapping is in a 'deep' or 'shallow' state is dependent on both the release time of the trap and the transit time of the carriers.

2.1 Early work on TOF experiment

The TOF experiment may be explained in terms of the MT model. Schmidlin (1977) has shown that the MT system of equations for the case of the TOF experiment could be solved analytically. The result obtained for a discrete set of traps, simply characterized by their capture and release times, appears in the form of convolutions of modified *Bessel* functions. Although the analysis is highly complex and not physically transparent a simple solution exists in two extreme cases corresponding to *pre* and *post-transit* régime.

The thermalization energy approach used by Orenstein and Kastner (1981), and Tiedje and Rose (1980), leads to an approximate solution with a limited range of applicability.

Seynhaeve (PhD thesis, 1989; Seynhaeve *et al*, 1989) has shown that *pre* and *post-transit* current in the TOF experiment could be used to extract information on density of localized states in $a-Si:H$. Post-transit spectroscopy has been used by numerous groups to determine the distribution of localised trapping states in amorphous semiconductors, such as amorphous silicon (Seynhaeve G. F. *et al*, (1989); Usala S., *et al*, (1991); Yan B.J. *et al*, (1996); Eliat A., *et al*, (1996); Fejfar A. *et al*, (1996)). In order to deduce the DOS the authors made use of a physical, and/or mathematical approximation. The assumed physical approximation is that instead of having an *average* release time, *all* trapped carriers at an energy E become free at $\gamma_i^{-1}(E)$, known as *thermalization energy* concept. Mathematically, a δ-function approximation makes the inversion analytic, and energy and time are related by the thermalization energy expression $E = kT\ln(\nu t)$. In both cases the approximations lead to diminished accuracy and resolution, discrete levels are broadened and sharp features cannot be resolved.

In this section focusing only on the post-transit régime:

i. A brief review of the mathematics behind the TOF experiment will be given,
ii. It will be shown that an exact solution for the DOS exists. This exact solution will be found by means of the *Tikhonov Regularization* method with an appropriately chosen kernel function reflecting the post-transit conditions of the experiment, and using the newly developed *ELT* method in a post-transit (post-recombination) régime. Both methods are termed 'exact' meaning that no mathematical approximations have been used in order to find DOS. No assumptions as to the form of the DOS have to be made, so both methods are truly 'spectroscopic'.

2.2 Multiple Trapping model in terms of TOF experiment

Brief mathematical outline

In terms of the MT model the created excess charge (free and trapped) is described by a system of coupled partial differential equations (Schmidlin, 1977) very similar to the system of MT equations in the context of the TPC experiment.

$$\frac{\partial n(x,t)}{\partial t} + \mu_0 F \frac{\partial n(x,t)}{\partial x} = -\sum_i \frac{\partial n_i(x,t)}{\partial t} + g(x,t) \tag{2.1}$$

$$\frac{\partial n_i(x,t)}{\partial t} = \omega_i n(x,t) - \gamma_i n_i(x,t) \tag{2.2}$$

$n(x,t)$ is the density of the created free charge at the moment of the flash, $n_i(x,t)$ is the density of the trapped charge at energy level i, F is the externally applied field, $g(x,t)$ is the probability of generation per unit volume per unit time, μ_0 is the microscopic mobility, and the density of localized states enters these equations via the capture and release rates:

$$\omega_i = \sigma \upsilon g_i(E), \qquad \gamma_i(E) = \nu \exp(-E_i / kT)$$

The initial/boundary conditions are:

i. Initial charge distribution at moment $t = 0$ is:

$$n(x, t=0) = \frac{Q_0}{eA\xi} e^{-x/\xi},$$

ξ being the penetration depth of the light, Q_0 - the created free charge, e - the elementary charge, A - the area of the sample and x - the distance from the interface. If $x/\xi >> 1$ then $n\ (x, t=0\ ) \to 0$

ii. No trapped charge at the moment of the flash, $n_i(x, t=0) = 0$

Under the assumption of a δ-function exposure and strongly absorbed light the term $g(x,t)$, describing the probability of generation per unit volume per unit time reads (Schmidlin, 1977):

$$g(x,t) = g(x)\delta(t-0) \xrightarrow[\alpha \to \infty]{} N_0 \eta(0) \delta(x-0)$$

N_0 is the total number of nonreflected photons in a flash exposure, α is the absorption coefficient and η is the effective conversion efficiency of an absorbed photon into a mobile carrier.

Applying *Laplace* transformation with respect to t to the system of partial differential equations (2.1) and (2.2), and taking into account the initial conditions (i) and (ii) leads to a system of ordinary differential equations.

$$s\hat{n}(x,s) - n(x,t=0) + \mu_0 F(s\frac{d\hat{n}(x,s)}{dx} - n(x,t=0)) = -\sum_i (s\hat{n}_i(x,s) - n_i(x,t=0)) + Const\delta(x)$$

$$s\hat{n}_i(x,s) - n_i(x,t=0) = \omega_i \hat{n}(x,s) - \gamma_i \hat{n}_i(x,s) \Rightarrow \hat{n}_i(x,s) = \frac{\omega_i}{s+\gamma_i}\hat{n}(x,s)$$

$$\frac{d\hat{n}(x,s)}{dx} + \frac{\hat{a}(s)}{\mu_0 F}\hat{n}(x,s) = Const\delta(x), \text{ where } \hat{a}(s) = s(1+\sum_i \frac{\omega_i}{s+\gamma_i}) \tag{2.3}$$

Again, applying *Laplace* transformation but this time with respect to x one obtains:

$$u\hat{n}(u,s) + \frac{\hat{a}(s)}{\mu_0 F}\hat{n}(u,s) = Const \Rightarrow \hat{n}(u,s) = Const\frac{1}{\hat{a}(s)(F\mu_0)^{-1} + u}$$

The inversion is analytic and gives: $\hat{n}(x,s) = Const\exp(\frac{-\hat{a}(s)}{\mu_0 F}x)$

$$\hat{I}(s) = Const\int_0^L \hat{n}(x,s)dx = Const\frac{1-\exp(-\hat{a}(s)t_0)}{\hat{a}(s)t_0} \tag{2.4}$$

where $t_0 = \frac{L}{\mu_0 F}$ is the free carrier transit time and L is the thickness of the sample.

The last expression is the result obtained by Schmidlin (1977) and evaluated by Seynhaeve *et al* (1989) in the case of *pre* and *post-transit* current spectroscopy. These two extreme cases correspond to $\hat{a}(s)t_0$ large and $\hat{a}(s)t_0$ small respectively.

In the *post-transit* régime, when the quantity $\hat{a}(s)t_0$ is small the exponent in equation (2.4) can be expanded into *Taylor* series and it leads to the following expression for the current in time-domain:

$$I(t) \propto Const \sum_i \omega_i \gamma_i e^{-\gamma_i t} \tag{2.5}$$

For the case of continuous distribution replacing the summation by integration the equation (2.5) reads:

$$I(t) = Const \int_{\gamma_1}^{\gamma_2} g(\gamma) \exp(-\gamma t) d\gamma \tag{2.6}$$

The limit γ_1 corresponds to release from the deepest states, and γ_2 is equal to ν. If these limits are approximated by zero and infinity respectively, it is immediately seen that the DOS is an inverse *Laplace* transform of *I-t* data. Taking into account the complexity of the equation the inversion in order to find the DOS should be done numerically. Seynhaeve *et al* (1989) proposed a solution of the problem employing a *delta* function approximation. The exponential waiting-time distribution for release out of a trap at an energy E, $\gamma(E)e^{-\gamma(E)t}$, is replaced by a δ-function. The *thermalization energy* approach was used (cf. Early work on TPC analysis). The energy scale $E = kT\ln(\nu t)$ is defined by associating the average release time from traps at energy depth E below the mobility edge with the elapsed time t. The attempt-to-escape frequency ν is assumed to be energy independent. Under these assumptions the authors obtain the following approximate expression for the DOS:

$$t \times I(t) \propto g(E) \tag{2.7}$$

In the last line the proportionality constant following directly from the multiple-trapping rate equations has been omitted. This simple relation is straightforward to apply, and has been quite widely used in the analysis of post-transit currents (Fejfar A. *et al*, 1996; Korevaar B. A. *et al*, 2000).

Unfortunately, because of the underlying assumption for thermalization, the method does not work for structured distributions of localized tail states (Seynhaeve *et al*, 1985) and for exponential states whose width is smaller than kT.

Main *et al* (2000) have shown that equation 2.6 may be solved numerically for the DOS *avoiding* the delta-function approximation, simply by least-squares fitting a sum of exponential

functions to *I-t* data. This approach offers improved accuracy and resolution, albeit at the expense of more intensive computation and somewhat greater susceptibility to experimental noise. By means of simulated decays, a resolution of typically 0.5 kT FWHM for discrete levels has been demonstrated, compared with more than 2 kT when equation 2.7 is used.

Here we present a further alternative method for inverting *I-t*, based on the use of Tikhonov regularization to solve equation 2.6, which is a *Fredholm* integral of the first kind. It has previously been shown (Nagase *et al*, 1999, Gueorguieva *et al*, 2001) that this approach is capable of high resolution and improved noise immunity over other methods when used to solve the general system of multiple-trapping rate equations in the *s*-domain.

2.3 Tikhonov Regularization and Exact Laplace Transform methods in the context of TOF experiment

Tikhonov Regularization method

The equation $I(t) \propto Const \int_{\gamma_1}^{\gamma_2} g(\gamma) e^{-\gamma t} d\gamma$ (Seynhaeve *et al*, 1989) is a *Fredholm integral equation of the first kind.* The numerical inversion in order to find the DOS, $g(\gamma)$, as a function of the release rates, γ, was done by means of the proprietary subroutine FTIKREG (Weese, 1992) based on the *Tikhonov* regularization technique.

As far as the release rates vary over many decades the integral equation which the FTIKREG program minimizes was chosen to be:

$$V(\lambda) = \sum_{i=1}^{n} \frac{1}{\sigma_i^2} \left(f(t) - \int_{\ln(\gamma_{min})}^{\ln(\gamma_{max})} K(\gamma,t) g(\ln\gamma) d(\ln\gamma) \right)^2 + \lambda \int_{\ln(\gamma_{min})}^{\ln(\gamma_{max})} g(\ln(\gamma))^2 d(\ln(\gamma)) \qquad (2.8)$$

In the discrepancy term the vector $f(t)$ contains either noisy experimental data points or simulated post-transit *I*-t data. The kernel function $K(\gamma,t)$ in this case is just an exponent, $\exp(-\gamma t)$, and is simpler in comparison with the kernel function in the case of the TPC experiment. In order to find the DOS as a function of energy the definition for release rates, $\gamma_i = \nu e^{-E_i}/kT$, was used with a value for the attempt-to-escape frequency $\nu = 10^{12}\ s^{-1}$ Although this leads to the familiar expression relating time and energy, $E_i = kT \ln(\nu/\gamma_i)$, it does not imply underlying *thermalization energy* approach. In the computation constant capture properties have been assumed, $\sigma\upsilon = const$.

The regularization term is motivated by the theory of *Tikhonov* regularization (Tikhonov A., 1963; Groetsch C. W., 1984) and prevents the experimental errors from having too large influence on the result. Furthermore, FTIKREG has been used with a requirement for positive values for the regularized solution.

Plus points of the Post - Transit (PT) *Tikhonov* regularization approach

i. No mathematical/physical approximations have been employed, so in principle information on the DOS distribution could be obtained to a high degree of accuracy.
ii. The input data for the *PT Tikhonov* method are in the time-domain. Consequently, the noise in the data is not correlated.
iii. The method is fast and straightforward.

ELT in a post-transit (post-recombination) régime

An alternative approach is to use the *ELT* method in a 'post-recombination' régime characterized with recombination time shorter than the trapping time into a group of traps. The *post-recombination* régime in coplanar geometry is nearly equivalent to the *post-transit* régime in sandwich configuration if one carrier type predominates and recombination is monomolecular.

Plus points of the *ELT* method:

i. The *ELT* method is exact and is characterized with very high resolution (4 $meV = kT/6$), higher than the resolution of the *Tikhonov* method (12 $meV = kT/2$).
ii. It gives a unique solution for a given set of current-time data. We could argue that this is an advantage over the *Tikhonov* method, which gives more than one solution.

According to the theory, this is the nature of ill-posed inverse problems, that many even very different solutions may explain equally well the input data. Regularization methods impose, through the regularization term, some prior information on the solution (e.g. the assumption that the solution is to some extent smooth) in order to choose among the possible solution (possible solutions due to a good data fitting) the 'unique' one.

Minus points of the *ELT* method:

i. As far as the *ELT* method is exact, it requires 'ideal' current-time data for input data. Any degree of noise introduced in photocurrent data results in a 'noisy' DOS. In order to use the method 'an ideal' *I-t* curve ('identical' to the experimental one) has to be reconstructed as a summation of exponents with given coefficients $\{A_i,\ \alpha_i, i = 1,...n\}$

(cf. Exact *Laplace* transform method and Appendix 1) and after that the method can be applied.

A point should be made that the 'noisiness' of the solution should not be considered as a deficiency of the *mathematical* model because the method is designed to give an exact solution using an array of data. But clearly from physical and/or practical point of view it could be considered as a deficiency.

ii. A further drawback for the *PT ELT* method is that the input data, $b_i(s_i)=\frac{1}{\sigma\upsilon}\left[\frac{1}{s_i}\left(\frac{2I(0)}{\hat{I}(s_i)}-\frac{1}{\tau_f}\right)-1\right]$, are in the *Laplace* domain. By definition, the *Laplace* transformation is an integral transformation with limits of the integration 0 and ∞ respectively. This means that in principle $\hat{I}(s_i)$ has to be inferred from the whole time series of *I-t* data. Obviously, this is impossible when working with experimental data and this inevitably leads to further error in the solution. Though, an improvement could be achieved if the current-time data could be appropriately extrapolated to very short times.

2.4 Application to simulated and experimental data

In the rest of this section the theoretical resolution of the approximate and the exact methods will be evaluated by means of computer simulations and application to noisy experimental data.

The procedure is as follows. First, the *I-t* response under post-transit conditions for several representative distributions of traps is generated by means of the *polynomial approach*. Then the DOS is calculated from the *I-t* data using $t\times I(t)$, the *Tikhonov*, and the *ELT* methods. At the end the *I-t* data from the already calculated DOS distributions is simulated. After evaluating the theoretical resolution of the methods they are applied to real data taken on $a-Si:H$ for which noise is inherent.

Simulated data

Two discrete levels

First, we start with a simple but rather extreme case of two discrete levels of equal density positioned at 0.3 and 0.5 eV below the conduction band edge. The line in fig. 2.1 represents the simulated *I-t* under *post-transit* conditions. The simulation was done by means of the polynomial approach with a very short recombination lifetime (10^{-12} s). It is seen, in figure 2.2, that the approximate method accurately recovers the energetic location of the states, but introduces significant broadening (with a FWHM as high as 70 meV, or $3kT$) of these features.

Contrastingly, the *Tikhonov* and *ELT* methods return only two values that are significantly greater than zero, which correspond very closely in energy to the originating levels. Closer investigation reveals a small difference in energy, of less than 0.01 eV, and a small inequality in the density.

As a further check, we have taken the DOS returned by each method as shown in figure 2.2 and used these to *re-calculate* the *I-t* decays. The results are shown in figure 2.1. It is seen that the data calculated from the *ELT* and *Tikhonov* DOS fit the original *I-t* decay obtained from the model DOS very closely. The shape of the *I-t* curve calculated from the approximate DOS is clearly quite different, which confirms that the improved resolution is not simply an artefact.

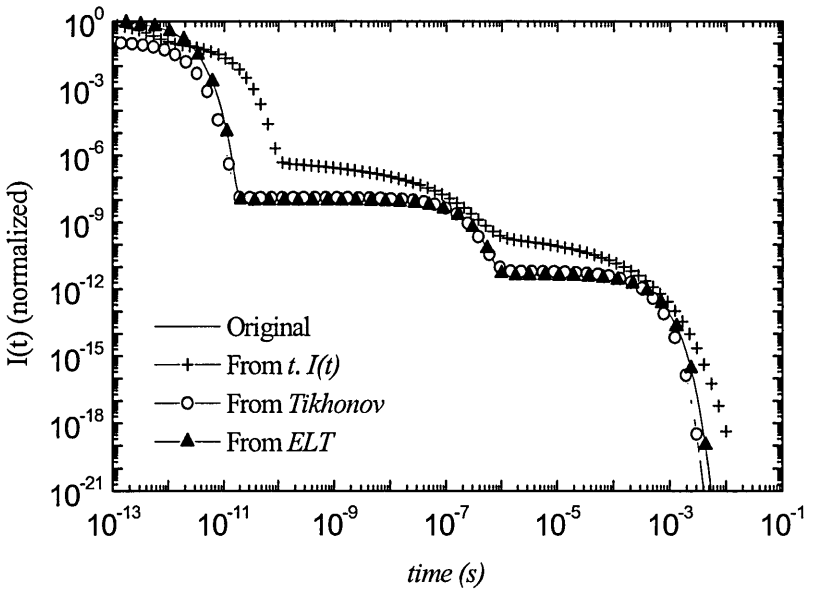

Figure 2.1 *Simulated post-transit data (line), and back-simulated data (symbols) using the DOS in figure 2.2.*

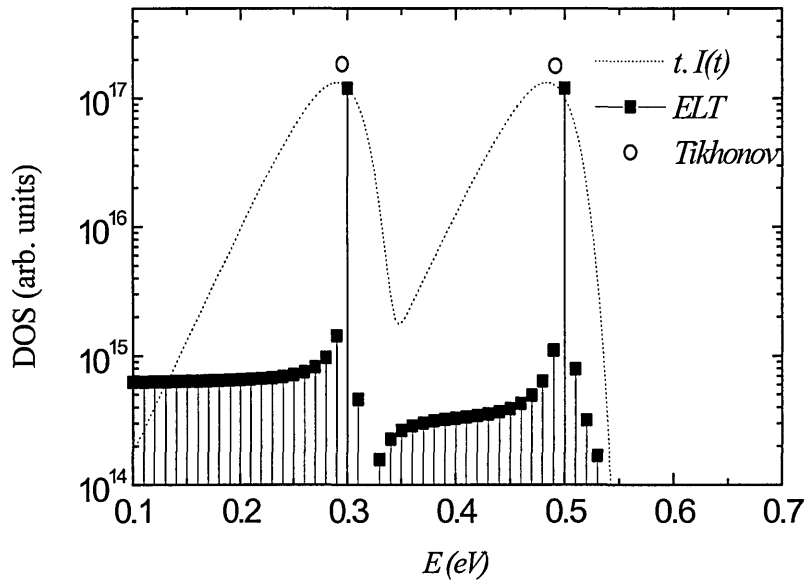

Figure 2.2 *Recovered DOS calculated using the approximate* $t \times I(t)$ *and the Tikhonov and ELT methods. The originated levels are positioned at 0.3 and 0.5* eV *.*

Exponential distribution with a *Gaussian* feature superimposed

Figure 2.3 shows the result of applying the approximate, *Tikhonov*, and *ELT* methods to a distribution of states, comprising an extensive exponential band-tail of characteristic energy 50 *meV* plus a *Gaussian* distribution. This kind of DOS is a more realistic model for a disordered semiconductor. It can be seen that while all three methods return the correct tail slope, the approximate method tends to broaden the *Gaussian* feature, especially on the shallower energy side. The *Tikhonov* and *ELT* methods reproduce all aspects of the originating DOS to a high degree of accuracy. The *I-t* re-calculation (figure 2.4) again confirms the improved fidelity of the exact methods.

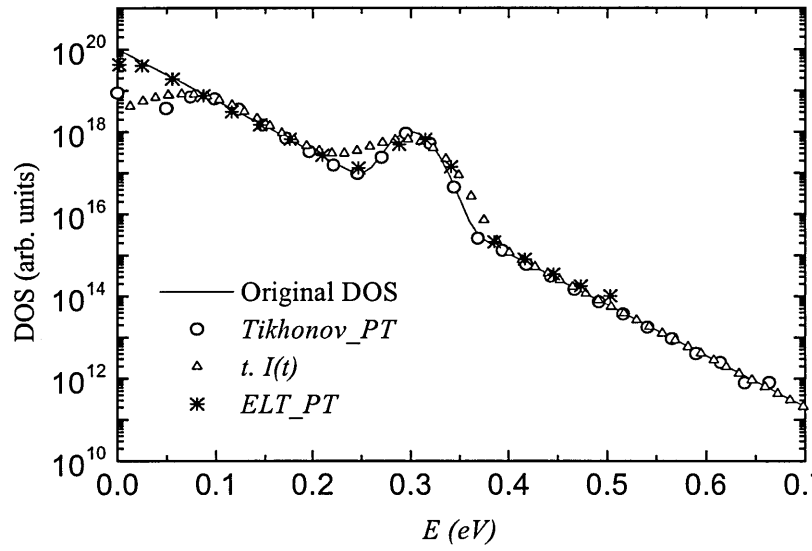

Figure 2.3 *DOS obtained using the approximate, $txI(t)$, and the exact Tikhonov and ELT methods.*

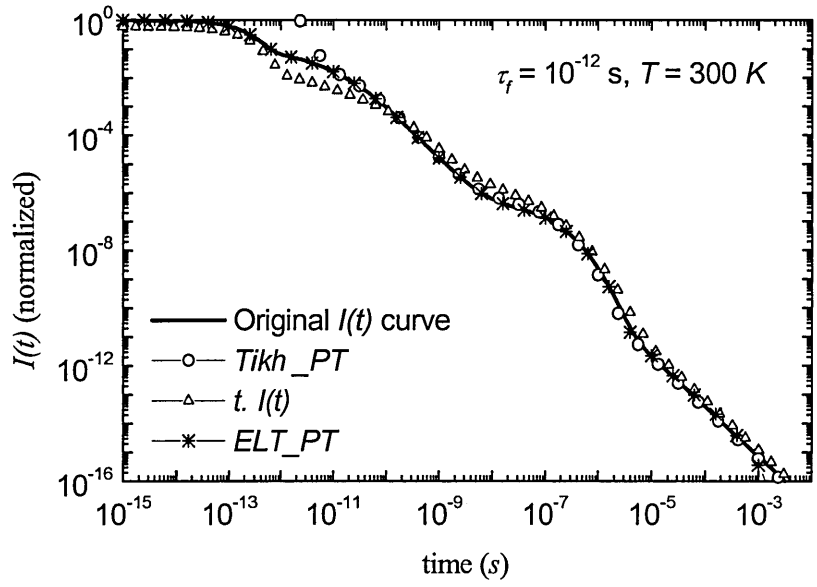

Figure 2.4 *The original $I(t)$ post-transit data (line) and simulated $I(t)$ data (symbols) using the recovered DOS in* figure *2.3.*

Experimental data

The work reported above demonstrates that the *ELT* and *Tikhonov* methods are capable of yielding good results when applied to simulated, noise-free, data. However, under experimental conditions, fluctuations in the current will occur, and may have some bearing on the practical success of the technique (Reynolds *et al*, 2001).

Figure 2.5 shows the result of applying the approximate and the *ELT* and *Tikhonov* methods to a typical electron post-transit decay for an $a-Si:H$ pin diode. This device was light-soaked prior to measurement, and the 'bump' in the DOS centred at 0.57 eV is associated, at least partially, with the creation of metastable defects. There is an additional peak centred at 0.33 eV, apparent in the DOS obtained using the approximate method but not reproduced by our exact techniques. Whether this feature is real or an artifact is unclear, as the range of validity for post-transit analysis, normally taken to extend from twice the carrier transit time, was approximately 60 ns, or an energy depth of some 0.28 eV. It is proposed to pursue this question by extending measurements to shallower energies, reducing the temperature and increasing the applied field.

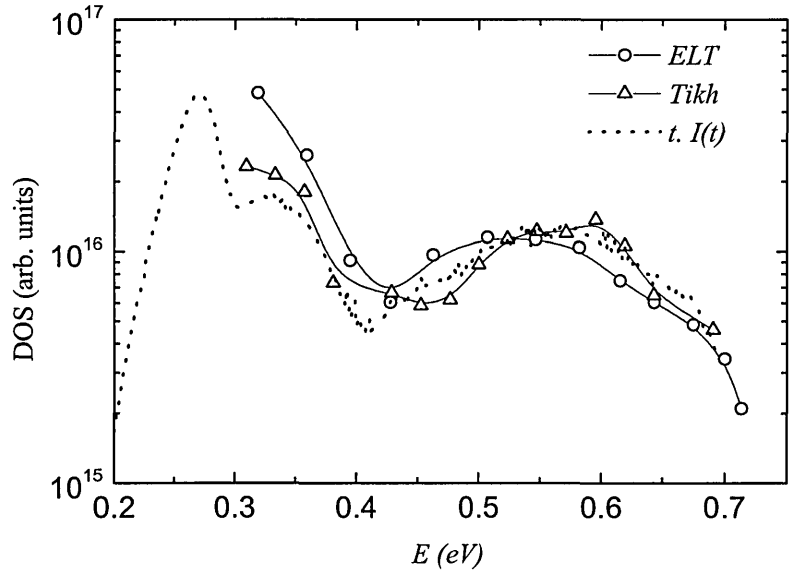

Figure 2.5 *Comparison of the DOS recovered from the experimental data in fig. 2.6 using the approximate* $t \times I(t)$, *and the exact ELT and Tikhonov methods.*

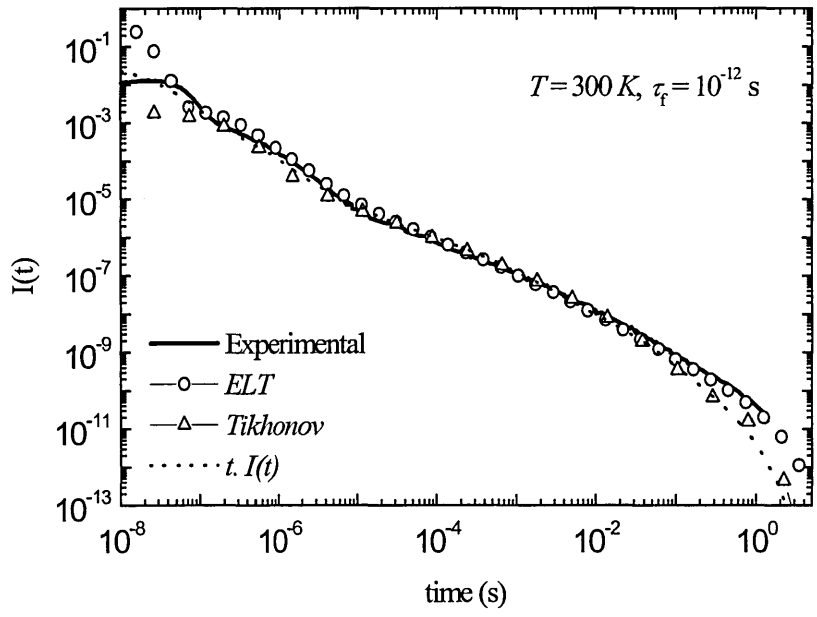

Figure 2.6 *Experimental post-transit data (line) and back-simulated I-t data (symbols) from DOS in figure 2.5.*

In conclusion, it has been shown by computer simulations that the density of localized states could be extracted from *post-transit* photocurrent data to a very high degree of accuracy retaining the exponential distribution function for the release time in the integral equation (2.6). As far as neither the Post-Transit *Tikhonov* regularization method nor the Post-Transit *ELT* method employ any kind of mathematical approximations the solution is 'exact'. It has been shown that the exact methods are capable of improved performance as a DOS spectroscopy over the frequently used approximate expression $t \times I(t)$. Obviously, the 'broadening' associated with the approximate $t \times I(t)$ method arises as a result of replacing the problematic part (the kernel function) of the *Fredholm* integral equation of the first kind with a δ-function positioned at a given energy where the kernel function has a maximum.

The potential benefits are most apparent when discrete levels or sharp distributions of states are investigated. The exact methods have also been applied to experimental post-transit data obtained from an amorphous silicon *pin* sample, and although the benefits of improved resolution were found to be unnecessary an acceptable tolerance to experimental noise present on the current decay was demonstrated.

Conclusions

The major contribution to the field arising from this work is that a new technique for DOS recovery via the *Laplace* transform of the transient photocurrent has been developed. The newly developed *ELT* method has been tested by applying it to simulated and experimental *I-t* data. The method yields very good agreement with the originating DOS when operating on *I-t* data simulated for model exponential and *Gaussian* continuous distributions, and can also resolve two discrete levels placed $kT/6$ apart in energy.

The performance of the *ELT* method when operating on experimental data has been compared with the results obtained from the *Tikhonov regularization* method, regarded as the best one for extracting information from noisy experimental data. Unfortunately, the 'exact' nature of the *ELT* method makes it susceptible to the presence of noise which may give rise to artifacts in the recovered DOS. This gives impetus to further work to determine the best way of coping with noise, maintaining acceptable energy resolution.

The *ELT* and the *Tikhonov* regularization methods have been applied to experimental data obtained on light-soaked PECVD $a-Si:H$, and single crystal $CdTe:Sn$. Both methods are found to perform equally well when applied to *I-t* data obtained on PECVD $a-Si:H$. Simulation of the current-time curves from the recovered DOS yields very good agreement in all cases with the originating experimental data over the range 10 ns – 1 s. It appears that although these methods do function correctly in the study of amorphous semiconductor systems, the capability to resolve discrete levels will seldom be required, and mathematically approximate methods (Naito H. *et al*, 1996; Nagase T. *et al*, 1998; Ogawa N. *et al*, 2000; Main C. *et al*, 1992; Main C. 1997) will suffice in most cases. In contrast, three gap states, have been identified in $CdTe:Sn$ using these techniques, suggesting that TPC experiments combined with these methods of analysis may provide useful supplementary information to the more common defect spectroscopies used on crystalline materials such as thermostimulated current (TSC), deep level transient spectroscopy (DLTS) and photo induced current transient spectroscopy (PICTS).

In chapter II we have shown by computer simulation that the use of the novel method based on the *Tikhonov* regularization for inverting the *post-transit* system of rate equations is capable of improved performance as a DOS spectroscopy over the frequently used approximate expression $g(E)=t\times I(t)$. The potential benefits are most apparent when discrete levels or sharp distributions of states are investigated. The method has also been applied to experimental post-transit data obtained from an amorphous silicon *pin* sample, and although the benefits of improved resolution were found to be unnecessary, an acceptable tolerance to experimental noise present on the current decay was demonstrated.

Appendices

Appendix A1

Fitting exponents to TPC *I-t* data.

Least Squares method of finding *A*s and *alphas*:

Let $\Delta = \sum_{i=1}^{n} (\ln I_i - \ln(Ae^{\alpha t_i}))^2$ Then:

$$\frac{\partial \Delta}{\partial A} = \sum_{i=1}^{n} \left(\frac{-2\ln I_i}{A} + \frac{2\ln A}{A} + \frac{2\alpha t_i}{A}\right) = 0 \Rightarrow \alpha \sum_{i=1}^{n} t_i + n\ln A - \sum_{i=1}^{n} \ln I_i = 0$$

$$\frac{\partial \Delta}{\partial \alpha} = \sum_{i=1}^{n} (-2t_i \ln I_i + 2t_i \ln A + 2\alpha t_i^{\,2}) = 0 \Rightarrow$$

$$\sum_{i=1}^{n} (-t_i \ln I_i) + \ln A \sum_{i=1}^{n} t_i + \alpha \sum_{i=1}^{n} t_i^2 = 0$$

If $S_t = \sum_{i=1}^{n} t_i$; $S_c = \sum_{i=1}^{n} \ln I_i$; $S_{tc} = \sum_{i=1}^{n} t_i \ln I_i$; $S_{tt} = \sum_{i=1}^{n} t_i^2$ then:

$$\alpha = \frac{nS_{tc} - S_c S_t}{nS_{tt} - S_t^2} \quad ; \quad \ln A = \frac{S_c - \alpha S_t}{n}$$

Procedure of fitting a minimum number of exponents to a given *I-t* data set:

We have a set of data: $\{I_i\}_{i=1}^{n}$ at points $\{t_i\}_{i=1}^{n}$.

First step: Applying equation (1) to the last tree points and finding exact values for *alpha* and the coefficient *A*.

Second step: Checking if the error $\left(1 - \frac{\ln I_{\exp}(t_i)}{\ln I_{calc}(t_i)}\right)$ is less than a given value (*e.g.* 0.01)

Third step: checking if $I_i - Ae^{\alpha t_i} > 0$ (they will be the 'new' data set $\{I_i\}_{i=1}^{n'<n}$ which will be used for the calculation of next A and *alpha*)

Fourth step: Adding another point and going through step one to three again. If the above three requirements are still fulfilled then another point is added and so on. The procedure of adding points to the first set of three starting points (which will be fitted with the first exponent) stops when one of the above requirements is no longer fulfilled.

Fifth step: The points found by the above procedure are 'ignored' and the value of the exponent is subtracted from all data $\{I_i\}_{i=1}^{n}$ (at all points $\{t_i\}_{i=1}^{n}$) and the same procedure starts with the 'new' set of $\{I_i\}_{i=1}^{n'<n}$ data. (Note that $n' = n - k$ where k is the number of points fitted with one exponent).

This procedure gives the minimum number of exponents required to fit a given *I-t* data set.

Appendix A2

Semi - analytical *Laplace* Transformation of TPC *I-t* data

For every two neighbouring *I-t* points, the following relations are fulfilled:

$$e^{a_i t + b_i} = I_i, \qquad e^{a_i t_{i+1} + b_i} = I_{i+1},$$

$$a_i = \frac{\ln(I_{i+1}/I_i)}{t_{i+1} - t_i}, \; e^{b_i} = \frac{I_i}{e^{a_i t_i}}.$$

Then the *Laplace* transformation of *I-t* data can be found analytically:

$$\hat{I}(s) = \sum_i \int_{t_i}^{t_{i+1}} e^{a_i t + b_i} e^{-st} dt = \sum_i \frac{e^{b_i}}{(a_i - s)} \left[e^{(a_i - s)t} \Big|_{t_i}^{t_{i+1}} \right]$$

The first and second derivative of $\hat{I}(s)$ is found using the theorem for multiplication by t^n (Spiegel M.R, 1965):

$$\hat{f}^{(n)}(s) = (-1)^n \int_0^\infty t^n f(t) e^{-st} dt$$

$$\hat{I}'(s) = -\int_0^\infty t I(t) e^{-st} dt = -\sum_i \frac{e^{b_i}}{(a_i - s)^2} \left[((a_i - s)t - 1) e^{(a_i - s)t} \Big|_{t_i}^{t_{i+1}} \right]$$

$$\hat{I}''(s) = \int_0^\infty t^2 I(t) e^{-st} dt = \sum_i \frac{e^{b_i}}{(a_i - s)^3} \left[((a_i - s)^2 t^2 - 2(a_i - s)t + 2) e^{(a_i - s)t} \Big|_{t_i}^{t_{i+1}} \right]$$

References

Anderson, P. W. (1958), *Phys. Rev.* **B109**, 1492.

Arkhipov, V.I., Rudenko, A.I. (1978), *J. Non-Cryst. Solids* **30**, 163.

Atkinson, L.V., Harley, P.J. and Hudson, J.D. (1989), *Numerical Methods with FORTRAN-77 A Practical Introduction*, Addison-Wesley.

Brüggemann, R., Main, C., Berkin, J. and Reynolds, S. (1990), *Phil. Mag.* **B62.**

Carlson, D. E. (1989) in: *Properties of Amorphous Silicon and its Alloys*, (Ed. T. Searle), IEE, London, UK, 264.

Eiche, C., Maier, D., Schneider, M., Sinerius, D., Weese, J., Benz, K.W. and Honerkamp, J. (1992), *J. Phys. Condens. Matter* **4**, 6131-6140.

Eliat, A., Yan, B.J., Adriaenssens, G.J. and Bezemer, J. (1996), *J. Non-Cryst. Solids*, **200**, 592.

Fejfar, A., Juška, G. and Kočka, J. (1996), *J. Non-Cryst. Solids* **198-200**, 190.

Garbow, B.S., Hillstrom, K.E. and More, J.J. (1980), *Subroutine LMDIF1, MINPACK project*, Argonne National Laboratory, IL.

Groetsch, C.W. (1984), *The theory of Tikhonov regularization for Fredholm equations of the first kind*, Boston, Pitman.

Groetsch, C.W. (1999), *Inverse problems – activities for undergraduates*, Published by the Mathematical Association of America.

Gueorguieva, M.J., Main, C. and Reynolds, S. (2000), *Mat. Res. Soc. Symp. Proc.* **vol. 609**, Materials Research Society.

Gueorguieva, M.J., Main, C. and Reynolds, S. (2001), Invited paper presented at the 11th International School on Condensed Matter Physics (ISCMP2000), Varna, Bulgaria, September 2000. Published in Materials for Information Technology in the New Millennium (Eds. J.M. Marshall, A.G. Petrov, A Vavrek, D Nesheva, D Dimova-Malinovska, J.M. Maud (Published by the Editors 2001) 332-335.

Gueorguieva, M.J., Main, C. and Reynolds, S. (2001a), *Mat. Res. Soc. Symp. Proc.*, **664**, A19.3.

Gueorguieva, M.J., Main, C. and Reynolds, S., Brüggemann, R. and Longeaud, C. (2002), *Journal of Non-Crystalline Solids*, **299-302,** 541-545.

Hadamard, J. (1923), *Lectures on the Cauchy Problem in Linear Partial Differential Equations*, Yale University Press, New Haven.

Kirsch, A. (1996), *An introduction to the mathematical theory of Inverse problems*, Applied Mathematical Sciences, **120**, Springer -Verlag, (Eds. J. E. Marsden, L. Sirovich and F. John).

Korevaar, B.A., Adriaenssens, G.J., Smets, A.H.M., Kessels, W.M.M., Song, H-Z, M.C.M. van de Sanden and Schram, D.C. (2000), *J. Non-Cryst. Solids* **266-269**, 380.

Lakin, W.D., Marks, L. and Noolandi, J. (1997), Model of photoconduction in amorphous medium, *Phys. Rev.* **B15**, 12.

Main, C., Brüggemann, R., Webb, D.P. and Reynolds, S. (1992), *Sol. St. Commun.* **83**, 401.

Main, C., Webb, D.P. and Reynolds, S. (1995), in: *Electronic, Optoelectronic and Magnetic Thin Films,* (Eds. J.M. Marshall, N. Kirov and A. Vavrek), John Wiley-Research Studies Press, New York, 12-25.

Main, C. (1997), in: *Amorphous and Microcrystalline Silicon Technology*, (Eds. M. Hack, E.A. Schiff, S. Wagner, A. Matsuda, R. Schropp), *Mater. Res. Soc. Proc.* Pittsburgh, PA, **467**, 167.

Main, C., Reynolds, S., Badran, R.I. and Marshall, J.M. (2000), *J. Appl. Phys.* **88**, 1190.

Marshal, J.M. (1983), *Rep. Prog. Phys.* **46**, 1235.

Marshall, J.M. and Main, C. (1983), *Philosophical Magazine* **B47**, 471.

Mathew, X. (2003), *Solar Energy Materials&Solar Cells*, **76**, issue 3.

Michiel, H. and Adriaenssens, G.J. (1985), *Phil. Mag.* **B51**, 27.

Michiel, H., Marshall, J.M. and Adriaenssens, G.J. (1983), *Phil. Mag.* **B48**, 187.

Mott, N.F. (1966). *Phil. Mag.*, **13,** 989.

Mott, N.F. (1987). *Conduction in non-crystalline materials*, Clarendon Press, Oxford.

Mott, N.F. and Davis, E.A.(1979). *Electronic processes in non-crystalline materials*, Oxford, Clarendon Press.

Naito, H., Ding, J. and Okuda, M. (1994), *Appl. Phys. Lett.* **64**, 1830.

Naito, H., Nagase, T., Ishii, T., Okuda, M., Kawaguchi, T., Maruno, S. (1996), *Journal of Non-Crystalline Solids* **198-200,** 363-366.

Nagase, T., Kishimoto, K. and Naito, H. (1999), *J. Appl. Phys.* **86**, 5026.

Noolandi, J. (1977), *Phys.Rev.* **B16**, 10.

Ogawa, N., Nagase, T. and Naito, H. (2000), *J. Non-Cryst. Solids*, **266-269**, 367-371.

Orenstein, J., Kastner, M.A. (1981) *Phys. Rev. Lett.* **46**, 1421.

Orenstein, J., Kastner, M.A. and Vaninov, V. (1982), *Philosophical Magazine* **B46**, 23.

Öztürk, F. and Akdeniz, F. (2000), *Linear Algebra and its Applications*, **321**, 295-305.

Panchuk, O., Savitskiy, A., Fochuk, P., Nykonyuk, Ye., Perfenyuk, O., Shcherbak, L., Ilashchuk, M., Yatsunyk, L., Feychuk, P. (1999), *Journal of Crystal Growth*, **197**, 607.

Press, W.H., Teukolsky, S., Vetterling, W. and Flannery, B. (1992), *Numerical Recipes in FORTRAN. The Art of Scientific Computing*, Second Edition, Cambridge University Press.

Reynolds, S., Main, C., Webb, D.P. and Rose, M.J. (2000), *Phil. Mag.* **B80**, 547.

Reynolds, S., Main, C., and Gueorguieva, M. (2001) in: *Materials for Information Technology in the New Millennium*, (Eds. J.M. Marshall, A.G. Petrov, A. Vavrek, D. Nesheva, D. Dimova-Malinovska and J.M. Maud), 152-159.

Reynolds, S., Main, C. and Gueorguieva, M. (2001a), *Mat. Res. Soc. Symp. Proc.* **664**, Materials Research Society.

Roths, T., Freiburger Materialforschungzentrum, Stefan-Meier-Strasse 21, Freiburg im Breisgau, Germany (private correspondence).

Roths, T. (2000), Ph.D. thesis, Albert-Ludvigs Universität Freiburg, Germany.

Schmidlin, F.W. (1997), *Phys. Rev.* **B16**, 6.

Seynhaeve, G., Adriaenssens, G.J., Michiel, H. (1985), *Solid State Communications*, **56**, 323.

Seynhaeve, G.F., Barclay, R.P., Adriaenssens, G.J. and Marshall J.M. (1989), *Phys. Rev.* **B 39**, 10 196.

Spiegel, M.R. (1965), *Theory and Problems of Laplace Transforms*, Schaum Publishing Co, New York.

Street, R.A. (1991), *Hydrogenated amorphous silicon*, Cambridge Solid State Science Series, Cambridge University Press.

Tiedje, T. and Rose, A.(1980), *Solid State Communications*, **37**, 49.

Tikhonov, A.N. (1963), English translation of *Dokl. Akad. Nauk. SSSR*, **151**, 501-504.

Usala, S., Adriaenssens, G.J., Öktu, Ö., Nesladek, M. (1991), *Appl. Surface Science* **50**, 265.

Webb, D.P. (1994), PhD thesis, University of Abertay Dundee.

Weese, J. (1992), FTIKREG: A program for the solution of Fredholm integral equations of the first kind. User manual. Published in: *Computer Physics Communications* **69**, 99. Programs FTIKREG & NLREG from the CPC Program Library, Queen's University of Belfast, N. Ireland.

Weese, J. (1993), NLREG: A program for solution of non-linear ill-posed problems, User manual. From Freiburger Materialforschungzentrum, Stefan-Meier-Strasse 21, Freiburg im Breisgau, Germany (free download).

Wolfram, S. (1991), *Mathematica, A System for Doing Mathematics by Computer*, 2nd edition, Addison-Wesley Publishing Company, Inc., The Advanced Book Program.

Yan, B.J., Han, D.X., Adriaenssens, G.J. (1996), *J. Appl. Phys.* **79**, 3597.

List of Publications

1. Gueorguieva, M. J., Main, C. and Reynolds, S. 2000, *A Laplace Transform Technique for Direct Determination of Density of Electronic States in Disordered Semiconductors from Transient Photocurrent Data.*, in: Collins R.W., Branz H.M., Guha S, Okamoto H., Stutzmann M. (Eds.), MRS Proceedings, Amorphous and Heterogeneous Silicon Thin Films, vol. 609, MRS, Warrandale, PA, 2000, p. A27.8.

2. Gueorguieva, M.J., Main, C. and Reynolds, S., 2001, *Laplace-Transform Transient Photocurrent Spectroscopy as a Probe of Metastable Defect Distributions in Hydrogenated Amorphous Silicon.* Paper presented at MRS Spring Meeting, San Francisco, April 2001, MRS Symp. Proc. 664, A19.3.

3. Reynolds, S., Main, C., and Gueorguieva, M.J., 2001, *Effect of Experimental Noise on Recovery of the Electronic Density of States From Transient Photocurrent Data.* Paper presented at MRS Spring Meeting, San Francisco, April 2001, MRS Symp. Proc. 664, A22.6.

4. Main, C., Reynolds, S., Gueorguieva, M and Badran, R.I., 2001 *New developments in the determination of the density of states from transient photocurrents in disordered semiconductors.* Invited paper presented at the 11th International School on Condensed Matter Physics (ISCMP2000), Varna, Bulgaria, September 2000. Published in Materials for Information Technology in the New Millennium eds. JM Marshall, AG Petrov, A Vavrek, D Nesheva, D Dimova-Malinovska, JM Maud (Published by the Editors 2001) 8-17.

5. Reynolds, S., Main, C. and Gueorguieva, M. 2001 *Noise and Bandwidth Limitations in Transient and Modulated Photocurrent DOS Spectroscopies.* Invited contribution in: Proceedings of the 11th International School on Condensed Matter Physics (ISCMP2000), Varna, Bulgaria, 3 - 8 September 2000. Published in Materials for Information Technology in the New Millennium, eds. J.M. Marshall, A.G. Petrov, A. Vavrek, D. Nesheva, D. Dimova-Malinovska, J.M. Maud (Published by the Editors 2001) 152-159.

6. Gueorguieva. M.J., Main. C. and Reynolds. S. 2001 *Comparison of Laplace transform methods for determination of density of states from transient photocurrent data.* Invited paper presented at the 11th International School on Condensed Matter Physics (ISCMP2000), Varna, Bulgaria, September 2000. Published in Materials for

Information Technology in the New Millennium eds. JM Marshall, AG Petrov, A Vavrek, D Nesheva, D Dimova-Malinovska, JM Maud (Published by the Editors 2001) 332-335.

7. Gueorguieva, M.J., Main, C., and Reynolds, S., 2002 *Probing defect distributions in semiconductors by Laplace transform transient photocurrent spectroscopy*. J Non-Cryst Solids 299: 541-545.

8. Gueorguieva, M.J., Main, C. and Reynolds, S. 2002, *Analysis of Post-Transit Photocurrent-Time Data by Application of Tikhonov Regularization*, Mat. Res. Soc. Symp. Proc. 715, A21.1.1-A21.1.6.